

Title	抗原の蛍光レシオ検出が可能な遺伝的にコードされた新規抗体バイオセンサーの開発
Author(s)	Huynh Nhat, Phuong Kim
Citation	
Issue Date	2016-03
Type	Thesis or Dissertation
Text version	ETD
URL	http://hdl.handle.net/10119/13532
Rights	
Description	Supervisor: 芳坂 貴弘, マテリアルサイエンス研究科, 博士

**Novel Genetically Encoded Antibody-based Biosensors
for Fluorescence ratio Detection of Antigens**

KIM PHUONG HUYNH NHAT

Japan Advanced Institute of Science and Technology

Doctoral Dissertation

**Novel Genetically Encoded Antibody-based Biosensors
for Fluorescence ratio Detection of Antigens**

KIM PHUONG HUYNH NHAT

Supervisor: Professor Takahiro Hohsaka, Ph.D.

School of Materials Science
Japan Advanced Institute of Science and Technology

March 2016

ABSTRACT

Fluorescence biosensor is an indispensable method for tracking of small biomolecules or biological processes not only *in vitro* but also in living cells. Recently, Quenchbody, a novel fluorescence biosensor consists of an N-terminal fluorescently labeled antibody single-chain variable domain (scFv) has been reported. This biosensor allowed detection of antigen based on antigen-dependent removal of quenching effect on the labeled fluorophore. However, fluorescence intensity of single labeled Quenchbody depends on not only concentration of antigen but also amount of the biosensor in measuring sample. In addition, Quenchbody requires the incorporation of fluorophore-labeled nonnatural amino acid in a cell-free translation system, thus, limit its application in live-cell imaging. In this study, a new strategy for construction of antibody-based fluorescence biosensor in combination of Förster (or fluorescence) resonance energy transfer (FRET) and fluorescence quenching mechanisms was introduced to overcome the limitations of Quenchbody. First, fluorescence biosensors for detection of phosphotyrosine-containing peptides were developed by incorporation fluorophore-labeled nonnatural amino acid into the N-terminus of anti-phosphotyrosine scFv. This biosensor showed antigen-dependent fluorescence increase upon addition of phosphotyrosine-containing peptides. Fusion of fluorescent protein (FP) to the labeled scFv generated double labeled biosensors which allowed FRET between FP and labeled fluorophore and detection of antigen based on antigen-dependent enhancement of fluorescence ratio of fluorophore/FP. Next, genetically-encoded antibody-based fluorescence biosensors were constructed by substituting fluorophore-labeled nonnatural amino acid by protein-tag and its fluorescent ligands. The obtained biosensors exhibited fluorescence enhancement in the presence of antigens. In addition, type of fluorophore, linker length between fluorophore–ligand and orientation of protein-tag to scFv largely affected fluorescence enhancement. Fusion of FP to protein-tag-scFv resulted in double labeled biosensors which showed FRET between FP and labeled fluorophore as well as antigen-dependent enhancement of the fluorophore, allowing fluorescent ratiometric detection of antigen. Finally, an application of the novel genetically-encoded antibody-based ratiometric fluorescent biosensor was demonstrated by expression of the biosensor on the surface of mammalian cells for detection of extracellular antigen. The advantage of the present strategy over conventional strategy for FRET-based biosensor construction is that no conformational change of backbone protein upon binding to analyte is required. Therefore, it is potentially applicable for various antigen-antibody pairs in not only diagnostic analysis but also live-cell imaging.

Key words: single-chain antibody, nonnatural amino acid, fluorescence biosensor, protein-tag, live-cell imaging.

Table of Contents

Chapter 1: Background and Overview	1
Chapter 2: Antibody-based fluorescent and fluorescent ratio biosensors for detection of phosphotyrosine	26
Chapter 3: Genetically-encoded antibody-based biosensors by fusion of protein-tag and fluorescent protein to scFv	49
Chapter 4: Application of genetically-encoded antibody-based biosensor to live-cell imaging	86
Chapter 5: Conclusion	101
List of publication.....	103
Acknowledgement	104

Chapter 1

Background and Overview

1-1. Introduction

Proteins present in all living organisms and play a central role in major biological processes. They are built up by 20 kinds of natural amino acids and form unique three-dimensional structures which can perform as catalysts, signaling molecules, receptors, transporters, etc. Based on approaches in elucidating protein structures and functions, proteins can be engineered to become useful biosensors to detect not only small biomolecules but also biological events *in vitro* and in living cells.

Fluorescent biosensor is one of the most powerful and popular tool for visualizing and quantifying target molecules or events. A fluorescent biosensor usually consists of a protein scaffold which can recognize the target and fluorophores which can convert the interaction of protein and target into fluorescent signal change. Most of fluorescent biosensors have been developed based on photoinduced energy transfer (PET) or Förster (or fluorescence) resonance energy transfer (FRET)¹ technologies. Fluorescent dyes can be incorporated into proteins by chemical labeling or incorporation of fluorophore-containing nonnatural amino acids. Proteins can also be labeled with fluorescent proteins or protein-tags which are subsequently labeled with fluorescent ligands. Since the discovery of *Aequorea victoria* green fluorescent protein (GFP)², variety of fluorescent protein derivatives have been reported³⁻⁴ and commonly used for protein labeling in cell biology. In addition, bioluminescent proteins (for example, luciferases)⁵, and other fluorescent proteins such as bacterial phytochromes⁶, rhodopsins⁷ and fatty acid binding protein (FABP) family⁸ provide additional choices for protein labeling.

Recently, together with the increasing demands in biological studies, various strategies for fluorescence labeling of proteins and fluorescent biosensors construction have been reported including antibody-based fluorescent biosensor⁹. Details of these strategies and achievements were described below.

1-2. Methods for fluorescent modification of protein

Proteins can be fluorescently labeled by chemical modification, incorporation of fluorophore-containing nonnatural amino acids, and fusion with fluorescent proteins or protein-tags.

1-2-1. Chemical modification of natural amino acid residues

Chemical modification of natural amino acid residues is a useful method for rapidly probing a protein. Targets for chemical modification are residues which have nucleophilic functional groups such as thiol group of cysteine and ϵ -amino group of lysine. Cysteine is often used for site-specific modification of protein because of its high nucleophilic thiol group and low occurrence on protein surface (about 2.3% genome-wide)¹⁰. For proteins lacking cysteine, this residue can be introduced to protein surface by site-direct mutagenesis. Thiol group can be labeled by reaction with maleimide or α -haloketone derivatives (Figure 1-1A). However, if protein contains undesired cysteines, these cysteines must be substituted by other amino acids, but such substitution may affect structure and function of protein. Alternatively, ϵ -amino group of lysine can be modified by activated esters, sulfonyl chlorides, isocyanates and isothiocyanates (Figure 1-1B). But, it is difficult to achieve site-specific labeling of ϵ -amino group because proteins always have multiple amino groups including N-terminal amino group.

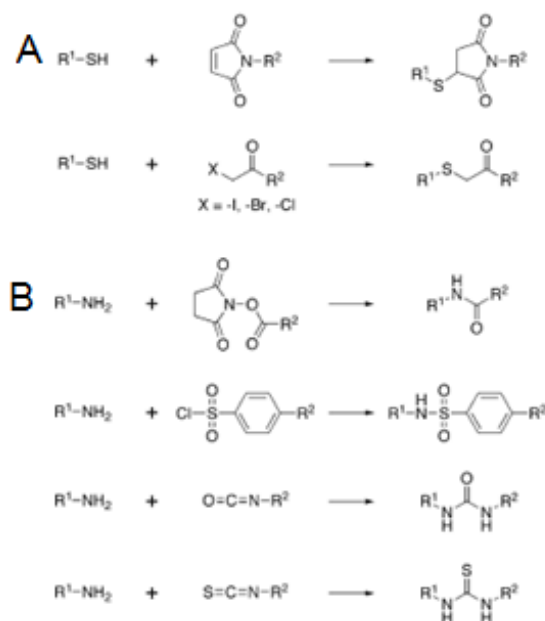


Figure 1-1. Chemical reactions for modification of (A) cysteine and (B) lysine (*Angew. Chem. Int. Ed.* **53**: 4088-4106 (2013))

In addition, Tsien *et al.* have reported a method for chemical labeling of protein using biarsenical ligands FAsH and its analogues, such as ReAsH, HoXAsH and CHoXAsH. These ligands can selectively bind to a tetracysteine motif CysCysProGlyCysCys with high affinity and specificity. Fluorescence of the ligands are reported considerably enhanced upon binding to tetracysteine motif. The advantages of this method are that the ligands can be prepared with ease and they can be used for labeling of proteins in living cells¹¹⁻¹³.

1-2-2 Incorporation of nonnatural amino acids into proteins

Proteins can be position-specifically fluorescent-labeled by incorporation of fluorophore-containing nonnatural amino acids. In addition, this method allows expansion of protein functions depending on the side groups of the nonnatural amino acids introduced. For incorporation of nonnatural amino acids into proteins using biological translation system, it requires the engineering of genetic code, synthesis of suppressor aminoacyl-tRNAs, designing of orthogonal tRNAs and designing of nonnatural amino acids.

Expansion of genetic code

The genetic code consists of 61 codons encoding 20 naturally-occurring amino acids and 3 nonsense (stop) codons. For incorporation of nonnatural amino acids, extended codons which are specific for nonnatural amino acids are necessary. Therefore, the amber stop codon (UAG) has been employed for incorporation of nonnatural amino acids by Schultz and Chamberlin groups¹⁴⁻¹⁶. In this method, an amber suppressor tRNA is chemically aminoacylated with nonnatural amino acid to obtain aminocyl-tRNA_{CUA}¹⁷⁻¹⁸. On the other hand, site-direct mutagenesis is used to generate DNA and mRNA containing amber stop codon at desired positions. Protein translation and incorporation of nonnatural amino acids were performed *in vitro* by a cell-free translation system. Even in the presence of amber suppressor aminocyl-tRNA_{CUA}, the release factor 1 (RF1) can bind to the amber stop codon and terminate the translation process, in this case, a truncated protein is produced (Figure 1-2). Hence, the yield of nonnatural amino acids incorporation is decreased due to this competition. Recently, a new strategy to increase the yield of nonnatural amino acids incorporation in response to amber stop codon by optimized pyrrolysyl tRNA synthetase/tRNA expression system and engineered release factor 1 has been reported. The study showed that this strategy improves the suppression of up to three UAG codons in mammalian cells significantly¹⁹.

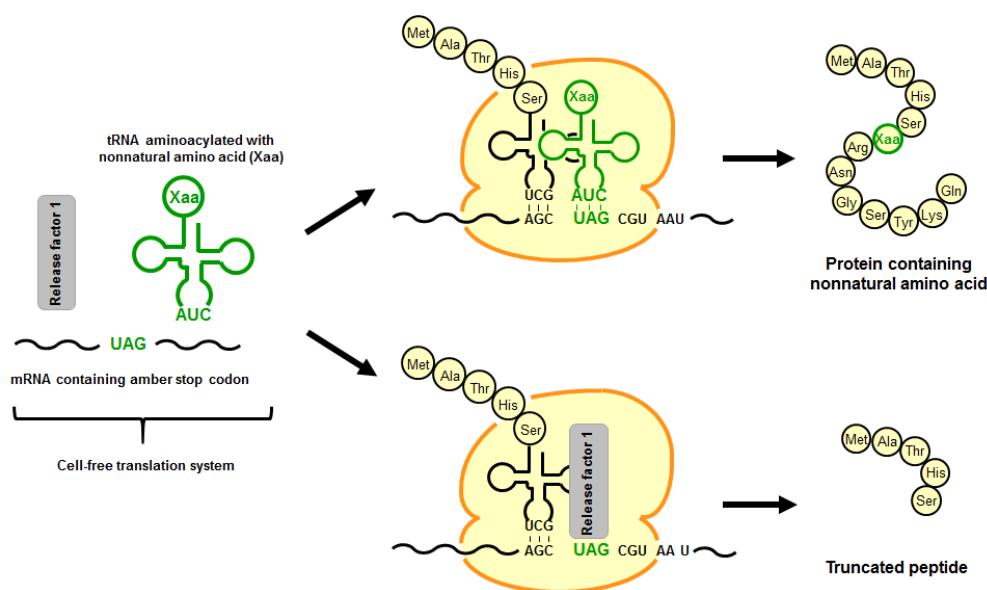


Figure 1-2. Site-specific incorporation of nonnatural amino acid into protein in response to amber stop codon in cell-free translation system. The incorporation competes with the termination of translation process by release factor 1.

However, the use of amber stop codon for incorporation of nonnatural amino acid is limited since it does not allow incorporation of multiple nonnatural amino acids into a single protein. To overcome this problem, Hohsaka *et al.* have developed the four-base codon method for incorporation of nonnatural amino acid. This method has two advantages: first, the competition of amber suppressor tRNA and RF1 is avoided. Four-base codons have been developed based on low occurrence codons such as CGG or AGG so that the competition of tRNA carrying four-base anticodon and endogenous tRNA can be minimized. Second, the four-base codon allows incorporation of multi-nonnatural amino acids into a single proteins. Various four-base codons have been developed, such as AGGU, CGGG, CGGU, CCCU, CUCU, CUAU, and GGGU²⁰⁻²¹. The DNA and mRNA containing four-base codon can be prepared by site-directed mutagenesis. In a cell-free translation system, if a four-base codon is successfully decoded by a nonnatural aminocyl-tRNA carrying corresponding anticodon, a full-length protein is synthesized. However, if four-base codon is recognized by an endogenous tRNA, the reading frame is shifted by 1 nucleotide by which a stop codon may be encountered. Thus, truncated protein is obtained (Figure 1-3). Kajihara and coworkers have reported an application of this strategy to incorporate two distinct fluorescent-labeled nonnatural amino acids in response to two four-base codon GGGU and CGGG in calmodulin and monitor its conformational change based on FRET signals²².

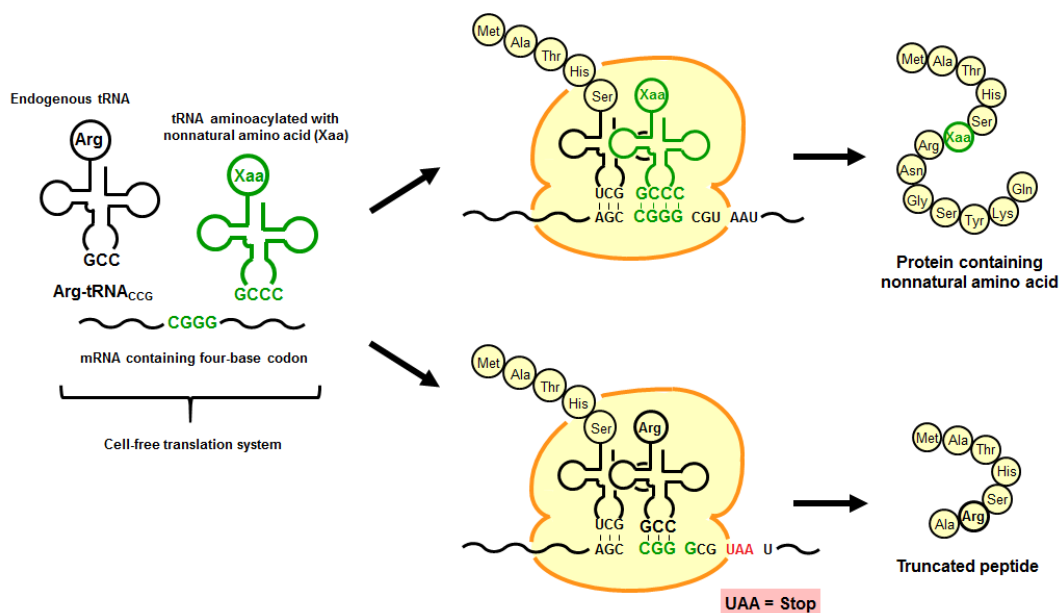


Figure 1-3. Site-specific incorporation of nonnatural amino acid into protein in response to four-base codon in cell-free translation system. Incorporation of natural amino acid in response to triplet codon results in the termination of translation process by frameshifting.

Aminoacylation of tRNAs with nonnatural amino acids

Aminoacylation of tRNAs with nonnatural amino acids is an important step for incorporation of nonnatural amino acids into protein. In early studies, Johnson and coworkers demonstrated that ϵ -amino group of Lys-tRNA which was prepared by LysRS was acetylated by N-acetoxysuccinimide, and the resulting acetyllysine was incorporated into hemoglobin using a rabbit reticulocyte cell-free translation system²³. This method was applied for modification of lysine with fluorescent probes²⁴ and cross-linking reagents for photo-affinity labeling²⁵. However, site-specific modification was not achieved because modified lysine was incorporated to multiple sites.

Alternatively, a chemical aminoacylation method in which synthesized aminoacylated dinucleotides pCpA was ligated to truncated tRNA lacking terminal pCpA by T4 RNA ligase was proposed by Hecht and coworkers¹⁷⁻¹⁸. The pCpA can be aminoacylated with various nonnatural amino acids. This method have been applied for not only *in vitro* translation system but also in live cells by microinjection²⁶⁻²⁷.

On the other hand, an approach in nonnatural amino acid acylation by evolved aminoacyl-tRNA synthetases (aaRSs) was reported by Schultz and coworkers²⁸⁻²⁹. A pair of amber suppressor tRNA^{Tyr}/TyrRS from *Methanococcus jannaschii* was engineered to

incorporate O-methyltyrosine into proteins in *E. coli*. Further improvement of this method allowed over 30 nonnatural amino acids to be incorporated into proteins in *E. coli* with high efficiency. In addition, pyrrolysyl-tRNA synthetase (PylRS)/tRNA^{Pyl} pairs from certain *Methanosarcina* species were also employed to introduce lysine derivatives into proteins not only in *E. coli* but also in eukaryotic cells³⁰⁻³³.

For non-enzymatic aminoacylation, Sisido *et al.* developed a peptide nucleic acid (PNA) which include a nonnatural amino acid thioester linked to a PNA that was complementary to the 3'-end of target tRNA³⁴ and micelle in which target tRNA was aminoacylated with activated ester of N-protected amino acids in the cationic micelle under ultrasonic agitation³⁵. Both non-enzymatic methods were reported as simple and applicable for variety of nonnatural amino acids.

Design of orthogonal tRNAs

Suppressor tRNAs are required for incorporation of nonnatural amino acids into proteins. This tRNA must be accepted by the translation machinery and orthogonal to endogenous aminoacyl-tRNA synthetase of the host translation system. An amber suppressor tRNA derived from yeast phenylalanine tRNA has been used in *E. coli* cell-free translation system²⁰. In addition, Taira *et al.* have developed an amber suppressor tRNA derived from *Mycoplasma capricolum* tryptophan tRNA which was reported to incorporate nonnatural amino acid into *E. coli* cell-free translation system with higher efficiency than the yeast phenylalanine tRNA³⁶. Recently, approaches in engineering of anticodon loop and anticodon stem of tRNA^{Pyl} for efficient incorporation of nonnatural amino acids in response to four-base codon have been reported³⁷⁻³⁸. The evolved tRNA^{Pyl}s were demonstrated to enhance incorporation of nonnatural amino acids into proteins in both *E. coli* and mammalian cells.

Design of nonnatural amino acids

Various nonnatural amino acids with diverse functional groups have been successfully incorporated into proteins (Figure 1-4)³⁹⁻⁴¹. For fluorescent labeling of proteins, proteins can be incorporated with either fluorescent nonnatural amino acids^{22,42} or nonnatural amino acids carrying biorthogonal chemical groups such as ketones, alkynes, anilines, etc. which are selectively labeled by fluorescent dyes⁴³. Incorporation of nonnatural amino acids allows studies of protein structures and functions as well as site-specific modification of proteins.

It is important to consider types of nonnatural amino acid which are efficiently incorporated into proteins. Hohsaka and coworkers have evaluated the incorporation efficiency

of nonnatural amino acids with various side chains in *E. coli* cell-free translation system. The results reveal that nonnatural amino acids with linearly expanded aromatic groups are more favorable for the translation system than those with widely expand or bend aromatic groups²⁰. Therefore, the side chain of nonnatural amino acids are very important and it should be carefully considered in designing of novel nonnatural amino acids.

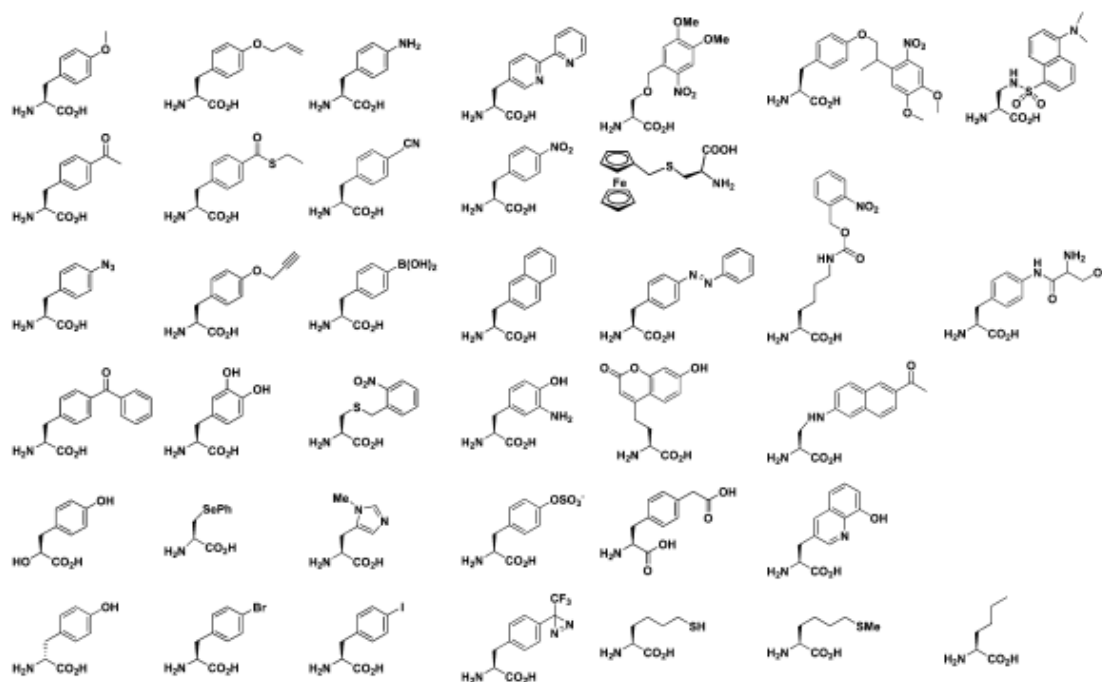


Figure 1-4. Examples of nonnatural amino acids that have been incorporated into proteins (*J. Am. Chem. Soc.* **131**: 12497-12515 (2009)).

1-2-3 Fusion with fluorescent proteins

Fluorescent proteins are indispensable tools for fluorescent labeling of proteins. The first discovered fluorescent protein is the *Aequorea victoria* green fluorescent protein (GFP)². GFP is encoded by about 240 amino acids which form an 11 β -strands barrel with molecular weight about 27 kDa. GFP can be fused to protein of interest and allow spatial, temporal imaging of proteins. Since the discovery of GFP, it has been continuously engineered to improve the brightness as well as stability. On the other hands, many of its derivatives with a wide range of fluorescent colors have been reported³. In addition, circular permuted fluorescent proteins which are found very useful in construction of fluorescent biosensors have been introduced by Tsien group and Miyawaki group^{4, 44-45}.

On the other hand, bioluminescent proteins such as luciferase are also commonly used for labeling. Luciferase is a family of photoproteins found in insects, marine organisms and prokaryotes. Luciferase reacts with its substrate luciferin and luminesces without requirement of excitation light. Thus, using luciferase can reduce background signals. To date, numerous studies have been carried out to investigate novel luciferases as well as engineer conventional luciferases to improve their optical properties, such as brightness, photostability, red-shift bioluminescence⁵.

Alternatively, near-infrared fluorescent proteins derived from bacterial phytochromes have been reported. The bacterial phytochromes utilize biliverdin which is ubiquitous in mammalian tissue as a reactive chromophore. Thus, phytochromes have been suggested as a candidate for fluorescence imaging in mammals. Currently, several phytochrome-based near-infrared fluorescent proteins have been developed, such as IFP1.4, iRFP and Wi-Phy⁶.

In addition, photoreceptor proteins rhodopsins which are found in proteobacteria and archaea have been used for biosensor construction^{7,46}. Recently, a novel fluorescent protein (UnaG) belongs to the fatty-acid binding protein family in eel has been reported. UnaG emits green fluorescence upon binding to its ligand bilirubin, a heme metabolite. UnaG has been applied for analyzing bilirubin of human clinical samples⁸. As mentioned above, up to date various fluorescent proteins with a wide range of colors as well as diversity in optical properties has been developed. Fluorescent proteins have become one of the most powerful tools for protein labeling and fluorescent biosensors construction.

1-2-4 Fusion with protein-tags

The most commonly used protein-tags for protein labeling are HaloTag, SNAP-tag and CLIP-tag. HaloTag is a 33 kDa protein derived from *Rhodococcus* haloalkane dehalogenase (DhaA). DhaA catalyzes a hydrolysis reaction in which it removes halides from aliphatic hydrocarbons by a nucleophilic displacement. HaloTag is a mutant of DhaA in which mutation is introduced to the active site so that catalysis reaction is trapped at the covalent ester bond intermediate between the enzyme and hydrocarbon substrate (Figure 1-5). As a results, various functional groups can be covalently linked to HaloTag. HaloTag was reported to have high affinity to its ligand, the binding of HaloTag and its ligand is rapid and irreversibly. A wide range of HaloTag ligands have been developed and enable its applications in not only protein fluorescence labeling but also protein isolation, purification, analysis of protein functions and interactions⁴⁷⁻⁴⁸.

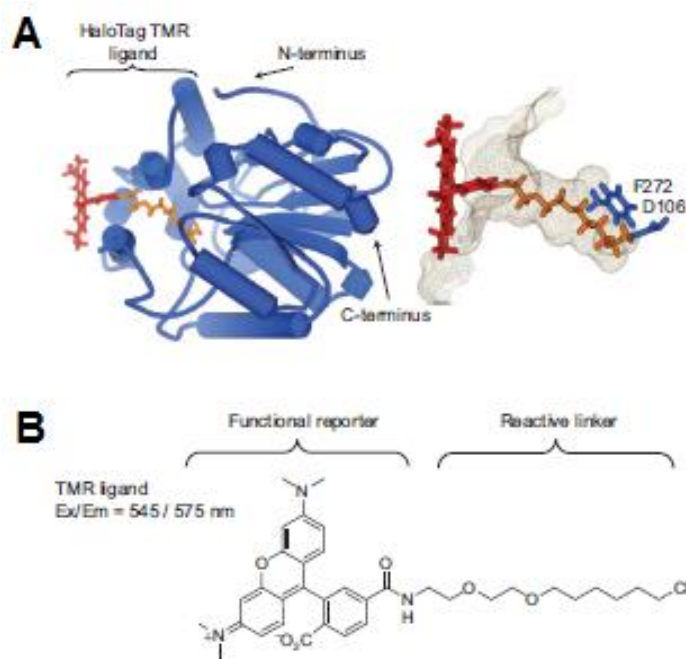


Figure 1-5. (A) Structure of HaloTag and its ligand tunnel with covalently bound TMR ligand. (B) Structure of TMR ligand (fluorescent ligand) (*ACS Chem. Biol.* **3**(6): 373-382 (2008)).

Another approach in protein-tag is SNAP-tag and its variant CLIP-tag. SNAP-tag and CLIP-tag are about 19 kDa proteins derived from human DNA repair protein O⁶-alkylguanine-DNA alkyltransferase (hAGT). SNAP-tag reacts with its substrates containing O⁶-benzylguanine (BG) moiety by transferring the alkyl group from substrates to its cysteine residues results in a covalent labeling with functional groups attached on substrate. Similarly, CLIP-tag can be covalently labeled by reacting with O²-benzylcytosine (BC) derivatives (Figure 1-6). The reaction of SNAP-tag and CLIP-tag with their substrates are specific, rapid and irreversible. Variety of fluorescent probes for SNAP-tag and CLIP-tag labeling have been developed. Since SNAP-tag and CLIP-tag are orthogonal, they can be used simultaneously for live cell imaging⁴⁹⁻⁵¹.

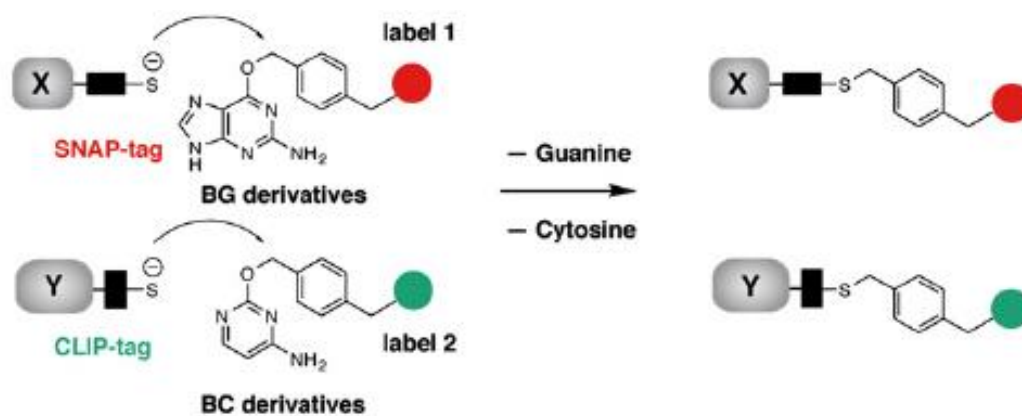


Figure 1-6. Labeling of SNAP-tag and CLIP-tag with BG derivatives and BC derivatives, respectively. (*Chem. Biol.* **15**: 128-136 (2008)).

1-3. Techniques for construction of fluorescent biosensors

Most of fluorescent biosensors have been developed based on Förster (or fluorescence) resonance energy transfer (FRET) and photoinduced electron transfer (PET).

1-3-1. FRET-based biosensors

FRET is a physical phenomenon which involves non-radiative energy transfer between a donor fluorophore and an acceptor fluorophore if the acceptor absorption spectrum is overlapped with the emission spectrum of donor (Figure 1-7A), they are in close distance (typically, less than 10 nm) and their orientations are favorable for dipole-dipole interaction. A Jablonski diagram of FRET is shown in Figure 1-7B. When donor is excited by a light source, its energy is promoted from ground state S_0^D to excitation state S_1^D . If the donor is at close proximity with an acceptor and emission energy of donor is match with excitation energy of acceptor, donor can transfer excited energy to acceptor directly. The energy transfer efficiency E is calculated as:

$$E = \frac{R_0^6}{R_0^6 + r^6}$$

where r is the distance between donor and acceptor, R_0 is the Förster distance – the distance at which FRET efficiency is 50%. R_0 is calculated based on the following equation:

$$R_0^6 = \frac{9000(\ln 10)\kappa^2 Q_D}{128\pi^5 N n^4} J(\lambda)$$

where κ^2 is the orientation factor that represents the geometric relationship between donor transition dipole and acceptor transition dipole, Q_D is quantum yield of donor, N is Avogadro's number, n is the refractive index of the medium, $J(\lambda)$ is the spectral integral expressing the degree of overlap between donor emission and acceptor absorption spectra⁵²⁻⁵³.

Thus, the extent of spectral overlap between donor and acceptor, the quantum yield of donor, the distance and relative orientations between them significantly affect FRET efficiency.

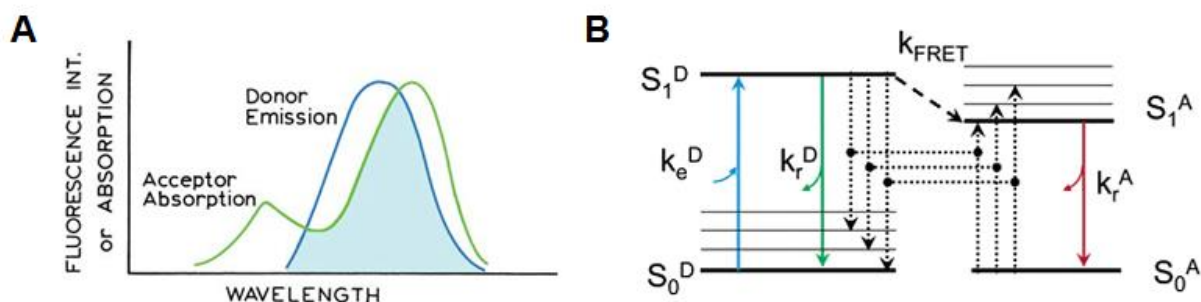


Figure 1-7. Mechanism of FRET. **(A).** Spectra of donor emission and acceptor absorption, and spectral overlap (blue filled region) (*Principles of Fluorescence Spectroscopy*, 3rd edition (Springer, New York) (2006)). **(B).** Jablonski diagram of energy transfer in FRET (*Chem. Rev.* **106**(5): 1785-1813 (2006)).

Typical FRET-based fluorescent biosensors are consisted of a protein backbone, which can interact with analyte, and tandemly linked two fluorophores at N- and C-termini. Upon interaction with analyte, protein backbone undergoes a conformational change which alters the relative orientation and distance of the labeled fluorophores, as a result, alter FRET efficiency between them. An example for FRET-based fluorescent biosensor is the ATP (adenosine 5'-triphosphate) indicator (ATeam). The bacterial ϵ subunit of F_0F_1 -ATP synthase was fused with monomeric super-enhanced cyan-emitting fluorescent protein (mseCFP) and monomeric yellow-emitting fluorescent protein (mVenus) at N- and C-termini, respectively. Upon binding of ATP, ϵ subunit changed its conformation from extended form to retracted form, thus, brought the two fluorophores closer and altered their relative orientation. The indicator showed increase in FRET efficiency in the presence of ATP (Figure 1-8). A series of ATeam for detection of wide range concentrations of ATP from μM to mM were developed⁵⁴.

Recently, FRET-based biosensor utilizing SNAP-tag and CLIP-tag (CLASH-AChE/HCA) to detect acetylcholine esterase (AChE) inhibitor tacrine has been reported (Figure 1-9). The biosensor was comprised of SNAP-tag and CLIP-tag linked by a rigid 30-proline linker, AChE fused to N-terminus of SNAP-tag, and a human carbonic anhydrase II (HCA) fused to C-terminus of CLIP-tag. The whole biosensor was displayed on cell surface. SNAP-tag was conjugated with a Cy5-labeled BG derivative containing an HCA ligand benzenesulfonamide (SA) and an inhibitor of AChE edrophonium (E). CLIP-tag was labeled with Cy3, which was FRET donor for Cy5. In the absence of tacrine (T), the interaction of edrophonium with AChE prevented the binding of benzenesulfonamide to HCA, thus, the biosensor was in low FRET state. When tacrine was added, the interaction of tacrine with AChE

allowed the binding of benzenesulfonamide to HCA and increased FRET efficiency. This strategy was also applied to regulate the activity of enzyme, for example, in this case, HCA can be switched on and off by addition of tacrine⁵⁵.

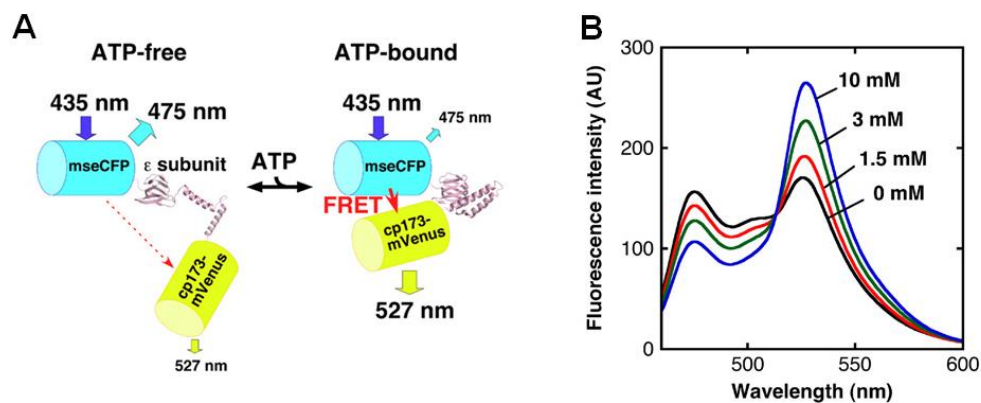


Figure 1-8. FRET-based ATP indicator (ATeam). (A). Schematic illustration of ATeam structure in ATP-free and ATP-bound forms. (B). ATP-dependent fluorescent spectral change of ATeam (*Proc. Natl. Acad. Sci. USA* **106**(37): 15651-15656 (2009)).

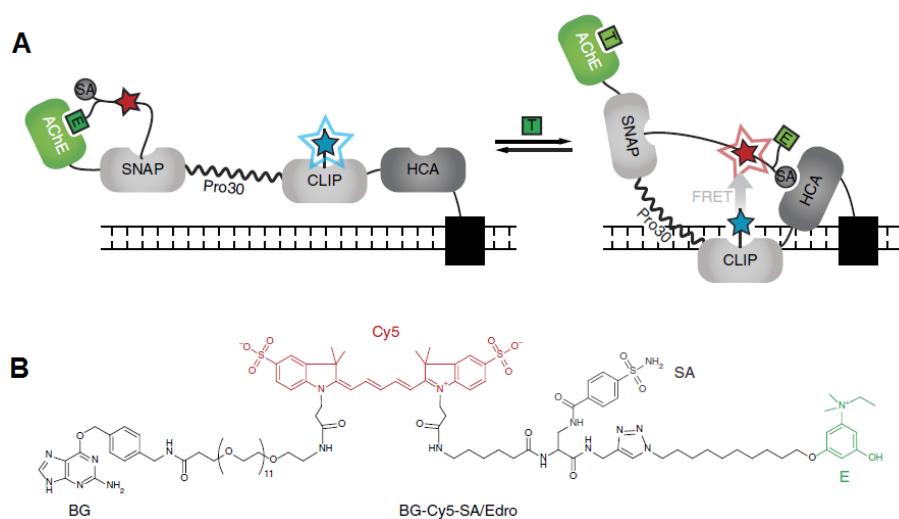


Figure 1-9. (A). Schematic illustration of CLASH-AChE/HCA. (B). Structure of BG derivative used for labeling of SNAP-tag (*Nat. Commun.* **6**:7830 (2015))

1-3-2. Photoinduced electron transfer (PET)

In contrast to FRET which results from a long-distance dipole-dipole interaction of two fluorophores, PET requires van de Waals contact between electron donor (D_P) and electron acceptor (A_P) molecules, yielding a complex $D_P^+A_P^-$ (Figure 1-10A). The complex can return to the ground state without emitting a photon though in rare cases exciplex emission is observed, then, the extra electron on acceptor is returned to donor. Thus, PET usually results in a quenching effect. In PET, excited fluorophore can be either donor or acceptor. Figure 1-10B presents an energy diagram of PET with the excited molecule being the donor. Excitation of donor results in turning an electron from ground state to excited state. Donor can transfer electron to acceptor and forms a complex $D_P^+A_P^-$. The complex returns to the ground state without emitting (quenching), or may emit exciplex emission in rare case⁵². Thus, the redox potential of donor and acceptor as well as their distance are important for PET efficiency.

In biology studies, nucleic acid such as guanine and amino acids such as tryptophan, methionine, and tyrosine are found to have quenching effect on various fluorophores since they have high tendency of donating electron⁵⁶⁻⁵⁸.

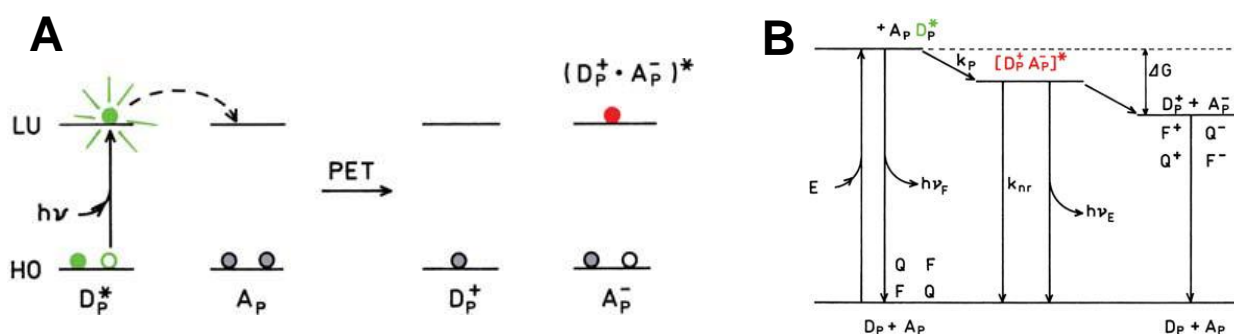


Figure 1-10. Mechanism of photoinduced electron transfer (PET). **(A)** Molecular orbital schematic for PET. HO is highest occupied orbital, LU is lowest unoccupied orbital. **(B)** Energy diagram of PET. F is fluorophore, Q is quencher, and ν_F and ν_E are emission of fluorophore and exciplex, respectively. (*Principles of Fluorescence Spectroscopy*, 3rd edition (Springer, New York) (2006)).

Iijima and coworkers have monitored the binding of maltose by site-specific incorporation of BODIPY-linked nonnatural amino acid into maltose binding protein (MBP). The binding of maltose was detected based on fluorescence quenching by PET. In the absence

of maltose, BODIPY dye incorporated at the ligand-binding site was quenched by tryptophan residue. Upon addition of maltose, BODIPY dye was removed from tryptophan residue and the quenching effect was depressed.

They utilized this PET system to generate a fluorescent ratiometric biosensor in combination with FRET (Figure 1-11). MBP was double-labeled with BODIPYFL (FRET donor) at the N-terminus and with BODIPY558 (FRET acceptor) at the ligand-binding site. FRET occurred regardless the absence and presence of maltose, but BODIPY558 was quenched only in the absence of maltose. Therefore, this biosensor showed significant increase of fluorescence intensity ratio and allow quantitative detection of maltose⁴².

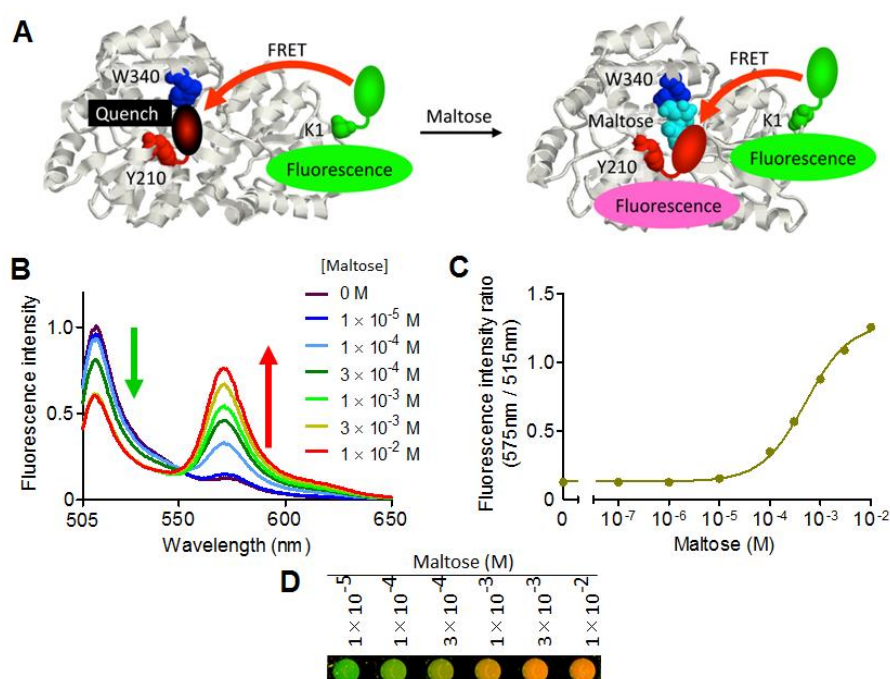


Figure 1-11. (A). Schematic illustration of the detection of maltose based on FRET and fluorescence quenching. (B). Maltose-dependent enhancement of FRET signals. (C). Titration curve of fluorescence ratio (575/515). (D). Fluorescence imaging on a microplate in the presence of maltose with excitation at 488 nm and emission at 520 nm (green) and 605 nm (red) (*Chem. Bio. Chem.* **10**: 999-1006 (2009)).

In addition, a new approach in PET-based biosensor, termed “Quenchbody”, has been reported. Quenchbody was developed based on the antigen-dependent removal of quenching effect on a fluorophore attached to N-terminal domain of an antibody single chain variable region (scFv) (Figure 1-12A). In the absence of antigen, the fluorophore is in close proximity

to tryptophan (Trp) residues located at the interface between the variable domains (V_H and V_L) of scFv, thus, fluorescence from the fluorophore is quenched by Trp via a PET mechanism. In the presence of antigen, this quenching is removed because the tight interaction of V_H and V_L prevented the interaction of fluorophore and Trp residues. Therefore, the fluorescence is significantly enhanced and this enhancement is antigen concentration dependent (Figure 1-12B). Quenchbodies have been proved to have a wide range of application in detection of not only small molecules but also peptides and proteins with high sensitivity⁹.

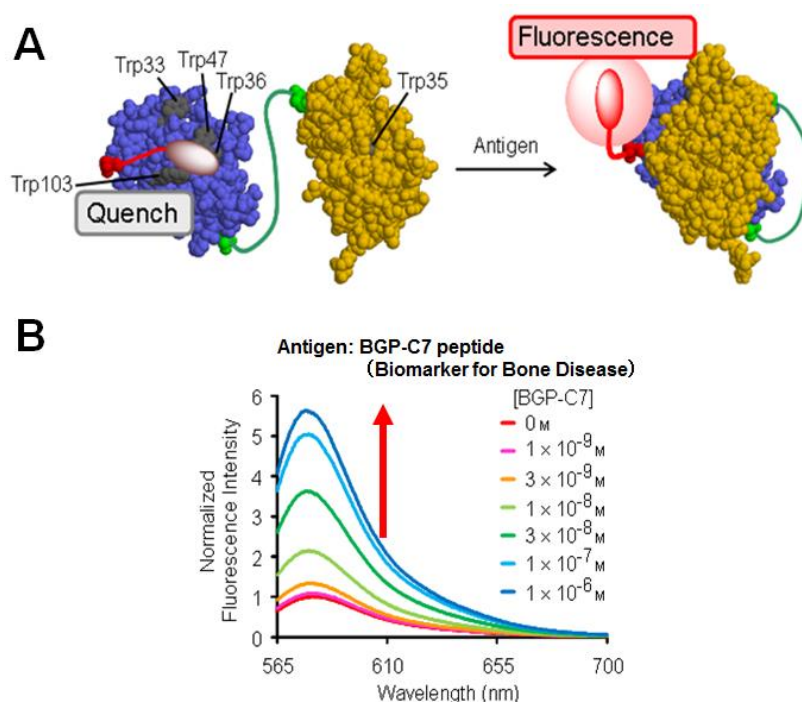


Figure 1-12. Fluorescent biosensor based on antibody single chain variable domain (scFv) (Quenchbody). (A) Illustration of Quenchbody in the absence and presence of antigen. (B) Antigen-dependent fluorescent enhancement of Quenchbody (*J. Am. Chem. Soc.* **133**: 17386-17394 (2011)).

1-4. Content of this thesis

While Quenchbody is a valuable biosensor strategy to detect a variety of target molecules, it has several drawbacks. Fluorescence intensity of single labeled Quenchbody increases upon antigen binding to scFv, however, fluorescence intensity also depends on the concentration of Quenchbody. Therefore, if Quenchbody is used under heterogeneous conditions such as inside the cell where local concentration of the biosensor cannot be controlled, it is difficult to distinguish the fluorescence signal is due to binding of antigen or non-uniform concentration of biosensor. In addition, incorporation of fluorescent-labeled nonnatural amino acid into Quenchbody requires the use of chemically synthesized aminoacyl-tRNA and cell-free translation system which also limit its application in live-cell imaging.

In this study, I developed novel types of antibody-based fluorescent and fluorescent ratiometric biosensors utilizing not only fluorescent-labeled nonnatural amino acid but also protein-tags and fluorescent proteins. I demonstrated that the present study successfully improved the disadvantages of Quenchbody and provided a general tool for fluorescent detection of various target molecules not only *in vitro* but also *in vivo*.

In chapter 2, N-terminal fluorescently labeled scFv against phosphotyrosine (pTyr) was newly synthesized. This fluorescent-labeled anti-pTyr scFv showed antigen-dependent fluorescent increase upon addition of pTyr-containing peptides (Figure 1-13A). In addition, double labeled scFv by fusion of fluorescent protein was generated. The double-labeled scFv showed FRET between fluorescent protein and labeled fluorophore and fluorescence enhancement of labeled fluorophore upon addition of pTyr peptide without affecting antigen binding affinity (Figure 1-13B).

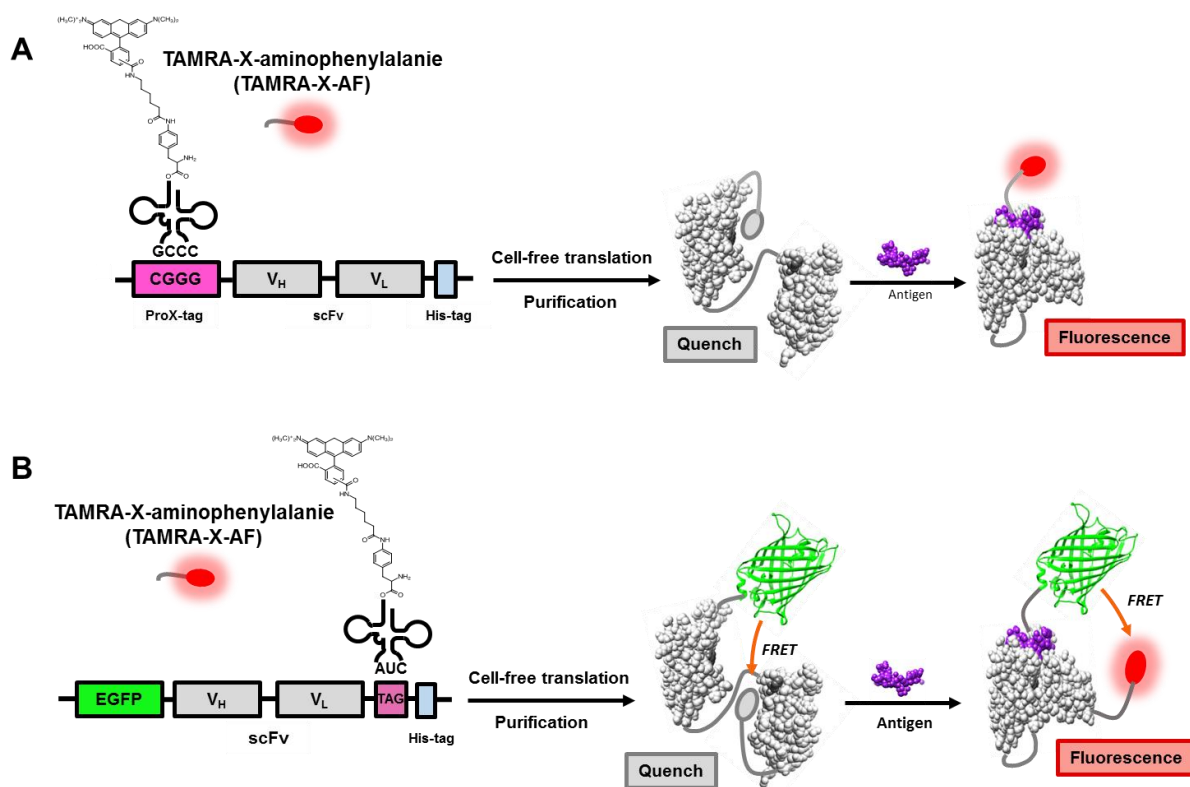


Figure 1-13. (A) Illustration of the synthetic procedure of TAMRA-scFv against pTyr and the detection of pTyr-containing peptide based on antigen-dependent removal of fluorescence quenching effect on TAMRA. (B) Illustration of the synthetic procedure of double labeled scFv(pTyr) in which EGFP was fused to N-terminus of scFv and the detection of pTyr-containing peptide based on FRET from EGFP to TAMRA and antigen-dependent removal of fluorescence quenching effect on TAMRA.

In chapter 3, protein-tags (HaloTag, SNAP-tag) and their fluorophore-labeled ligands were used for N-terminal fluorescent labeling of scFvs without using nonnatural amino acid mutagenesis. The resulting fusion proteins showed fluorescence enhancement upon antigen-binding (Figure 1-14A). In addition, type of fluorophores, linker length between fluorophore–ligand, and orientation of protein-tag to scFv largely affected the fluorescence enhancement. This result demonstrated that genetically encoded Quenchbody can be obtained by substituting fluorescent nonnatural amino acid by protein-tag. Subsequent fusion of fluorescent protein to protein-tag-scFv generated double labeled biosensors which allowed FRET between fluorescent protein and fluorophore and the antigen-dependent fluorescence enhancement to detect antigen in a ratiometric manner. (Figure 1-14B).

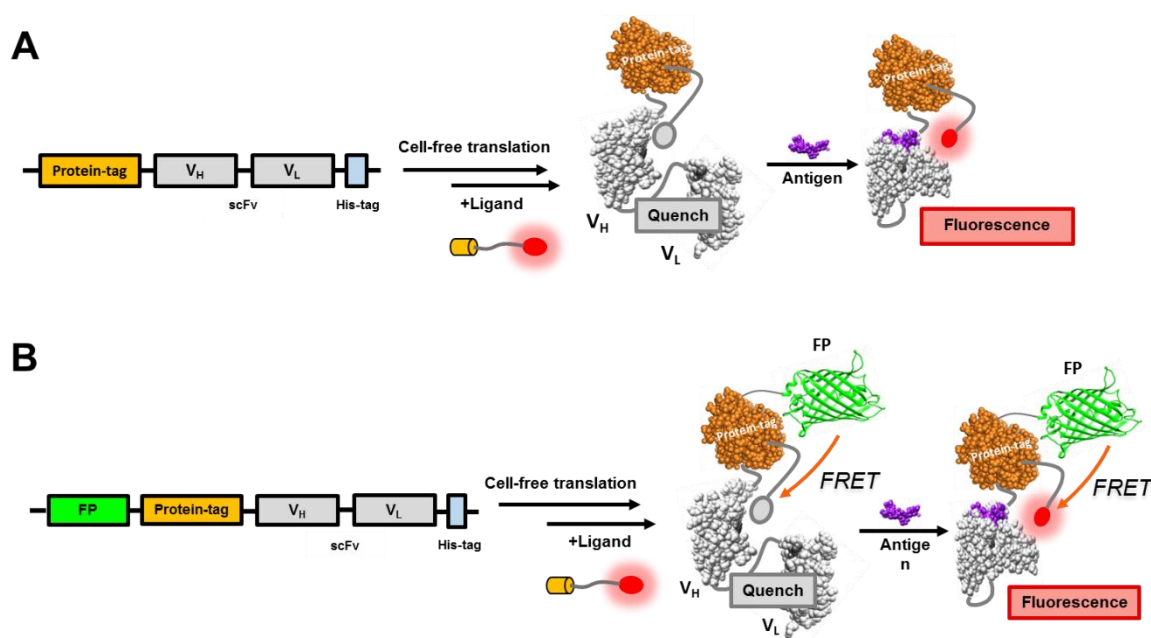


Figure 1-14. (A) Synthetic procedure of fusion of scFv and protein-tag labeled with fluorescent ligand and detection of antigen based on antigen-dependent removal of quenching effect on fluorophore. (B) Synthetic procedure of double labeled scFv with fluorescent protein (FP) and protein-tag, and fluorescence ratio detection of antigen based on FRET from FP to fluorophore and antigen-dependent removal of quenching effect on fluorophore.

In chapter 4, I expressed the newly constructed biosensor consisted of fluorescent protein, SNAP-tag, and scFv on surface of mammalian cells (HeLa S3 cells and osteosarcoma U2OS cells) and observed fluorescence of the cells in the absence and presence of antigen (BGP) (Figure 1-15).

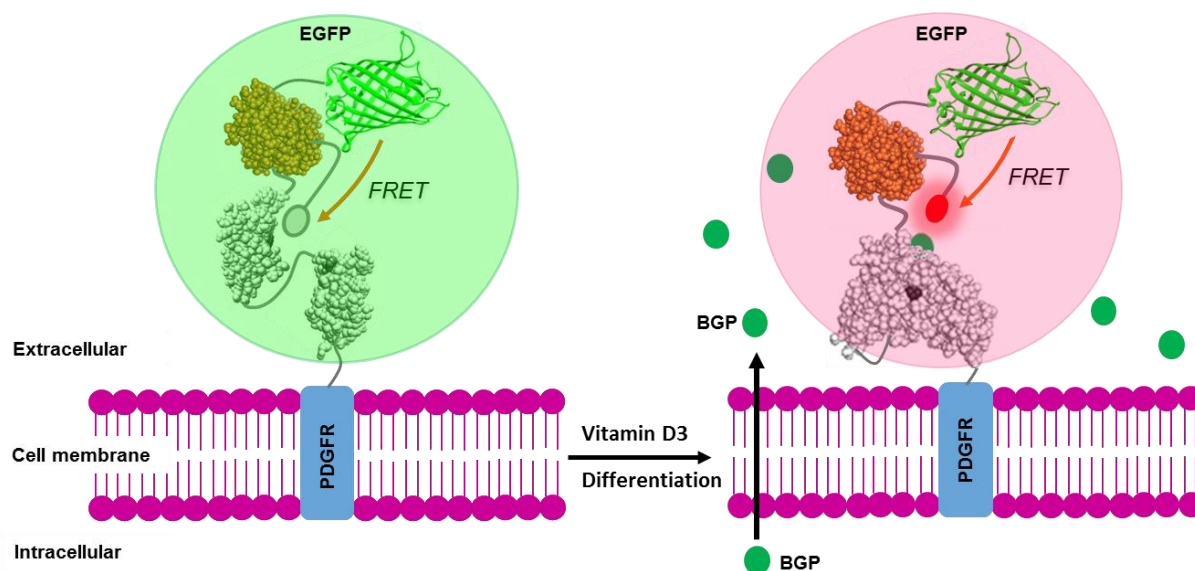


Figure 1-15. Detection of BGP secreted by osteosarcoma U2OS cells during differentiation to osteoblasts. Anti-BGP scFv fused with EGFP and SNAP tag was expressed and incorporated on the membrane of U2OS cells. Expressed EGFP-SNAP-scFv is labeled by fluorophore-SNAP ligand. Without BGP, fluorescence ratio of fluorophore/EGFP is low because of quenching of fluorophore. When U2OS cells are induced to differentiate to osteoblast, they secrete BGP to extracellular environment. Binding of BGP to EGFP-SNAP-scFv results in fluorescence enhancement of fluorophore, and as consequence, enhancement of fluorescence ratio.

1-5 References

- (1) Förster T. Zwischenmolekulare Energiewanderung und Fluoreszenz. *Annalen der Physik* **437**: 55-75 (1948)
- (2) Shimomura O., Johnson F. H., Saiga Y., *J. Cell. Comp. Phys.* **59**(3): 223-239 (1962)
- (3) Shaner N. C., Steinbatch P. A., Tsien R. Y. A guide to choosing fluorescent proteins. *Nat. Methods* **2**(12): 905-909 (2005)
- (4) Baird G. S., Zacharias D. A., Tsien R. Y., Circular permutation and receptor insertion within green fluorescent proteins. *Proc. Natl. Acad. Sci. USA* **96**(20): 11241-11246 (1999)
- (5) Ozawa T., Yoshimura H., Kim S.B. Advances in fluorescence and bioluminescence imaging. *Anal. Chem.* **85**(2): 590-609 (2013)
- (6) Piatkevich K. D., Subach F. V., Verkhusha V. V., Engineering of bacterial phytochromes for near-infrared imaging, sensing, and light-control in mammals. *Chem. Soc. Rev.* **42**(8): 3441–3452 (2013)
- (7) Van de Horst M. A., Hellingwerf K. J. Photoreceptor proteins, “star actors of modern times”: a review of the functional dynamics in the structure of presentative members of six different photoreceptor families. *Acc. Chem. Res.* **37**:13-20 (2004)
- (8) Kumagai A., Ando R., Miyatake H., Greimel P., Kobayashi T., Hiabiayashi Y., Shimogori T., Miyawaki A. A bilirubin-inducible fluorescent protein form eel muscle. *Cell* **153**(7): 1602-1611 (2013)
- (9) Abe R., Ohashi H., Iijima I., Ihara M., Takagi H., Holsaka T., Ueda H. “Quenchbodies”: Quench-based antibody probes that show antigen-dependent fluorescence. *J. Am. Chem. Soc.* **133**: 17386-17394 (2011)
- (10) Takaoka Y., Ojida A., Hamachi I. Protein organic chemistry and applications for labeling and engineering in live-cell systems. *Angew. Chem. Int. Ed.* **53**: 4088-4106 (2013)
- (11) Griffin B. A., Adams S. R., Tsien R. Y. Specific covalent labeling of recombinant protein molecules inside live cells. *Science* **281**(5374): 269-272 (1998)
- (12) Adams S. R., Campbell R. E., Gross L. A., Martin B. R., Walkup G. K., Yao Y., Llopis J., Tsien R. Y. New biarsenical ligands and tetracysteine motifs for protein labeling in vitro and in vivo: synthesis and biological applications. *J. Am. Chem. Soc.* **124**(21): 6063-6076 (2002)

- (13) Adams S. R., Tsien R. Y. Preparation of the membrane-permeant biarsenicals FIAsh-EDT2 and ReAsH-EDT2 for fluorescent labeling of tetracysteine-tagged proteins. *Nat. Protoc.* **3**(9): 1527-1534 (2008)
- (14) Noren C. J., Anthony-Cahill S. J., Griffith M.C., Schultz P. G. A general method for site-specific incorporation of unnatural amino acids into proteins. *Science* **244**: 182-188 (1989)
- (15) Anthony-Cahill S. J., Griffith M. C., Noren C. J., Suich D. J., Schultz P. G. Site-specific mutagenesis with unnatural amino acids. *Trends, Biochem. Sci.* **14**: 400-403 (1989)
- (16) Bain J. D. Glabe C. g., Dix T.A., Chamberlin A. R. Biosynthetic site-specific incorporation of a non-natural amino acid into a polypeptide. *J. Am. Chem. Soc.* **111**: 8013-8014 (1989)
- (17) Hecht S. M., Alford B. L., Kuroda Y., Kitano S. "Chemical aminoacylation: of tRNA's. *J. Biol. Chem.* **253**: 4517-4520 (1978)
- (18) Heckler T. G., Chang L. H. Zama Y., Naka T., Chorghade M. S., Hecht S. M. T4 RNA ligase mediated preparation of novel "chemically misacylated" tRNA^{Phe}s. *Biochemistry* **23**: 1468-1473 (1984)
- (19) Schmied W.H., Elsässer S.J., Uttamapinant C. Chin J. W. Efficient multisite unnatural amino acid incorporation in mammalian cells via optimized pyrrolysyl tRNA synthetase/tRNA expression and engineered eRF1. *J. Am. Chem. Soc.* **136**(44): 15577-15583 (2014)
- (20) Hohsaka T., Kajihara D., Ashizuka Y., Murakami H., Sisido M. Efficient incorporation of non-natural amino acids with large aromatic groups into streptavidin in in vitro protein synthesizing systems. *J. Am. Chem. Soc.* **121**: 34-40 (1999)
- (21) Hohsaka T., Ashizuka Y., Taira H., Murakami H., Sisido M. Incorporation of non-natural amino acids into proteins by using various four-base codons in an Escherichia coli in vitro translation system. *Biochemistry* **40**: 11060-11064 (2001)
- (22) Kajihara D., Abe R., Iijima I., Komiyama C., Sisido M., Hohsaka T. FRET analysis of protein conformational change through position-specific incorporation of fluorescent amino acids. *Nature Methods* **3**(11): 923-929 (2006)
- (23) Johnson A.E., Woodward W. R., Herbert E., Menninger J. R., N epsilon-acetyllysine transfer ribonucleic acid: a biologically active analogue of aminoacyl transfer ribonucleic acids. *Biochemistry* **15**: 569-575 (1976)

- (24) Crowley K. S., Liao S., Worrell V. E., Reinhart G. D., Johnson A.E. Secretory proteins move through the endoplasmic reticulum membrane via an aqueous, gated pore. *Cell* **78**: 461-471 (1994)
- (25) Kreig U. C., Walter P., Johnson A. E. Photocrosslinking of the signal sequence of nascent preprolactin to the 54-kilodalton polypeptide of the signal recognition particle. *Proc. Natl. Accad. Sci. USA* **83**: 8604-8608 (1986)
- (26) Beene D. L., Dougherty D. A., Lester H. A. Unnatural amino acid mutagenesis in mapping ion channel function. *Curr. Opin. Neurobiol.* **13**(3): 264-270 (2003)
- (27) Lummis S. C., Beene D. L. Lee L.W., Lester H. A. Broadhurst R. W., Dougherty D. A. Cis-trans isomerization at proline opens the pore of a neurotransmitter-gated ion channel. *Nature* **438**(7065): 248-252 (2005)
- (28) Wang L., Brock A., Herberich B., Schultz P. G. Expanding the genetic code of *Escherichia coli*. *Science* **292**: 498-500 (2001)
- (29) Xie J., Schultz P.G. An expanding genetic code. *Methods* **36**: 227-238 (2005)
- (30) Polycarpo C. R., Herring S., Bérubé A., Wood J. L., Söll D., Ambrogelly A. Pyrrolysine analogues as substrates for pyrrolysyl-tRNA synthetase. *FEBS Lett.* **580**(28-29): 6695-6700 (2006)
- (31) Yanagisawa T., Ishii R., Fukunaga R., Kobayashi T., Sakamoto K., Yokoyama S. Multistep engineering of pyrrolysyl-tRNA synthetase to genetically encode N(epsilon)-(o-azidobenzyloxycarbonyl) lysine for site-specific protein modification. *Chem. Biol.* **24**; 15(11): 1187-1197 (2008)
- (32) Nguyen D.P., Elliott T., Holt M., Muir T. W., Chin J. W. Genetically encoded 1,2-aminothiols facilitate rapid and site-specific protein labeling via a bio-orthogonal cyanobenzothiazole condensation. *J. Am. Chem. Soc.* **113**: 11418-11421 (2011)
- (33) Mukai T., Kobayashi T., Hino N., Yanagisawa T., Sakamoto K., Yokoyama S. Adding l-lysine derivatives to the genetic code of mammalian cells with engineered pyrrolysyl-tRNA synthetases. *Biochem. Biophys. Res. Commun.* 371(4): 818-822 (2008)
- (34) Ninomiya K., Minohata T., Nishimura M., Sisido M. In situ chemical aminoacylation with amino acid thioesters linked to a peptide nucleic acid. *J. Am. Chem. Soc.* **126**: 15984-15989 (2004)
- (35) Hashimoto N., Ninomiya K., Endo T., Sisido M. Simple and quick chemical aminoacylation of tRNA in cationic micellar solution under ultrasonic agitation. *Chem. Commun. (Camb)* 4321-4323 (2005)

- (36) Taira H., Matsushita T., Kojima K., Shiraga K., Hohsaka T. Comprehensive screening of amber suppressor tRNAs suitable for incorporation of non-natural amino acids in a cell-free translation system. *Biochem. Biophys. Res. Commun.* **19**; 374(2)304-308 (2008)
- (37) Niu W., Schultz P.G., Guo J. An expanded genetic code in mammalian cells with a functional quadruplet codon. *ACS Chem. Biol.* **19**; 8(7): 1640-1645 (2013)
- (38) Wang K., Sachdeva A., Cox D. J., Wilf N. W., Lang K., Wallace S., Mehl R. A., Chin J. W. *Nature Chemistry* **6**: 393-403 (2014)
- (39) Wang L., Schultz P.G. Expanding the genetic code. *Angew. Chem. Int. Ed.* **44**: 34-66 (2005)
- (40) Wu X., Schultz P.G. Synthesis at the interface of chemistry and biology. *J. Am. Chem. Soc.* **131**: 12497-12515 (2009)
- (41) Hohsaka T., Sisido M. Incorporation of non-natural amino acids into proteins. *Curr. Opin. Chem. Biol.* **6**(6): 809-815 (2002)
- (42) Iijima I., Hohsaka T. Position-specific incorporation of fluorescent non-natural amino acids into maltose-binding protein for detection of ligand binding by FRET and fluorescence quenching. *Chem. Bio. Chem.* **10**: 999-1006 (2009)
- (43) Lang K., Chim J. W. Cellular incorporation of unnatural amino acids and biorthogonal labeling of proteins. *Chem. Rev.* **114**: 4764-4806 (2014)
- (44) Nagai T., Sawano A., Park E. S., Miyawaki A. Circular permuted green fluorescent proteins engineered to sense Ca²⁺. *Proc. Natl. Acad. Sci. USA* 98(6): 3197-3202 (2001)
- (45) Nagai T., Yamada S., Tominaga T., Ichikawa M., Miyawaki A. Expanded dynamic range of fluorescent indicators for Ca²⁺ by circular permuted yellow fluorescent proteins. *Proc. Natl. Acad. Sci. USA* 101(29): 10554-10559 (2004)
- (46) Gong Y. The evolving capabilities of rhodopsin-based genetically encoded voltage indicators. *Curr. Opin. Chem Biol.* **27**: 84-89 (2015)
- (47) Los G. V., Encell L.P., McDougall M. G., Hartzell D.D., Karassina N., Zimprich C., Wood M. G., Learish R., Ohana R. F., Urh M., Simpson D., Mendez J., Zimmerman K., Otto P., Vidugiris G., Zhu J., Darzins A., Klaubert D. H., Bulleit R. F., Wood K.V. HaloTag: A novel protein labeling technology for cell imaging and protein analysis. *ACS Chem. Biol.* **3**(6): 373-382 (2008)
- (48) England C. G., Luo H., Cai W. HaloTag technology: a versatile platform for biomedical application. *Bioconjugate Chem.* **26**: 975-986 (2015)

- (49) Juillerat A., Gronemeyer T., Keppler A., Gendreizig S., Pick H., Vogel H., Johnsson K. Direct evolution of O6-alkylguanine-DNA alkyltransferase for efficient labeling of fusion proteins with small molecules in vivo. *Chem. Biol.* **10**: 313-317 (2003)
- (50) Keppler A., Gendreizig S., Gronemeyer T., Pick H., Vogel H., Johnsson K. A general method for the covalent labeling of fusion proteins with small molecules in vivo. *Nat. Biotechnol.* **21**: 86-89 (2003)
- (51) Gautier A., Juillerat A., Heinis C., Corrêa Jr.I.R., Kindermann M., Beaufils F., Johnsson K. An engineered protein tag for multiprotein labeling in living cells. *Chem. Biol.* **15**: 128-136 (2008)
- (52) Lakowicz J. R. *Principles of Fluorescence Spectroscopy*, 3rd edition (Springer, New York) (2006)
- (53) Arai Y., Nagai T. Extensive use of FRET in biological imaging. *Microscopy (Tokyo)* **62**(4): 419-428 (2013)
- (54) Imamura H., Huynh Nhat K.P., Togawa H., Saito K., Iino R., Kato-Yamada Y., Nagai T., Noji H. Visualization of ATP levels inside single living cells with fluorescent resonance energy transfer-based genetically encoded indicators. *Proc. Natl. Acad. Sci. USA* **106**(37): 15651-15656 (2009).
- (55) Schena A., Griss R., Johnsson K. Modulating protein activity using tethered ligands with mutually exclusive binding sites. *Nat. Commun.* **6**:7830 (2015)
- (56) Michalet X., Weiss S., Jäger M. Single-molecule fluorescence studies of protein folding and conformational dynamics. *Chem. Rev.* **106**(5): 1785-1813 (2006)
- (57) Torimura M., Kurata S., Yamada K., Yokomaku T., Kamagata Y., Kanagawa T., Kurame R., Fluorescence-Quenching phenomenon by photoinduced electron transfer between a fluorescent dye and a nucleotide base. *Anal. Sci.* **17**:155–160 (2001)
- (58) Knemeyer J. P. Sauer M., Wolfrum J. Inter- and Intramolecular Fluorescence Quenching of Organic Dyes by Tryptophan. *Bioconjugate Chem* **14**: 1133-1139 (2003)

Chapter 2

Antibody-based fluorescent and fluorescent ratio biosensors for detection of phosphotyrosine

2-1 Introduction

Protein phosphorylation is an important post-translational process which affects protein structure and function. In mammalian cells, serine (Ser), threonine (Thr) and tyrosine (Tyr) are phosphorylated in response to extracellular stimuli. For example, in signal transduction the autophosphorylation of Tyr in epidermal growth factor (EGF) receptor upon binding of EGF activates a kinase cascade that relays the signal to the transcriptional apparatus in the nucleus which then triggers cell growth and differentiation. Abnormal protein phosphorylation may cause pathogenesis or even carcinogenesis. Therefore, methods for studies of protein phosphorylation are very important in not only fundamental biology but also biomedical applications.

To study protein phosphorylation kinases and phosphatases activities, genetically-encoded fluorescent indicators for protein phosphorylation have been developed. Fluorescence resonance energy transfer (FRET)-based indicators consists of a substrate domain specific for the kinase of interest linked with a phosphorylation recognition domain through a flexible linker and sandwiched by cyan and yellow fluorescent proteins (CFP and YFP, respectively). Phosphorylation of substrate domain and binding of substrate domain to recognition domain generate a large conformational change of the indicator which alter the distance and/or relative orientation of CFP and YFP, induced increase in FRET signals. In contrast, dephosphorylation of substrate domain decreases FRET signals (Figure 2-1A). The indicators are applicable to real-time monitoring protein phosphorylation and dephosphorylation in live cells¹⁻⁴. Alternatively, a phosphorylation-mediated assembly of semisynthetic GFP-based biosensor for protein kinases has recently reported. The biosensor consists of S-peptide fused with 10th β -strand of GFP (s10) and a kinase substrate peptide. Phosphorylation of the substrate peptide by kinase can protect s10 from cleavage by carboxypeptidase Y (CPY). Binding of s10 to truncated GFP (tGFP, lack of s10) results in an intact GFP which fluoresces. If peptide is not phosphorylated, S-peptide is degraded by CPY and no fluorescence is observed (Figure 2-1B). The biosensor has demonstrated high sensitivity in analysis of kinase and phosphatase activities *in vitro*⁵.

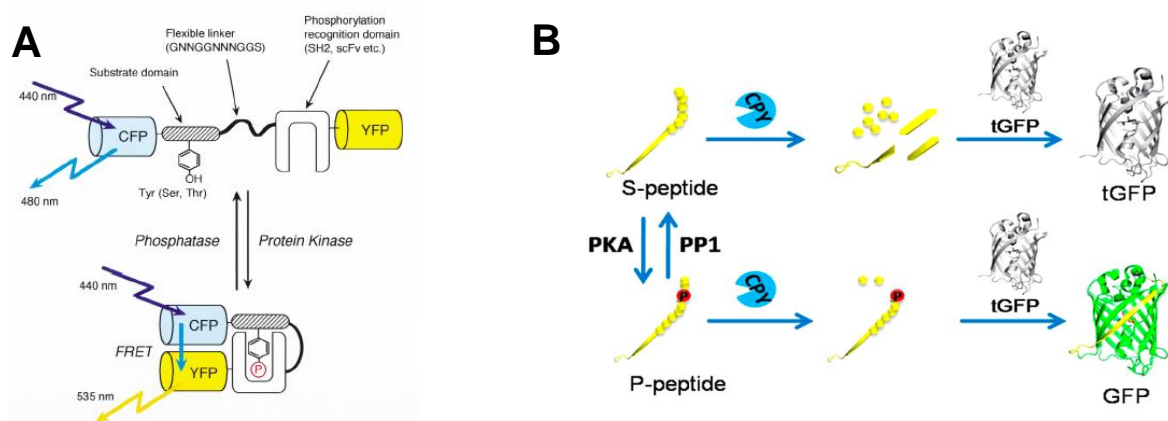


Figure 2-1. Genetically-encoded fluorescent indicators for protein phosphorylation. **(A)** Schematic illustration of the indicator named “phocus”, the phosphorylation and dephosphorylation of substrate domain was converted to FRET signals between CFP and YFP (*Nat. Biotechnol.* **20**: 287-294 (2002)). **(B)** Principle of phosphorylation-mediated assembly of semisynthetic GFP-based biosensor for protein kinases (*Anal. Chem.* **87**: 6311-6318 (2015)).

Another method for studying protein kinase is analyzing the phosphorylation of substrate proteins of kinases. Although above indicators successfully monitor kinases activities, they cannot directly detect naturally occurred phosphorylated proteins. Most of strategies for detection of phosphorylated proteins are based on immunoassay recruiting antibodies specific for phosphorylation sites by Western blotting or *in situ* labeling of phosphorylated molecules by immunohistochemistry on a tissue section⁶⁻¹⁰. The use of antibodies allows us to detect various phosphorylated antigens; however, it requires tedious and time-consuming process. In addition, it is difficult to detect antigens in a real-time manner.

Ohiro and co-workers have reported a fluorescent biosensor for homogeneous competitive immunoassay for detection of phosphorylated protein based on enhanced FRET technology. The enhanced FRET has a characteristic that FRET efficiency is significantly enhanced by interaction of leucine zippers (Lzip) which are tethered with donor and acceptor fluorescent proteins. In this system, the extracellular signal-regulated kinase (ERK) is employed as a model antigen. A synthetic diphosphorylated peptide that mimics the regulatory site of ERK is linked to donor FRET probe (ECFP-Lzip) and an anti-diphosphorylated ERK antibody fragment (Fab) is linked to acceptor FRET probe (EYFP-Lzip). The indicator exhibits high FRET signal in the absence of antigen, but FRET signal decreases in the presence of antigen due to the competitive binding of diphosphorylated ERK to antibody (Figure 2-2A). *In vitro*

assay using this indicator allows detection of diphosphorylated ERK in the range from 15 nM to 250 nM (Figure 2-2B)¹¹. Although this strategy is potentially available for detection of various phosphorylated antigens, the preparation procedure is complicated and it requires careful design of the synthetic phosphorylated peptide so that the binding affinity of antibody-synthetic peptide must be lower than that of antibody-antigen.

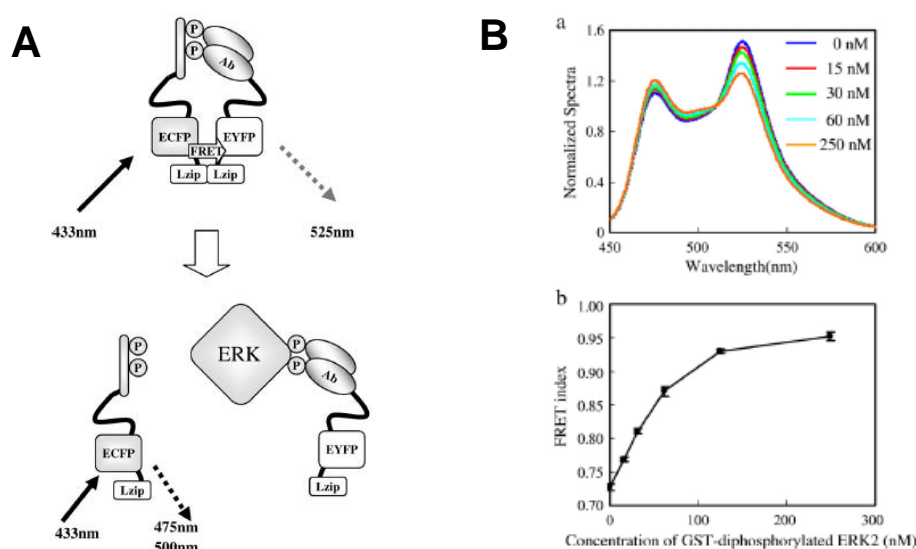


Figure 2-2. (A) Principle of the competitive immunoassay for phosphorylated protein antigen. (B) Assay for diphosphorylated ERK, (a) Fluorescence spectra show decrease in FRET signal upon addition of Glutathione-S-transferase (GST)-fused diphosphorylated ERK, (b) Dose-response curve for GST-diphosphorylated ERK (*J. Biosci. Bioeng.* **109**(1): 15-19 (2010)).

To develop a simple and widely-applicable fluorescent biosensor for protein phosphorylation, the synthesis of fluorescent biosensor utilizing “Quenchbody” (Qbody) technology¹² is introduced in this chapter. An anti-phosphotyrosine antibody single-chain variable domain (scFv) was fluorescently labeled at the N-terminus by incorporating a 5(6)-carboxytetramethylrhodamine (TAMRA)-linked nonnatural amino acid in response to a four-base codon CGGG¹³⁻¹⁴ (Figure 2-3). The biosensor showed fluorescence enhancement upon addition of peptides containing phosphotyrosine (pTyr).

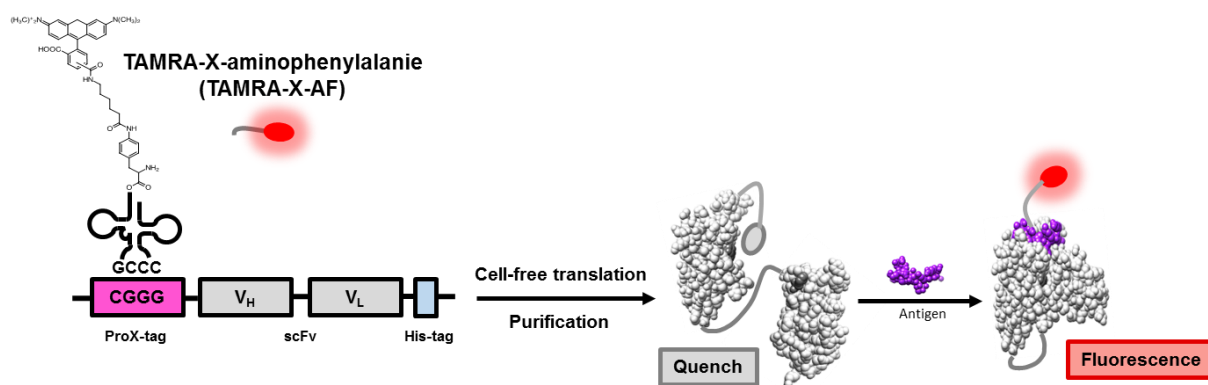


Figure 2-3. Schematic illustration of the synthetic procedure of TAMRA-scFv against pTyr and the detection of pTyr-containing antigen based on antigen-dependent removal of fluorescence quenching effect on TAMRA.

In the second part of this chapter, I attempt to construct fluorescent ratio biosensors in combination of FRET and Qbody technologies. Although Qbody is a powerful method for constructing of simple and sensitive biosensor, fluorescence intensity of single labeled Qbody is also dependent on the amount of this biosensor in measuring sample. It is a difficulty in the application of this technique to detection of antigens in the cells where the local concentration of the biosensor cannot be controlled. Therefore, double labeled scFv was developed and the change in fluorescence of this biosensor was based on FRET and fluorescent quenching. The scFv was labeled at C-terminus by TAMRA and fused at either N- and C-terminus with EGFP (enhanced green fluorescent protein) (Figure 2-4) or HaloTag which was subsequently labeled by a 5(6)-RhodamineGreen-linked HaloTag ligand. An expected mechanism for detection of antigen using double labeled scFv is as follows: double labeled scFv exhibits FRET from EGFP or RhodamineGreen (RhG) to TAMRA because emission spectra of EGFP and RhG overlap with absorption spectrum of TAMRA. However, fluorescence of TAMRA is quenched in the absence of antigen. As consequence, the biosensor mainly emits green fluorescence. In the presence of antigen, the quenching effect is eliminated and the biosensor emits both green and red fluorescence.

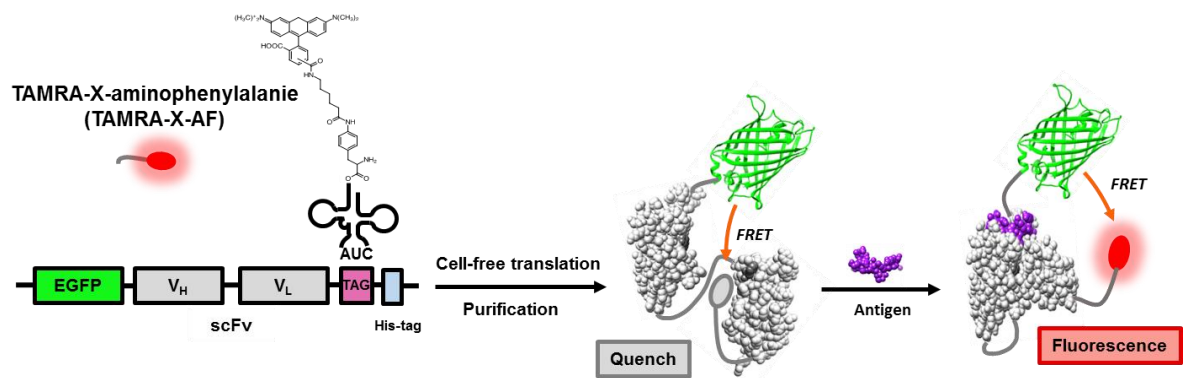


Figure 2-4. Schematic illustration of the synthetic procedure of double labeled scFv against pTyr in which EGFP was fused to N-terminus of scFv and the detection of pTyr-containing antigen based on FRET from EGFP to TAMRA and antigen-dependent removal of fluorescent quenching effect on TAMRA.

2-2. Materials and Methods

2-2-1. Materials

KOD-Plus DNA polymerase, Thermo T7 RNA polymerase were purchased from TOYOBO (Osaka, Japan). Primers for PCR were custom synthesized by Invitrogen (Life technologies Japan). QIAquick PCR purification kit, QIAquick gel extraction kit were purchased from QIAGEN (Venlo, Netherlands). pGEMEX1, MagneHis Ni-particles, *E. coli* S30 extract for linear templates, HaloTag Amine (O₂) were from Promega (WI, USA). In-Fusion HD Cloning kit was from Clontech (CA, USA). T4 RNA ligase was obtained from TaKaRa Bio (Otsu, Japan), *Nde*I, *Hind*III restriction enzymes, Quick Ligase, Prestained protein marker (7-175 kDa) and T7 RNA polymerase were from New England BioLabs (MA, USA), Zeba desalting spin columns (7K MWCO) were from ThermoFisher Scientific (MA, USA), EGF receptor substrate 2 (Phospho-Tyr⁵), insulin receptor (1142-1153) (Phospho-Tyr^{1146,1150,1151}) were obtained from GenScript (NJ, USA), pp60^{src} SH2 domain-binding peptide (Ac-pTyr-Glu-Glu-Ile-Glu-OH) was from Bachem (Bubendorf, Switzerland), pFN18A Halo Tag® (WI, Promega) was a kind gift from Prof. Masaru Kawakami (Yamagata University).

2-2-2. Construction scFv(pTyr) genes

cDNA sequences of heavy chain and light chain of anti-pTyr antibody 4G10 was obtained from the National Center for Biotechnology Information USA (NCBI) Nucleotide database¹⁵. Accession number for heavy chain is DD058293.1 and accession number for light chain is DD058294.1. The original sequences of anti-pTyr antibody from database are heavy chain (V_H): 1365 base pairs and light chain (V_L): 645 base pairs. The sequence of scFv against BGP (scFv(BGP)) in Qbody¹² was used as reference for designing of scFv against pTyr (scFv(pTyr)). Alignment of amino acid sequences of scFv(BGP) and scFv(pTyr) was performed by “T-Coffee”¹⁶⁻¹⁷ and “ESPrpt 3.0”¹⁸. The sequence from base 1 to 354 of V_H and the sequence from base 1 to 324 of V_L was linked by a (Gly₄Ser)₃ linker to make scFv(pTyr), All codons encoded for arginine was modified to be different from CGG. The N- and C-termini of scFv(pTyr) were fused with ProX-tag containing a four-base codon (5'-ATG TCT AAA CAA ATC GAA GTA AAC CGGG TCT AAT GAG-3') and His₆-tag, respectively. The scFv(pTyr) gene was custom synthesized by Biomatik (DE, USA), amplified for incorporation of *Nde*I and *Hind*III restriction sites respectively to N- and C-termini by PCR with forward primer (5'-GGA ATT CCA TAT GTC TAA ACA AAT CGA AG-3') and reverse primer (5'-CCC AAG CTT AAT GAT GAT GAT GAT GAT GAG-3'). The PCR product was purified

by QIAquick PCR purification kit and digested by the restriction enzymes. The digested DNA fragments were introduced into pre-digested pGEMEX1 between T7 promoter and T7 terminator by Quick Ligase.

The incorporation of linker (Gly₃Ser)₃ between ProX-tag and scFv(pTyr) was done by separately amplification of (Gly₃Ser)₃ and pGEMEX1 containing ProX-scFv(pTyr). After purification, the (Gly₃Ser)₃ was introduced between ProX-tag and scFv(pTyr) by In-Fusion HD cloning kit yielding ProX-(GGGS)₃-scFv(pTyr). The insertion of (Gly₃Ser)₅ linker between ProX-tag and scFv(pTyr) was performed by Quickchange mutagenesis with primers containing (Gly₃Ser)₂ and ProX-(GGGS)₃-scFv(pTyr) as template. The DNA sequences of all constructs were confirmed by DNA sequencing.

The encoding regions of ProX-(GGGS)_x-scFv(pTyr) genes were amplified by PCR with forward primer (5'-CCC GCG CGT TGG CCG ATT CA-3') and reverse primer (5'-CCG GAT AAC CTG GCG TAA TA-3'). The PCR product was purified and transcribed with Thermo T7 RNA polymerase as described before¹³.

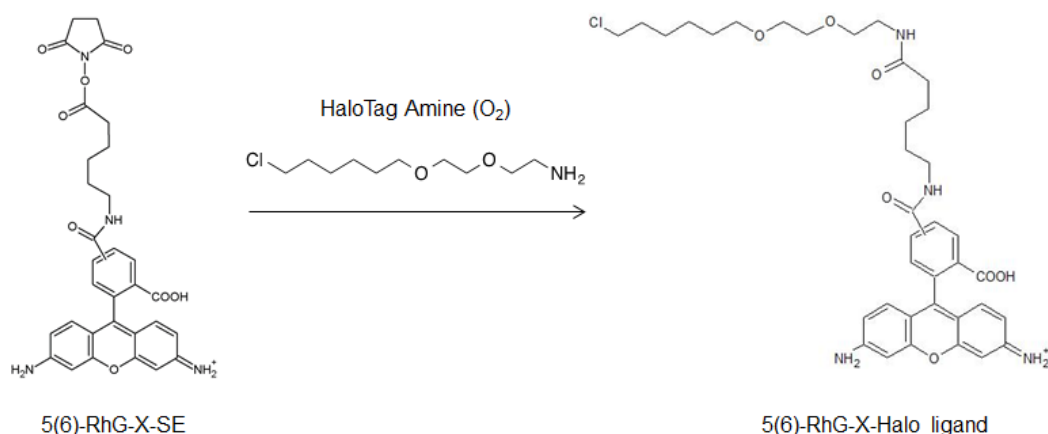
2-2-3. Construction of double labeled scFv(pTyr) genes

The cDNA of EGFP variant (F64L, S65T, Q80R, F99S, M153T, V163A, I167T, and S208L) was amplified by PCR with forward primer (5'-GAA GGA GAT ATA CAT ATG AGT AAA GGA GAA GAA CTT TTC ACT GGA GTT GTC CC-3') and reverse primer (5'-GCT GCA GCT GGA CCT CTT TGT AGA GCT CATCCA TGC CAT GTG TAA TCC CAG C-3') for fusion of EGFP to N-terminus of scFv(pTyr). For the fusion of EGFP to C-terminus of scFv(pTyr), the forward primer (5'-GGT GGC GGT GGC TAG AGT AAA GGA GAA GAA CTT TTC ACT GGA GTT GTC C-3') and the reverse primer (5'-ATA GAA TAC TCA AGC TTA GTG GTG GTG GTG GTG TTT GTA GAG CTC ATC-3') were used. The plasmid pGEMEX1 containing scFv(pTyr) linked with amber codon (TAG) at C-terminus through Gly₄ or Gly₃SerGly₄ linker (scFv(pTyr)-G₄-TAG or scFv(pTyr)-G₃SG₄-TAG) was amplified by PCR with forward primer (5'-GAG GTC CAG CTG CAG CAG TCT GGA CCT GAA CTG G-3') and reverse primer (5'-ATG TAT ATCT CCT TCT TAA AGT TAA ACA AAA TTA TTT C-3') for incorporation of EGFP to N-terminus. For incorporation of EGFP to C-terminus, the forward primer (5'-GCT TGA GTA TTC TAT AGT GTC ACC TAA ATC CCA GC-3') and reverse primer (5'-CTA GCC ACC GCC ACC TGA ACC GCC ACC ACG TTT G-3') were used. The resulting PCR products were purified by gel extraction from agarose gel. The plasmid and EGFP PCR products were joined by In-Fusion cloning to introduce EGFP to either N- or C-termini of scFv(pTyr). Similar procedure was performed for fusion with HaloTag to

make pGEMEX-Halo-scFv(pTyr)-G₃SG₄-TAG. The forward and reverse primers for amplification of HaloTag were 5'-GAA GGA GAT ATA CAT ATG GCA GAA ATC GGT ACT GGC TTT CCA TTC GAC C-3' and 5'-CTG CAG CTG GAC CTC GCC GGA AAT CTC GAG CGT CGA CAG CCA GCG CGC G-3', respectively. The DNA sequences of all constructs were confirmed by DNA sequencing.

2-2-4. Synthesis of RhodamineGreen-linked HaloTag ligand

To a mixture of 50 mM DMSO solution of 5(6)-RhodamineGreen-X-succinimide ester (5(6)-RhG-X-SE) (8 μ L, 400 nmol), 100 mM DMSO solution of HaloTag Amine (O₂) (2 μ L, 200 nmol) and 100 mM NaHCO₃aq (4 μ L) were added. The mixture was kept on ice for 60 min, and applied to an analytical scale reversed-phase HPLC (XBridge, 2.5 μ m, 4.6x20 mm, flow rate 1.5 ml/min, with a linear gradient of 0-100% methanol in 0.38% formic acid, over 10 min) to afford RhG-X-Halo ligand (188 nmol; 94% yield). The product was confirmed by MALDI-TOF MS (calcd. 693.30 for MH⁺, found 693.34).



Scheme 2-1. Synthetic scheme of RhG-X-Halo ligand

2-2-5. Cell-free translation

The synthesis of TAMRA-X-AF-tRNA_{CCCG} by ligating TAMRA-X-AF-pdCpA with a yeast phenylalanine tRNA_{CCCG} (lacking the 3'-terminal two nucleotides C and A (-CA)) that contained a CCCG anticodon was carried out as described before¹³. The reaction mixture (93.6 μ L) contained 2.3 nmol tRNA_{CCCG}, 6.8 nmol TAMRA-X-AF-pdCpA, 55 mM HEPES-Na (pH 7.5), 1 mM ATP, 15 mM MgCl₂, 3.3 mM DTT, 0.002% BSA and 112.4 units T4 RNA ligase.

After incubation of 2 hours at 4°C, potassium acetate (pH 4.5) was added to the reaction to final concentration 0.3 M. The TAMRA-X-AF-tRNA_{CCCG} was isolated by ethanol precipitation and the pellet was dissolved with 12 µL pre-chilled 1 mM potassium acetate (pH 4.5). TAMRA-X-AF-tRNA_{CUA} was prepared in a similar manner using an amber suppressor tRNA_{CUA} derived from *Mycoplasma capricolum* tryptophan tRNA¹⁹.

Coding regions of scFv fusions were amplified by PCR and the PCR products were purified by QIAquick PCR purification kit. The transcription to mRNA was performed as described before¹³.

To incorporate TAMRA-X-AF into scFvs, a 120 µL cell-free translation mixture was prepared with 55 mM HEPES-KOH (pH 7.5), 210 mM GluK, 6.9 mM CH₃COONH₄, 12 mM (CH₃COO)₂Mg, 1.2 mM ATP, 0.28 mM GTP, 26 mM phosphoenolpyruvate, 1 mM spermidine, 1.9% PEG-8000, 35 µg/ml folinic acid, 0.1 mM of each of the 19 natural amino acid except arginine, 0.01 mM arginine, 2 mM glutathione oxidized, 0.8 µg/µL mRNA, 2.3 nmol TAMRA-X-AF-tRNA_{CCCG} (or TAMRA-X-AF-tRNA_{CUA}) and 24 µL *E. coli* S30 extract. The mixture was incubated at 37°C for 1 hour.

For HaloTag-containing protein, after protein was synthesized by cell-free translation, DMSO solution of RhG-X-Halo ligand was added to the crude translation mixture to final concentration 50 µM and incubated at 25°C for 30 minutes to achieve fluorescent labeling of HaloTag with RhG.

2-2-6. Protein purification

The translation mixture was diluted with buffer A (20 mM sodium phosphate, 0.5M NaCl, 5 mM imidazole, pH 7.5) containing 10M urea to final volume 480 µL and mixed with 48 µL MagneHis Ni-Particles. After shaking for 30 minutes at room temperature, the supernatant was removed and the beads were washed once with buffer A, once with buffer A containing 8 M Urea and followed by three times with buffer A. The His-tagged protein was eluted by buffer B (20 mM sodium phosphate, 0.5M NaCl, 500 mM imidazole, pH 7.5) and was gel-filtrated by Zeba Spin Desalting column (7K MWCO) equilibrated with phosphate buffer saline containing 0.05% Tween (PBS-T). For EGFP-fused scFvs, buffer A containing 4 M urea was used for dilution of the translation mixture and for second wash step.

Samples for SDS-PAGE were taken at each purification step and mixed with SDS-PAGE sample buffer to final volume 20 µL. All samples were heated at 95°C for 5 min before SDS-PAGE. 5 µL of each sample and Prestained protein marker were applied to 15% SDS-PAGE gel. In case of EGFP and Halo-tag fusions, 12% polyacrylamide gel was used. SDS-

PAGE gel was visualized by a fluorescence scanner (FMBIO-III; Hitachi Software Engineering, Japan). RhG was excited at 488 nm and visualized at 520 nm, and TAMRA was excited at 532 nm and visualized at 580 nm. Prestained marker was visualized with excitation at 635 nm and detection at 670 nm.

2-2-7. Fluorescence measurement

The purified TAMRA-labeled scFv was diluted in PBS-T buffer to 80 μ L with various final concentrations (0 M, 10^{-9} M, 10^{-8} M, 10^{-7} M, 10^{-6} M, 10^{-5} M, 10^{-4} M) of pTyr-containing peptides, EGF receptor substrate 2 (ERS-pTyr), insulin receptor substrate (IRS), and pp60^{src} SH2 domain-binding peptide (Ac-pYEEIE). The mixture was incubated at 25°C for 12 hours.

The emission spectra were measured by a Fluorolog-3 instrument (Horiba, Japan) at 25°C. TAMRA was excited at 550 nm and emission was recorded from 565 nm to 700 nm. In case of double labeled scFvs with EGFP, EGFP was excited at 470 nm and emission was scanned from 490 nm to 700 nm. In cases of double labeled scFvs with HaloTag and RhG-X-Halo ligand, RhG was excited at 495 nm and emission was scanned from 510 nm to 700 nm. Fluorescence intensities of TAMRA, EGFP, and RhG was obtained at 580 nm, 509 nm, and 529 nm, respectively, and fluorescence ratio (accepter/donor) was calculated using these values.

The apparent dissociation constant (K_d) was calculated by fitting the fluorescence intensity or fluorescence ratio values to a sigmoidal dose-response (variable slope) model using Graphpad Prism (Graphpad, CA, USA). All data were normalized by the value in the absence of antigen.

2-3 Results and discussion

2-3-1. Synthesis of TAMRA-labeled scFv(pTyr)

To construct a fluorescent biosensor for detection of phosphorylated proteins, an anti-phosphotyrosine monoclonal antibody 4G10^{15, 20} was employed since it has been isolated and characterized, moreover, its amino acid sequence can be obtained from the Nucleotide databank. The anti-pTyr has three Trp residues on V_H (Trp36_H, Trp47_H, and Trp103_H using the Kabat numbering scheme) and two Trp residues on V_L (Trp35_L and Trp47_L). These Trp residues except Trp47_L are conserved among various IgGs, and could contribute to the antigen-dependent quenching effect as in the cases of previously developed Quenchbodies. The TAMRA-labeled scFv(pTyr) was designed with reference to the existing scFv against BGP¹². According to the result of amino acid alignment of anti-BGP and anti-pTyr, the sequence from amino acid 1 to 118 terminated at conserved residues TVSS and the sequence from amino acid 1 to 113 terminated at KLEIKR were chosen for heavy chain (V_H) and light chain (V_L), respectively (Figure 2-5). The V_H and V_L fragments were joined by a flexible linker (Gly₄Ser)₃ and fused at N-terminus with ProX-tag carrying a four-base codon to yield ProX-scFv(pTyr). The sequence of ProX-tag (ATG TCT AAA CAA ATC GAA GTA AAC CGGG TCT AAT GAG) has been designed so that if the four-base codon is recognized by an Arg-tRNA_{CCG}, the downstream stop codon (TAA) terminates the translation process. At the C-terminus of scFv, His₆-tag was fused for purification. In addition, flexible peptide linkers (Gly₃Ser)_n (n = 3 or 5) were introduced between ProX-tag and scFv(pTyr), because the mobility of TAMRA had been proved to affect the quenching of scFv to fluorophore¹².

To avoid the mistranslation of CGG triplet to nonnatural amino acid, all the arginine were encoded by CGT. On the other hand, to reduce the possibility that four-based codon CGGG is decoded by Arg-tRNA_{CCG}, concentration of arginine in cell-free translation mixture was reduced 10-fold lower than other 19 kinds of natural amino acids.

The four-base codon was decoded by TAMRA-X-AF-tRNA_{CCCG} in an *E. coli* cell-free translation system. The resulting His₆-tagged scFvs were purified by Ni-NTA beads followed by gel-filtration to completely remove free TAMRA-labeled amino acid. SDS-PAGE analysis and fluorescent imaging of SDS-PAGE gel revealed that TAMRA was successfully incorporated into full-length scFv(pTyr) (molecular weight \approx 28 kDa) (Figure 2-6).

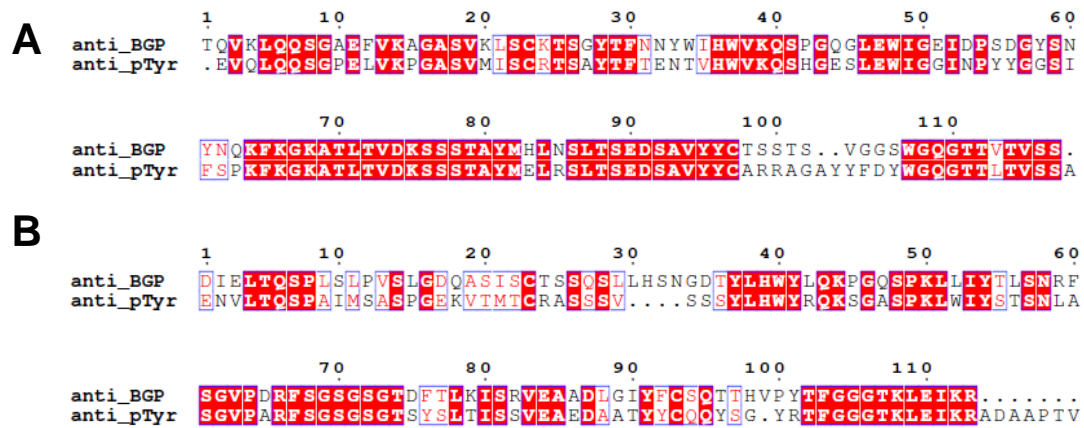


Figure 2-5. (A). Alignment of heavy chains (V_H) of scFv(BGP) against scFv(pTyr). (B). Alignment of light chains (V_L) of scFv(BGP) against scFv(pTyr). Conserved residues are boxed in red-filled boxes. Amino acids with same side-chain properties are in red and boxed in empty boxes.

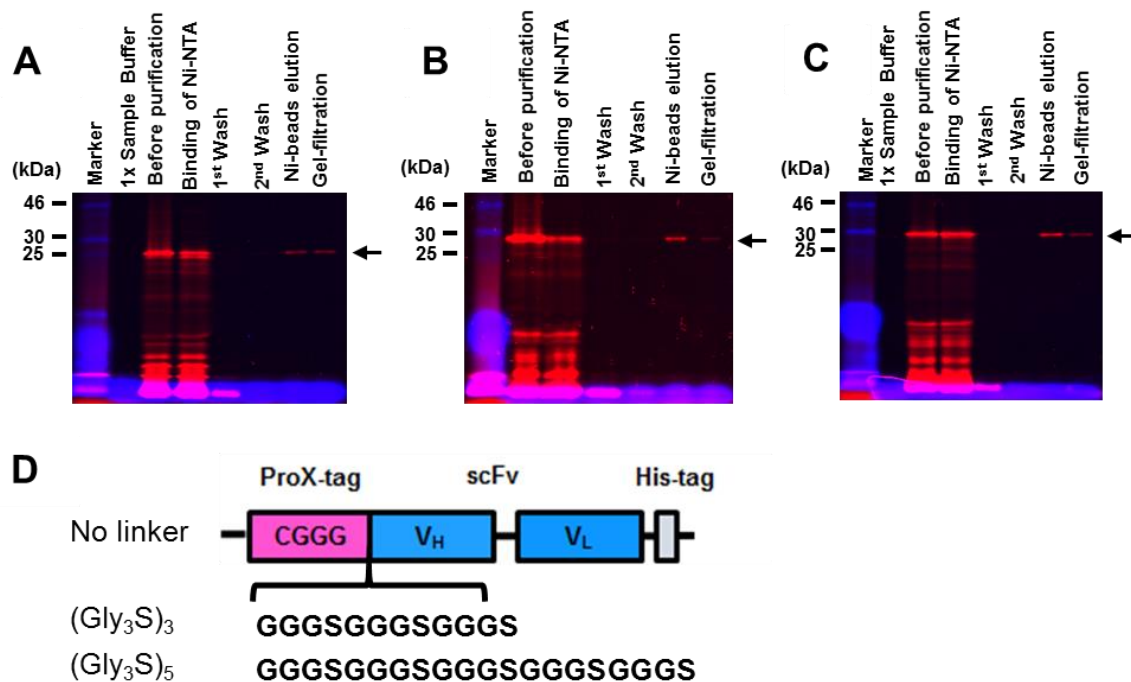


Figure 2-6. Fluorescent images of SDS-PAGE gels of TAMRA-scFv(pTyr) (A), TAMRA-(GGGS)₃-scFv(pTyr) (B), and TAMRA-(GGGS)₅-scFv(pTyr) (C), arrows indicated full-length TAMRA-scFvs. (D). Illustration of the gene structures of ProX-(GGGS)_n-scFv(pTyr) (n=0, 3, 5).

2-3-2. Fluorescence measurement of TAMRA-scFv(pTyr) with pTyr-containing peptides

Fluorescence spectra of TAMRA-scFv(pTyr) were measured with excitation of TAMRA at wavelength 550 nm in the absence and presence of various concentrations of pTyr-containing peptides. When EGF receptor substrate 2 (ERS-pTyr) with sequence DADE-pY-LIPQQG was used as antigen, TAMRA-scFv(pTyr) without Gly₃Ser linker between TAMRA and scFv showed increase of TAMRA intensity to 1.15-fold upon addition of antigen (Figure 2-7A). This result indicated that TAMRA was quenched by Trp residues in the interface of scFv in the absence of the antigen, but the binding of antigen removed the quenching effect and enhanced TAMRA fluorescence. Interestingly, the enhancement of TAMRA fluorescence was depended on the length of linker between TAMRA and scFv (Figure 2-7B and C). The variant with (GGGS)₅ linker exhibited the largest fluorescence enhancement, while that with (GGGS)₃ linker exhibited 1.19-fold enhancement. The titration curve of fluorescence intensity of TAMRA at 580 nm revealed the apparent dissociation constant (K_d) of TAMRA-(GGGS)_n-scFv(pTyr) (n=0, 3, and 5) to the pTyr-containing peptide was 1.1×10^{-5} M, 3.3×10^{-6} M, and 2.6×10^{-6} M, respectively. This suggests that the linker is effective to improve not only the fluorescence enhancement upon the antigen binding but also the antigen binding affinity.

Next, the fluorescence response of TAMRA-(GGGS)₅-scFv(pTyr) to different pTyr-containing peptides was examined. Insulin receptor tyrosine kinase substrate peptide (TRDI-pY-ETD-pY-pY-RK) (IRS) which has three pTyr residues and pp60^{src} SH2 domain-binding peptide (Ac-pY-EEIE) were used. Titration of TAMRA-(GGGS)₅-scFv(pTyr) with IRS showed 1.17-fold fluorescence enhancement with apparent K_d of 4.3×10^{-7} M (Figure 2-8A). On the contrary, the addition of pYEEIE led to only 1.05-fold fluorescence enhancement of TAMRA even when 10^{-4} M of antigen was added (Figure 2-8B). Titration of TAMRA-scFv(pTyr) without linker with IRS and pYEEIE was also carried out and gave similar results.

These results suggest that amino acid residues adjacent to pTyr significantly affect the binding affinity. scFv may interact with not only pTyr residue but also adjacent residues and this interaction was essential for the binding of antigen peptides to scFv. In fact, the anti-pTyr 4G10 antibody had been reported to show some context preference in antigen amino acid sequence²⁰. Leucine at position +1 and proline at position +3 were favorable for the 4G10 antibody. This explained the good K_d value against ERS-pTyr peptide. On the other hand, aspartic acid at position -1 was not preferable, suggesting that the binding of the second pTyr residue of IRS peptide was less effective. This might reduce the binding affinity against IRS peptide to some extent even though it has multiple pTyr residues. In the case of Ac-pY-EEIE

peptide, amino acid residues upstream of pTyr may be important for interaction with the antibody. While the binding affinity was different between IRS and ERS peptides, the fluorescence enhancement was found to be comparable (1.17- and 1.23-fold), suggesting that the antigen peptides bound to the scFv may not interact with TAMRA. In the case of Ac-pYEEIE peptide, the addition of antigen at 10^{-4} M may not be enough for saturation of the antigen-binding site, and as consequence, the quenching effect on TAMRA is partially removed.

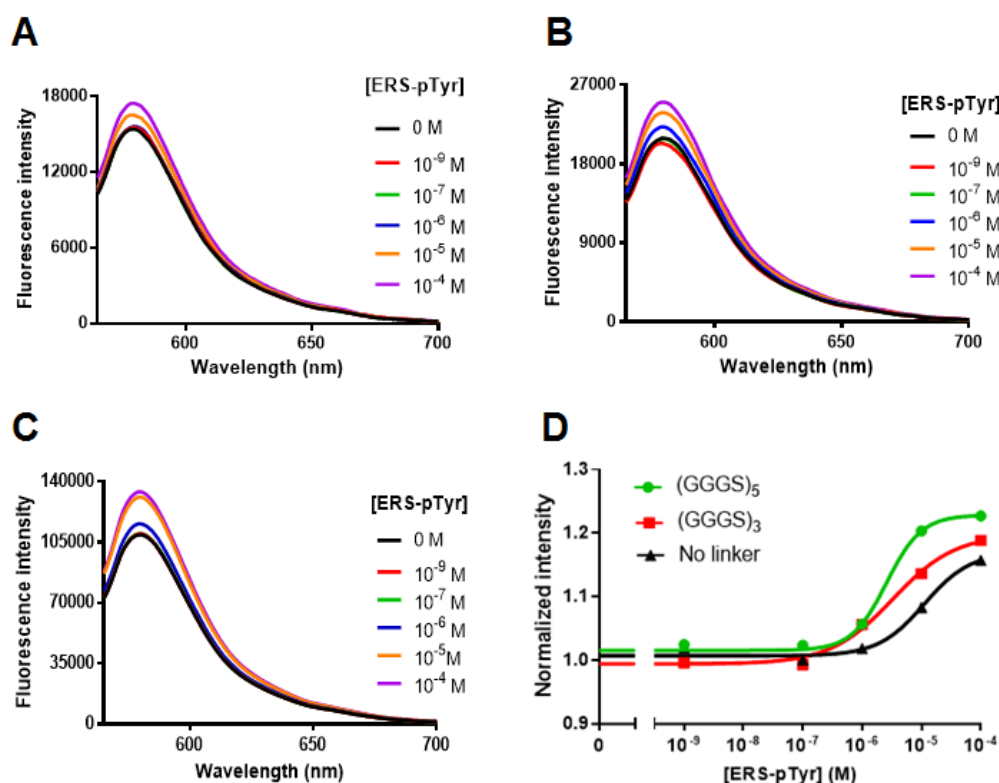


Figure 2-7. Fluorescent spectra of TAMRA-scFv(pTyr) (A), TAMRA-(GGGS)₃-scFv(pTyr) (B), TAMRA-(GGGS)₅-scFv(pTyr) (C). (D) Titration curves of TAMRA-scFv(pTyr)s with different linker length. The data were normalized by the value without antigen.

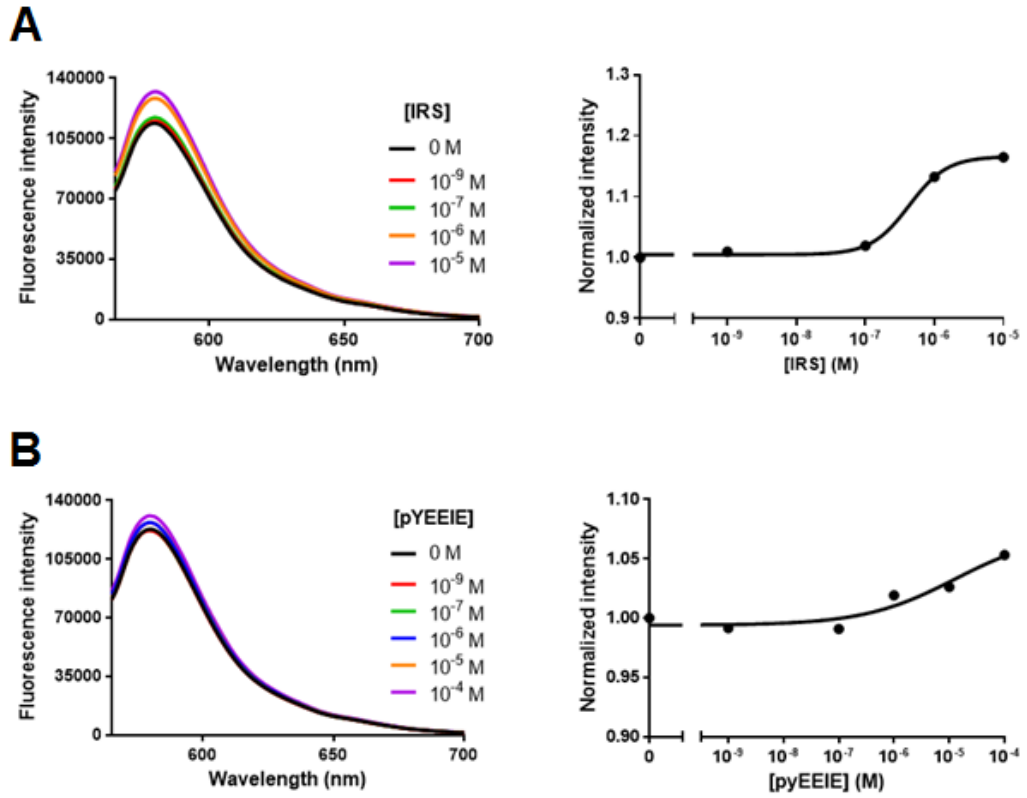


Figure 2-8. Fluorescence spectra and titration curves of TAMRA-(GGGS)₅-scFv(pTyr) with two different pTyr-containing peptides, (A) Insulin receptor tyrosine kinase substrate peptide (IRS), (B) pp60^{src} SH2 domain-binding peptide (pYEEIE). The data were normalized by the value without antigen.

2-3-3. Synthesis and fluorescence measurement of double labeled scFv(pTyr)

A simple, single-chain fluorescent biosensor for detection of protein phosphorylation was successfully constructed based on the principle of antigen-dependent removal of quenching effect of scFv on attached fluorophore. This biosensor recognized pTyr residues and showed fluorescence enhancement upon addition of pTyr-containing antigens. However, fluorescence intensity of single labeled scFvs is also dependent on the amount of this biosensor in measuring sample. It is a difficulty in the application of this technique to detect antigen in the cells where the local concentration of the biosensor cannot be controlled. Further improvement was examined to obtain double labeled scFvs that show antigen-dependent fluorescence ratio change by combining FRET and fluorescence quenching.

To synthesize double fluorescent labeled biosensor for protein phosphorylation, EGFP was fused to TAMRA-labeled scFv(pTyr). Because the emission spectrum of EGFP well overlaps with absorption spectrum of TAMRA, FRET from EGFP to TAMRA was expected to occur. In addition, HaloTag was fused to TAMRA-scFv and conjugated with RhodamineGreen (RhG)-labeled HaloTag ligand. RhG is also suitable FRET donor for TAMRA. According to a finding that scFv(pTyr)s labeled with TAMRA at the C-terminus through Gly₄ or Gly₃SerGly₄ linker improved in fluorescent enhancement upon addition of antigen (Yoshikoshi K., personal communication), TAMRA was introduced at the C-terminus of scFv(pTyr) for double labeling. EGFP and HaloTag were fused at the N-terminus of TAMRA-labeled scFv(pTyr)s to generate EGFP-scFv(pTyr)-G₄-TAMRA, EGFP-scFv(pTyr)-G₃SG₄-TAMRA, and Halo-scFv(pTyr)-G₃SG₄-TAMRA. Figure 2-4 shows a schematic illustration of this strategy. In the absence of antigen, although FRET between EGFP and TAMRA occurs since they are in close distance, fluorescence of TAMRA is not detected because it is quenched by Trp residues in the interface of V_H and V_L. In the presence of antigen, binding of antigen induces a tight interaction of V_H and V_L and release TAMRA from quenching effect. By excitation of EGFP, fluorescence of both EGFP and TAMRA can be detected as a result of FRET and fluorescent intensity of TAMRA increases dependently on concentration of antigen.

The double labeled scFv(pTyr) proteins were synthesized in *E. coli* cell-free translation system. TAMRA-nonnatural amino acid was incorporated into protein in response to an amber codon (UAG). Proteins with His₆-tag were purified by Ni-NTA beads and subsequently gel-filtration. Analyzing of protein purification procedure by SDS-PAGE and fluorescence imaging of SDS-PAGE gels revealed that synthetic efficiency of double labeled scFv(pTyr) is lower than that of single labeled protein (Figure 2-9). Probably, the bulky size of double labeled

proteins reduced the translation yield of cell-free translation system, molecular weight of EGFP fusions and HaloTag fusion are about 53 kDa and 60 kDa, respectively.

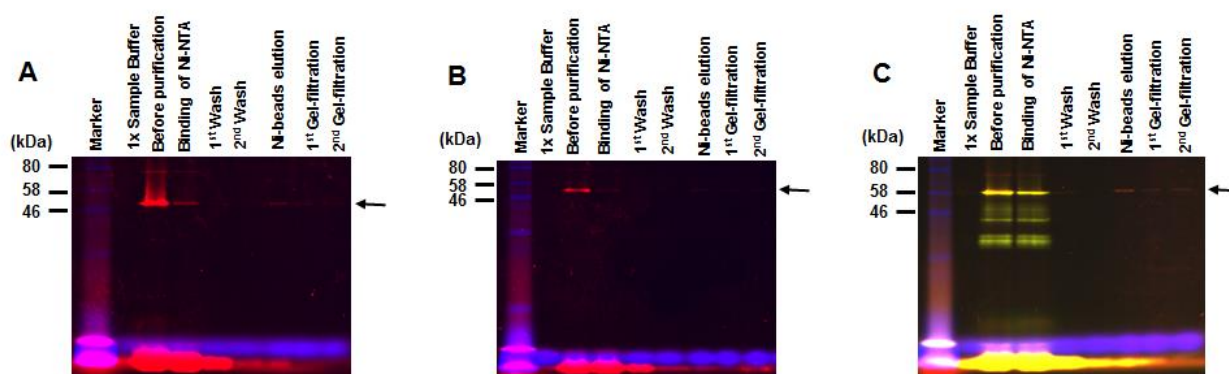


Figure 2-9. Fluorescent images of SDS-PAGE gels of EGFP-scFv(pTyr)-G₄-TAMRA (A), EGFP-scFv(pTyr)-G₃SG₄-TAMRA (B), and Halo-scFv(pTyr)-G₃SG₄-TAMRA (C), arrows indicated full-length proteins.

To examine FRET between EGFP and TAMRA, EGFP was excited at 470 nm and fluorescence was recorded from 490 nm to 700 nm. In the absence of antigen, only the peak of EGFP fluorescence at 509 nm was recorded and TAMRA fluorescence was negligible. Upon the addition of antigen (ERS-pTyr peptide), the peak of TAMRA at 580 nm appeared and increased with antigen concentration while fluorescence of EGFP was almost identical. Fluorescence ratio was calculated as fluorescence intensities of TAMRA/EGFP, and plotted against the antigen concentration (Figure 2-10A and B). When directly excited TAMRA at 550 nm, the antigen-dependent increase of fluorescence intensity was also observed.

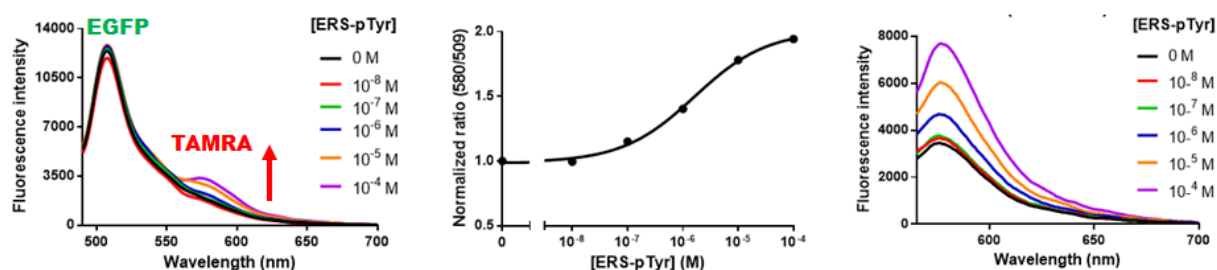
These results confirm that FRET between EGFP and TAMRA always occurred, but the fluorescence of TAMRA was quenched in the absence of antigen. In the presence of antigen, however, the quenching effect was eliminated and the fluorescence of TAMRA was detected. The elimination of the quenching effect was evidenced by the fluorescence enhancement of TAMRA excited at 550 nm. FRET efficiency was not altered by the antigen-binding in all the double labeled scFvs, indicating that average distance between the donor and acceptor pairs is nearly constant.

EGFP-scFv(pTyr)-G₄-TAMRA showed 1.94-fold increase in fluorescence ratio of TAMRA/EGFP (580 nm/509 nm) upon addition of 10^{-4} M ERS-pTyr peptide. By fitting the fluorescence ratio against the antigen concentration, apparent K_d was calculated as 1.6×10^{-6} M.

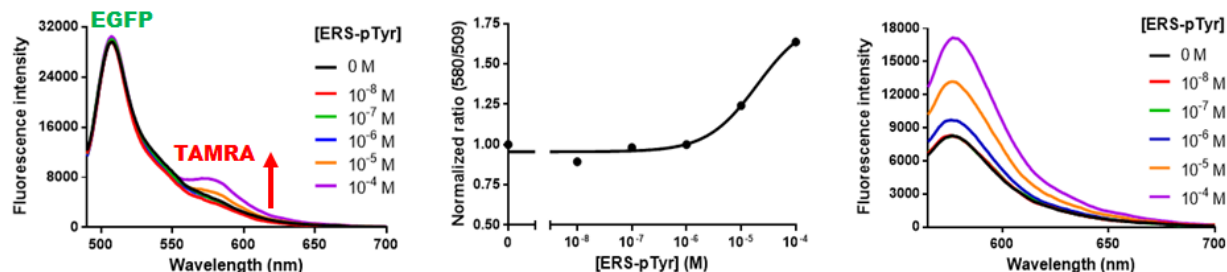
EGFP-scFv(pTyr)-G₃SG₄-TAMRA also exhibited increase in the fluorescence ratio although it was slightly lower than that having shorter linker.

In case of Halo-tagged scFv(pTyr), Halo-tag was labeled by RhG-X-Halo ligand after protein translation. FRET between RhG and TAMRA was monitored by exciting RhG at 495 nm, and fluorescence was recorded from 510 nm to 700 nm. The fluorescence of TAMRA was negligible in the absence of antigen, but the addition of the antigen increased the TAMRA fluorescence as in the case of the EGFP fusions. The increase in fluorescence ratio of TAMRA/RhG (580 nm/529 nm) upon addition of 10⁻⁴ M ERS-pTyr peptide was 1.33-fold, lower than the EGFP fusions, suggesting that FRET between RhG-labeled HaloTag and TAMRA may occur in lower efficiency than between EGFP and TAMRA (Figure 2-10C).

A. EGFP-scFv(pTyr)-G₄-TAMRA



B. EGFP-scFv(pTyr)-G₃SG₄-TAMRA



C. Halo(RhG)-scFv(pTyr)-G₃SG₄-TAMRA

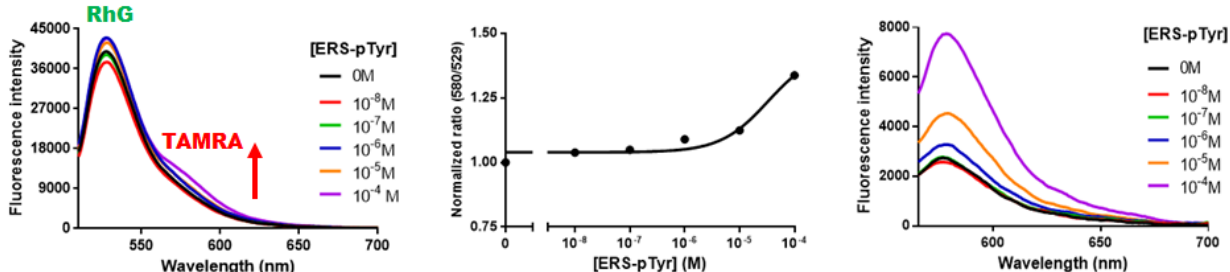
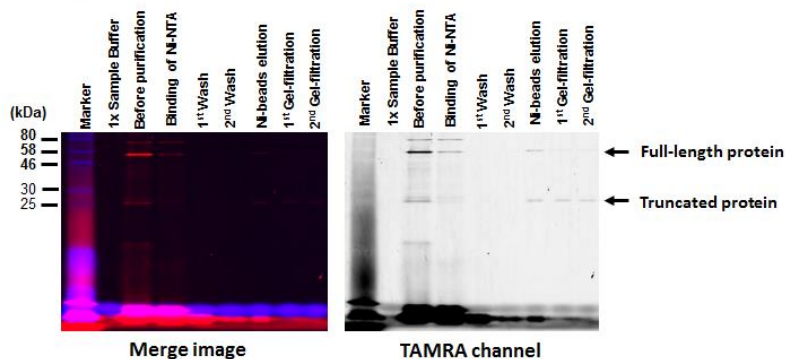


Figure 2-10. Fluorescence analysis of double labeled Qbody variants in which EGFP and HaloTag were fused at N-terminus of scFv(pTyr). *Left:* FRET measurement by excitation at 470 nm (EGFP) or 495 nm (RhG). *Middle:* Titration curve. *Right:* Fluorescent spectra of TAMRA upon excitation at 550 nm.

The above double labeled scFvs with FRET donor and acceptor pairs at the N- and C-termini, respectively, showed weak fluorescence of TAMRA even in the presence of antigen, suggesting a low FRET efficiency between the donor proteins and TAMRA. This probably due to the long distance and/or unfavorable orientations of two fluorophores. To improve FRET efficiency, EGFP was fused downstream of the C-terminal TAMRA through (Gly₃Ser)₂ linker. The C-terminus double labeled scFv(pTyr)s having Gly₄ or Gly₃SerGly₄ linker between scFv and TAMRA (scFv(pTyr)-G₄-TAMRA-EGFP and scFv(pTyr)-G₃SG₄-TAMRA-EGFP) were expressed in the cell-free translation system and purified. Fluorescence image of SDS-PAGE gels showed that the full-length protein was synthesized, however, a truncated protein was also included after purification (Figure 2-11). The truncated protein was between 25 - 30 kDa, co-purified by Ni-NTA beads and contained TAMRA-nonnatural amino acid, probably, this protein was TAMRA linked with EGFP. These proteins might produce background signal of TAMRA under excitation of EGFP, removal of these truncated products may further improve the fluorescence ratio change of the scFv-TAMRA-EGFP fusions. However, in this experiment, these purified proteins were used for fluorescence measurement without further purification because it was difficult to remove the truncated proteins due to low yield of the protein synthesis.

A. scFv(pTyr)-G₄-TAMRA-EGFP



B. scFv(pTyr)-G₃SG₄-TAMRA-EGFP

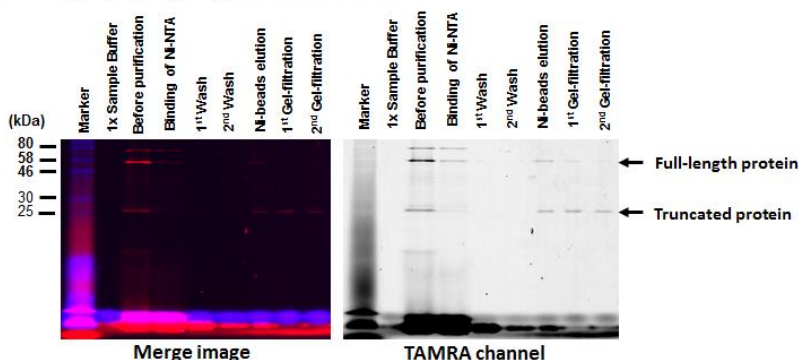
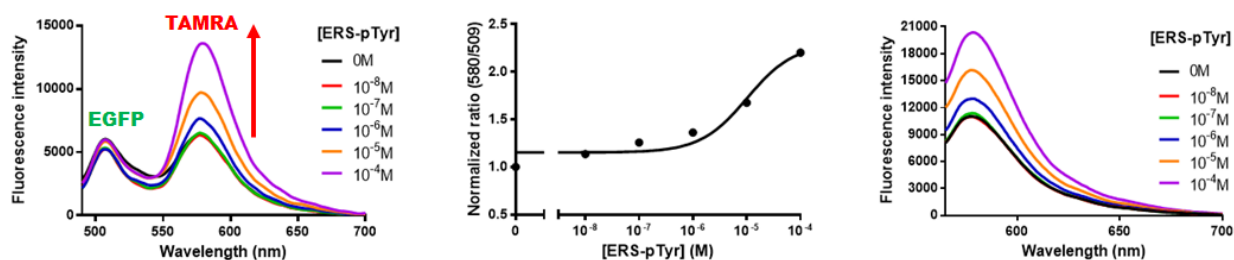


Figure 2-11. Fluorescence images of SDS-PAGE gels of scFv(pTyr)-G₄-TAMRA-EGFP (A), and scFv(pTyr)-G₃SG₄-TAMRA-EGFP (B).

Fluorescence spectra of the C-terminus double labeled scFv(pTyr)s showed distinct fluorescence peak of TAMRA (Figure 2-12), which suggests that FRET efficiency between EGFP and TAMRA was significantly improved. The increase in fluorescence ratio was 2.20 and 1.73-fold for Gly₄ and Gly₃SerGly₄ linkers, respectively. These values are comparable to those of N-terminus EGFP-labeled scFvs. In addition, high intensity of TAMRA fluorescence would contribute to improve signal-to-noise ratio. The fluorescence intensity of EGFP was nearly constant upon the antigen-binding as in the case of N-terminus EGFP-labeled scFvs, suggesting again that FRET efficiency was not altered by the antigen-binding. Apparent K_d value of scFv(pTyr)-G₃SG₄-TAMRA-EGFP was determined as 2.4×10^{-6} M, which is nearly the same as that of EGFP-scFv(pTyr)-G₄-TAMRA, while scFv(pTyr)-G₄-TAMRA-EGFP did not show saturated binding at 10^{-4} M antigen. Bulky EGFP may interfere with the binding of antigen when it was fused to the C-terminus without relatively long linker.

A. scFv(pTyr)-G₄-TAMRA-EGFP



B. scFv(pTyr)-G₃SG₄-TAMRA-EGFP

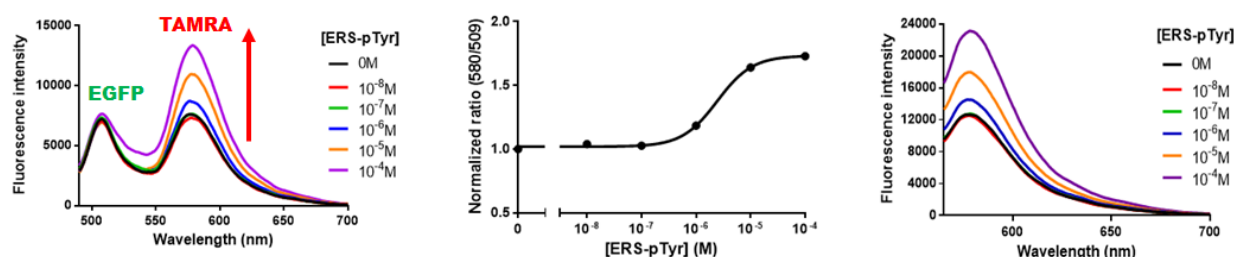


Figure 2-12. Fluorescence analysis of double labeled Qbody variants in which EGFP was fused downstream of TAMRA-natural amino acid at C-terminus of scFv(pTyr). *Left:* FRET measurement by excitation at 470 nm (EGFP). *Middle:* Titration curve. *Right:* Fluorescent spectra of TAMRA upon excitation at 550 nm.

2-4. Conclusion

In this study, I developed new, single-chain fluorescent biosensors for detection of phosphotyrosine (pTyr). TAMRA-labeled anti-pTyr scFv in which TAMRA-nonnatural amino acid was incorporated at N-terminal domain of anti-pTyr scFv showed antigen-dependent enhancement of TAMRA fluorescence intensity upon addition of antigen peptides containing pTyr at different positions. This experiment also revealed that adjacent residues to pTyr on antigen peptides affected the binding affinity to scFv.

Upon fusion of fluorescent proteins (EGFP) and protein-tag (HaloTag-RhG) to TAMRA-labeled scFv(pTyr), double labeled biosensors for pTyr-containing peptides were generated. The double labeled anti-pTyr scFvs exhibited fluorescence ratio enhancement in the presence of antigen based on FRET and antigen-dependent fluorescence quenching effect. While the double labeled scFv with EGFP and HaloTag at N-terminus resulted in low FRET efficiency, the fusion of EGFP at C-terminus significantly improved FRET efficiency. We expect that fluorescent biosensors obtained in this study will become a novel tool for analysis of protein phosphorylation.

Our strategy in combination of PET and FRET technologies for biosensor construction has an advantage compared with conventional FRET-based biosensors as it does not require large conformational change of protein scaffold upon interaction with analyte. Therefore, this strategy makes it easy to design fluorescent ratiometric biosensors and has a potential for wide range application to various antibody-antigen pairs.

2-5. References

- (1) Ting A. Y., Kain K. H., Klemke R. L., Tsien R. Y. Genetically encoded fluorescent reporters of protein tyrosine kinase activities in living cells. *Proc. Natl. Acad. Sci. USA* **98** (26): 15003-15008 (2001)
- (2) Sato M., Ozawa T., Inukai K., Asano T., Umezawa Y. Fluorescent indicators for imaging protein phosphorylation in single living cells. *Nat. Biotechnol.* **20**: 287-294 (2002)
- (3) Offterdinger M., Georget V., Girod A., Bastiaens P. I. H. Imaging phosphorylation dynamic of the epidermal growth factor receptor. *J. Biol. Chem.* **279**(35): 36972-36981 (2004)
- (4) Oldach L., Zhang J. Genetically-encoded fluorescent biosensors for live-cell visualization of protein phosphorylation. *Chem. Biol.* **21**: 186-197 (2014)
- (5) Yin C., Wang M., Lei C., Wang Z., Li P., Li Y., Li W., Huang Y., Nie Z., Yao S. Phosphorylation-mediated assembly of semisynthetic fluorescent protein for label-free detection of protein kinase activity. *Anal. Chem.* **87**: 6311-6318 (2015)
- (6) Kameshita I., Fujisawa H. A sensitive method for detection of calmodulin-dependent protein kinase II activity in sodium dodecyl sulfate-polyacrylamide gel. *Anal. Biochem.* **183**: 139-143 (1989)
- (7) Ishida A., Kameshita I., Sueyoshi N., Taniguchi T., Shigeri Y., Recent advances in technologies for analyzing protein kinases. *J. Pharmacol. Sci.* **103**: 5-11 (2007)
- (8) Bockus L.B., Scifiel R. H. Phosphoprotein detection on protein electroblot using a phosphate-specific fluorophore. *Methods Mol. Biol.* **1314**: 263-271 (2015)
- (9) Sasaki A., Arawaka S., Sato H., Kato T. Sensitive Western blotting for detection of endogenous Ser129-phosphorylated α -synuclein in intracellular and extracellular spaces. *Sci. Rep.* **5**:14211 (2015)
- (10) Mandell J. W. Phosphorylation state-specific antibodies: applications in investigative and diagnostic pathology. *Am. J. Pathol.* **163**(5): 1687-1698 (2003)
- (11) Ohiro Y., Ueda H., Shibata N., Nagamune T. Development of a homogeneous competitive immunoassay for phosphorylated protein antigen based on the enhanced fluorescence resonance energy transfer technology. *J. Biosci. Bioeng.* **109**(1): 15-19 (2010)

- (12) Abe R., Ohashi H., Iijima I., Ihara M., Takagi H., Hohsaka T., Ueda H.
“Quenchbodies”: Quench-based antibody probes that show antigen-dependent fluorescence. *J. Am. Chem. Soc.* **133**: 17386-17394 (2011)
- (13) Hohsaka T., Kajihara D., Ashizuka Y., Murakami H., Sisido M. Efficient incorporation of nonnatural amino acids with large aromatic groups into streptavidin in vitro protein synthesizing systems. *J. Am. Chem. Soc.* **121**: 34-40 (1999)
- (14) Kajihara D., Abe R., Iijima I., Komiyama C., Sisido M., Hohsaka T. FRET analysis of protein conformational change through position-specific incorporation of fluorescent amino acids. *Nat. Methods* **3**(11): 923-929 (2006)
- (15) Easinger D., Stiles L., Ramarsh A., Jelinek T. A recombinant monoclonal antibody specific for phosphotyrosine-containing proteins. Patent JP 2004526408-A1 and JP2004526408A2 (2004)
- (16) Notredame C., Higgins D.G., Heringa J. T-Coffee: A novel method for fast and accurate multiple sequence alignment. *J. Mol. Biol.* **302**(1): 205-217 (2000)
- (17) Di Tommaso P., Moretti S., Xenarios I., Orobittg M., Montanyola A, Chang JM, Taly JF, Notredame C. T-Coffee: A web server for the multiple sequence alignment of protein and RNA sequences using structural information and homology extension. *Nucleic Acids Res. (Web server issue)* **39**: W13-17 (2011)
- (18) Robert X., Gouet P. Deciphering key features in protein structures with the new ENDscript server. *Nucleic Acids Res. (Web server issue)* **39**: W320-324 (2014)
- (19) Taira H., Matsushita Y., Kojima K., Shiraga K., Hohsaka T. Comprehensive screening of amber suppressor tRNAs suitable for incorporation of non-natural amino acids in a cell-free translation system. *Biochem. Biophys. Res. Commun.* **374**: 304-308 (2008)
- (20) Tinti M., Nardoza A. P., Ferrari E., Sacco F., Corallino S., Castagnoli L., Cesareni G. The 4G10, pY20 and p-TYR-100 antibody specificity: profiling by peptide microarrays. *N. Biotechnol.*, 29, 571–577 (2012).

Chapter 3

Genetically-encoded antibody-based biosensors by fusion of protein-tag and fluorescent protein to scFv

3-1. Introduction

FRET-based genetically-encoded fluorescent biosensor is a powerful and popular tool for biological studies since it allows not only quantifying but also tracking the analyte in living cells. The biosensor usually consists of a protein scaffold linked with two fluorescent proteins which are energy donor and acceptor. Interaction of protein scaffold and analyte is converted into change in FRET signals which can be observed¹⁻².

In previous chapter, I have developed biosensors for phosphotyrosine (pTyr)-containing peptides by fusion of fluorescent protein (EGFP) or protein-tag (HaloTag-RhG) to anti-pTyr scFv which have been site-specifically labeled by a fluorescent dye (TAMRA). The resulting double labeled biosensors exhibit FRET between donor (EGFP or HaloTag-RhG) and acceptor (TAMRA) as well as enhancement of acceptor fluorescence in the presence of antigen. However, this type of FRET-based biosensors requires the incorporation of nonnatural amino acid in a cell-free translation system, thus, limit its application in live-cell.

To overcome this problem, protein-tag (i.e. HaloTag³, SNAP-tag, CLIP-tag⁴⁻⁶) and its fluorescent ligand may be employed to substitute the fluorescent nonnatural amino acid. Protein-tags have important advantages for substituting fluorescent nonnatural amino acids, such as (1) they are genetically-encoded which can be fused to scFv gene and expressed in living cells, (2) protein-tag ligand can be obtained by chemical synthesis, which means it can be linked to various fluorophores and the linker length between ligand and fluorophore can be regulated.

In this chapter, I developed novel genetically-encoded fluorescent biosensors using protein-tag and its ligand. A protein-tag (HaloTag or SNAP-tag) is fused to N-terminus of scFv and subsequently labeled by a fluorophore-ligand conjugate. The linker between fluorophore and protein-tag ligand is adjusted so that fluorophore is in close proximity with the interface of V_H and V_L and can be quenched by Trp residues. In the presence of antigen, binding of antigen to scFv remove the quenching effect on fluorophore, thus, intensity of fluorophore increases dependently on antigen concentration (Figure 3-1A).

In addition, fusion of protein-tag and scFv was linked with a fluorescent protein (FP) for detection of antigen based on FRET between FP and fluorophore and antigen-dependent fluorescence quenching effect (Figure 3-1B). I have synthesized fluorescent biosensors for osteocalcin (bone gla protein; BGP), pTyr, and bisphenol-A (a chemical compound which is commonly found in plastics and have been proved to be responsible for many human diseases⁷⁻⁸, BPA). Antigen titration of these biosensors reveal that orientation of protein-tag, type of labeled fluorophore, length of linker between fluorophore-ligand and properties of scFv significantly affect fluorescence response of biosensors to antigens. Through optimization of these factors, novel types of genetically-encoded fluorescent and fluorescent ratio biosensors have been developed.

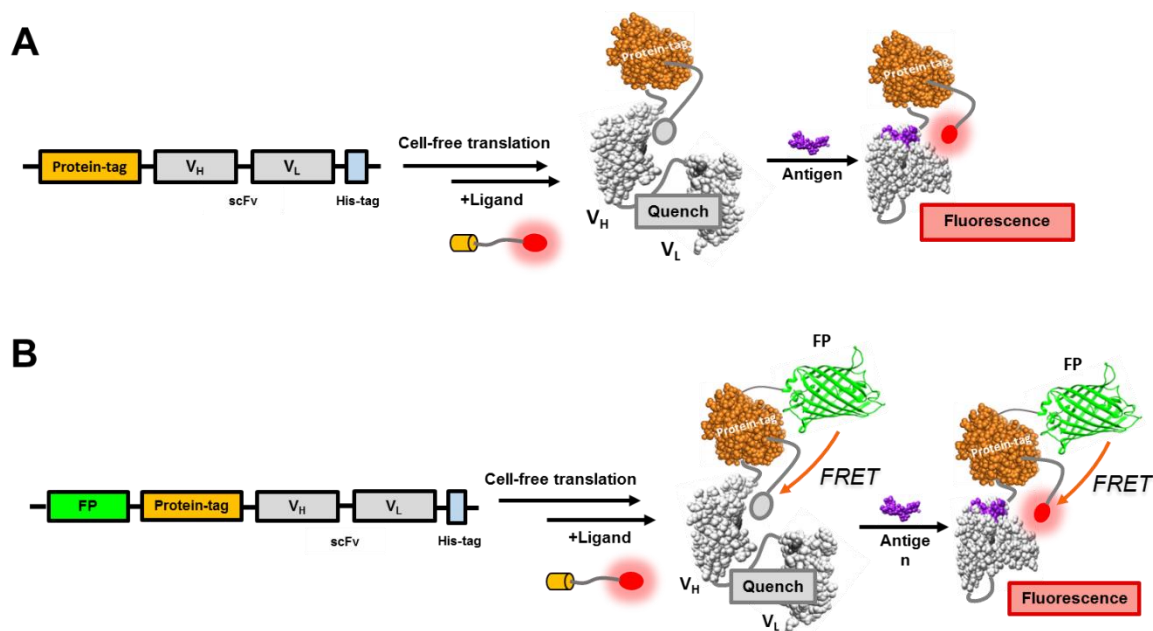


Figure 3-1. (A) Synthetic procedure of fusion of scFv and protein-tag labeled with fluorophore, and fluorescence detection of antigen based on antigen-dependent removal of quenching effect on fluorophore. (B) Synthetic procedure of double labeled scFv with fluorescent protein (FP) and protein-tag, and fluorescence ratio detection of antigen based on FRET from FP to fluorophore and antigen-dependent removal of quenching effect on fluorophore.

3-2. Materials and Methods

3-2-1. Materials

KOD-Plus DNA polymerase, Thermo T7 RNA polymerase were purchased from TOYOBO (Osaka, Japan). Primers for PCR were custom synthesized by Eurofins Genomics (Italy). QIAquick PCR purification kit, QIAquick gel extraction kit were purchased from QIAGEN (Venlo, Netherlands). MagneHis Ni-particles, *E.coli* S30 extract for linear templates, HaloTag Amine (O₂) were from Promega (WI, USA). In-Fusion HD Cloning kit was from Clontech (CA, USA). T4 RNA ligase was obtained from TaKaRa Bio (Otsu, Japan). Prestained protein marker (7-175 kDa), T7 RNA polymerase, SNAP-tag Ligand (BG-NH₂) were from New England BioLabs (MA, USA). YFP (yellow fluorescent protein) gene was a kind gift from Assoc. Prof. Hidekazu Tsutsui (JAIST).

Boc- ϵ -amino caproic acid succinimide ester was purchased from Bachem (Switzerland) or GmbH (Germany), Boc-amino-PEO₁₂-COOH and amino-PEO₂₄-COOH were from Quanta BioDesign (USA), 5-TAMRA succinimide ester, 5(6)-TAMRA-X-succinimide ester, 5(6)-Rhodamine Green-X-succinimide ester and 5-RhodamineRed-X succinimide ester were from Invitrogen (USA), 5-TAMRA-PEO₈ succinimide ester and 5-TAMRA-PEO₁₂ succinimide ester were purchased from Biotium (USA), 5-RhodamineGreen succinimide ester was obtained from Anaspec (USA), 5-FAM-X succinimide ester was purchased from Research Organics (USA).

Zeba desalting spin columns (7K MWCO) were from ThermoFisher Scientific (MA, USA), EGF Receptor Substrate 2 peptide (Phospho-Tyr⁵) was obtained from GenScript (USA), C-terminal peptides for human osteocalcin (BGP-C7, BGP) were custom synthesized by MBL (Japan), bisphenol-A (BPA) was from Tokyo Chemistry Industry (Japan).

3-2-2. Construction of HaloTag- and SNAP tag-scFv genes

HaloTag gene in pFN18A HaloTag was amplified by PCR with forward primer (5'-AGA AGG AGA TAT ACC ATG GCA GAA ATC GGT ACT GGC TTT CC-3') and reverse primer (5'-GCC TGA ACC GCC ACC GCC GGA AAT CTC GAG CGT CGA CAG CC-3'). The pIVEX2.3d vector containing ProX-(GGGS)₅-scFv against BPA with C-terminal His tag was linearized by PCR with forward primer (5'-GGT GGC GGT TCA GGC GGC GGA TCA GGC GGC GGA TCA GGT GG-3') and reverse primer (5'-GGT ATA TCT CCT TCT TAA AGT TAA ACA AAA TTA TTT CTA GAG-3'). The two PCR products were analyzed by

agarose gel and purified. Then, the HaloTag fragment was clone into linearized vector in place of ProX-tag by In-Fusion cloning to form pIVEX-Halo-(GGGS)₅-scFv(BPA).

pIVEX-Halo-(GGGS)₅-scFv genes against BGP and pTyr were constructed by simply substituted anti-BPA scFv by anti-BGP and anti-pTyr scFvs by In-Fusion cloning. In this case, the vector was amplified by PCR with 5'-GGC GGT GGC TCT CAT CAT CAT CAT CAT CAT TAA TAA AAG-3' and 5'-TGA ACC GCC ACC TGA ACC GCC ACC TGA TCC GCC GCC-3' as forward and reverse primers, respectively. Anti-BGP scFv gene was amplified by forward primer (5'-GTT CAG GTG GCG GTT CAA CCC AAG TAA AGC TGC AGC AGT CTG GGG C-3') and reverse primer (5'-GAT GAG AGC CAC CGC CCC GTT TTA TTT CCA GCT TGG TCC CCC CTC-3'). The forward primer (5'-GTT CAG GTG GCG GTT CAG AGG TCC AGC TGC AGC AGT CTG GAC CTG AAC TGG-3') and reverse primer (5'-GAT GAG AGC CAC CGC CAC GTT TGA TTT CCA GCT TGG TGC CTC CAC CGA ACG-3') were used for amplification of anti-pTyr scFv gene. The cloning of anti-BGP and anti-pTyr scFv genes to linearized vector was performed by In-Fusion cloning. The linker (GGGS)₅ peptide between HaloTag and scFv was varied by Quichchange mutagenesis to construct Halo-GGGS-scFv(BGP) using forward primer (5'-CCG GCG GTG GCG GTT CAA CCC AAG TAA AGC TGC-3') and reverse primer (5'-GCA GCT TTA CTT GGG TTG AAC CGC CAC CGC CGG-3').

E. coli codon-optimized SNAP-tag gene was designed according to SNAPf gene (New England BioLabs) and custom synthesized by Integrated DNA technology (IA, USA). To construct pIVEX-SNAP-(GGGS)₅-scFv genes, we substituted HaloTag in above constructs by SNAP-tag. SNAP-tag was amplified by PCR with forward primer (5'-AGG AGA TAT ACC ATG GAT AAG GAT TG-3') and reverse primer (5'-GCC TGA ACC GCC ACC TCC AAG TCC TGG-3') while the pIVEX vector was linearized by PCR with same primers as in the first construct to substitute ProX-tag by HaloTag. The SNAP-tag gene and linearized vector were analyzed by agarose gel electrophoresis and purified. Then, the two DNA fragments was ligated by In-Fusion cloning to make pIVEX-SNAP-(GGGS)₅-scFv. The linker (GGGS)₅ peptide between SNAP-tag and scFv was varied by Quickchange mutagenesis. pIVEX-SNAP-(GGGS)₃-scFv(BGP) was generated by Quickchange mutagenesis with forward primer (5'-CTT GGA GGT GGC GGT TCA GGC GGC GGA TCA GGT GGC GGG TCA ACC CAA GTA AAG CTG CAG-3') and reverse primer (5'-CTG CAG CTT TAC TTG GGT TGA CCC GCC ACC TGA TCC GCC GCC TGA ACC GCC ACC TCC AAG-3'). Similarly, pIVEX-SNAP-scFv(BGP) without peptide linker was generated with forward primer (5'-CGT CTT GGC AAA CCA GGA CTT GGA ACC CAA GTA AAG CTG CAG CAG TC-3') and reverse

primer (5'-GAC TGC TGC AGC TTT ACT TGG GTT CCA AGT CCT GGT TTG CCA AGA CG-3').

3-2-3. Construction scFv(BGP)-EGFP and scFv(BGP)-Halo genes

To synthesize anti-BGP scFv-EGFP, the cDNA of EGFP was amplified by PCR with forward primer (5'-GGT GGC AGT GGT GGC TCG AGT AAA GGA GAA GAA CTT TTC-3') and reverse primer (5'-GAA TTC GCC CTT TTA CTA TAG AAT ACT CAA GCT TA-3'). The pIVEX2.3d vector containing ProX-scFv(BGP) was linearized by PCR with forward primer (5'-TAA AAG GGC GAA TTC CAG CAC ACT GG-3') and reverse primer (5'-CGA GCC ACC ACT GCC ACC ACG TTT TAT TTC CAG CTT GGT CCC CCC-3'). Then, EGFP was cloned into linearized vector by In-Fusion cloning to generate pIVEX-ProX-scFv(BGP)-(GGG)₂-EGFP.

To synthesize anti-BGP scFv fused with HaloTag at the C-terminus (scFv(BGP)-(GGG)₂-Halo), the cDNA of HaloTag was amplified by PCR with forward primer (5'-GGT GGC AGT GGT GGC TCG GCA GAA ATC GGT ACT GGC TTT CCA TTC-3') and reverse primer (5'-GAA TTC GCC CTT TTA GTG GTG GTG GTG GTG GTG GCC GGA AAT CTC GAG CGT CGA CAG CCA G-3') and cloned into linearized vector of pIVEX-ProX-scFv(BGP) by In-Fusion cloning to generate pIVEX-ProX-scFv(BGP)-(GGG)₂-Halo. Then, ProX-tag might be deleted by Quickchange mutagenesis with forward primer (5'-CTT TAA GAA GGA GAT ATA CCA TGA CCC AAG TAA AGC TGC AGC AG-3') and reverse primer (5'-CTG CTG CAG CTT TAC TTG GGT CAT GGT ATA TCT CCT TCT TAA AG-3').

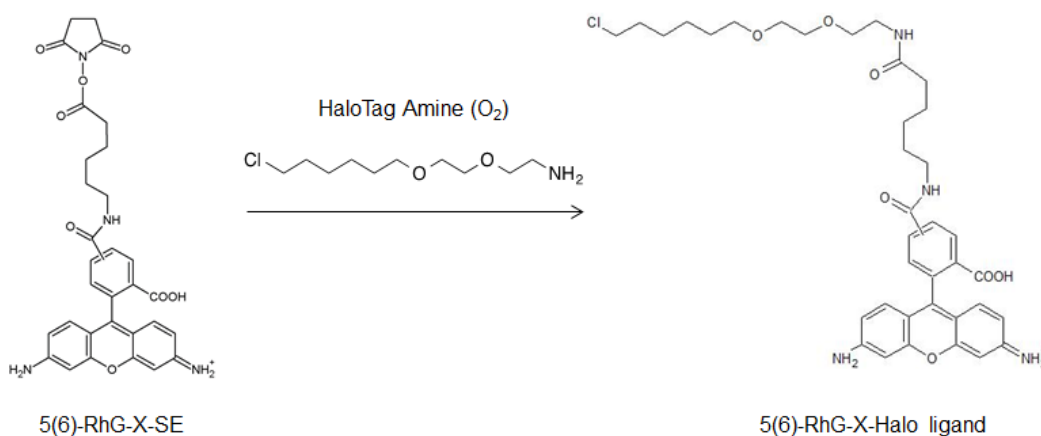
3-2-4. Construction of FP-SNAP-scFv genes

cDNA of EGFP was amplified by PCR with forward primer (5'-AAG AAG GAG ATA TAC CAT GAG TAA AGG AGA AGA ACT TTT CAC TGG AGT TGT C-3') and reverse primer (5'-CTT ATC CGA GCC ACC ACT GCC ACC TTT GTA GAG CTC ATC CAT GCC ATG TGT AAT C-3'). The vector pIVEX-SNAP-(GGG)₅-scFv was linearized by PCR with 5'-TGG TGG CTC GGA TAA GGA TTG CGA AAT GAA GCG GAC TAC C-3' and 5'-GGT ATA TCT CCT TCT TAA AGT TAA ACA AAA TTA TTT CTA GAG-3' as forward and reverse primers, respectively. The EGFP and linearized vector were analyzed by agarose gel electrophoresis and purified. Then, In-Fusion cloning was performed to clone EGFP into pIVEX-SNAP-scFv vector, yielding pIVEX-EGFP-SNAP-scFv.

cDNA of YFP was amplified from the plasmid pCs4+ carried a voltage probe (Mermaid2)⁹ by PCR with forward primer (5'-AAG AAG GAG ATA TAC CAT GGT GAG CAA GGG CGA GGA GCT GTT CAC CGG-3') and reverse primer (5'-TTT CGC AAT CCT TAT CCT TGT ACA GCT CGT CCA TGC CGA GAG TGA TC-3'). pIVEX-SNAP-scFv was linearized by PCR with forward primer (5'-GAT AAG GAT TGC GAA ATG AAG CGG ACT ACC-3') and reverse primer (5'-GGT ATA TCT CCT TCT TAA AGT TAA ACA AAA TTA TTT CTA GAG-3'). The PCR products were purified from agarose gel and ligated by In-Fusion cloning to produce pIVEX-YFP-SNAP-scFv.

3-2-5. Synthesis of fluorophore-linked HaloTag ligand compounds

RhodamineGreen-X-HaloTag ligand: To a mixture of 50 mM DMSO solution of 5(6)-RhodamineGreen-X-succinimide ester (5(6)-RhG-X-SE) (8 μ L, 400 nmol), 100 mM DMSO solution of HaloTag Amine (O₂) (2 μ L, 200 nmol) and 100 mM NaHCO₃aq (4 μ L) were added. The mixture was kept on ice for 60 min, and applied to an analytical scale reversed-phase HPLC (XBridge, 2.5 μ m, 4.6x20 mm, flow rate 1.5 ml/min, with a linear gradient of 0-100% methanol in 0.38% formic acid, over 10 min) to afford RhG-X-Halo ligand (188 nmol; 94% yield). The product was confirmed by MALDI-TOF MS (calcd. 693.30 for MH⁺, found 693.34).

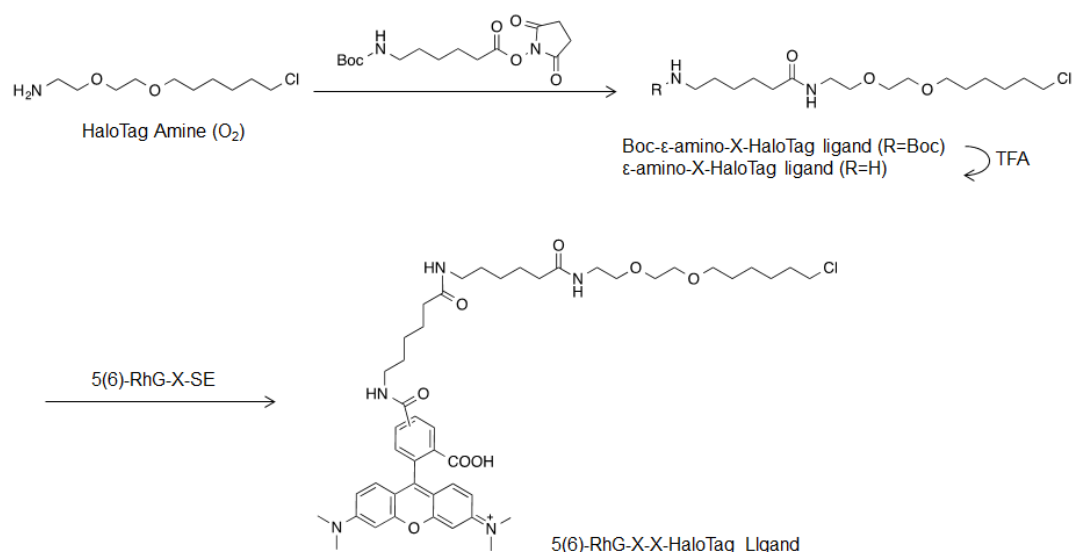


Scheme 3-1. Synthetic scheme of RhG-X-Halo ligand

RhodamineGreen-X-X-HaloTag ligand: To a mixture of 100 mM DMSO solution of HaloTag Amine (O₂) (4 μ L, 400 nmol) and 100 mM DMSO solution of Boc- ϵ -amino caproic acid succinimide ester (5 μ L, 500 nmol), 100 mM NaHCO₃aq (9 μ L) was added. The mixture

was kept on ice for 1 hour. 5% KHSO_4aq (13 μL) was added to the solution, and the resulting mixture was extracted with ethyl acetate. The organic layer was removed by evaporation. The dried product was dissolved in trifluoroacetic acid (TFA) (30 μL) and placed on ice for 10 min to remove Boc group. After evaporation of TFA by vacuum centrifuge, the pellet was washed with diethyl ether (200 μL), and dried under vacuum to afford amino-X-HaloTag ligand. The product was dissolved in DMSO (4 μL).

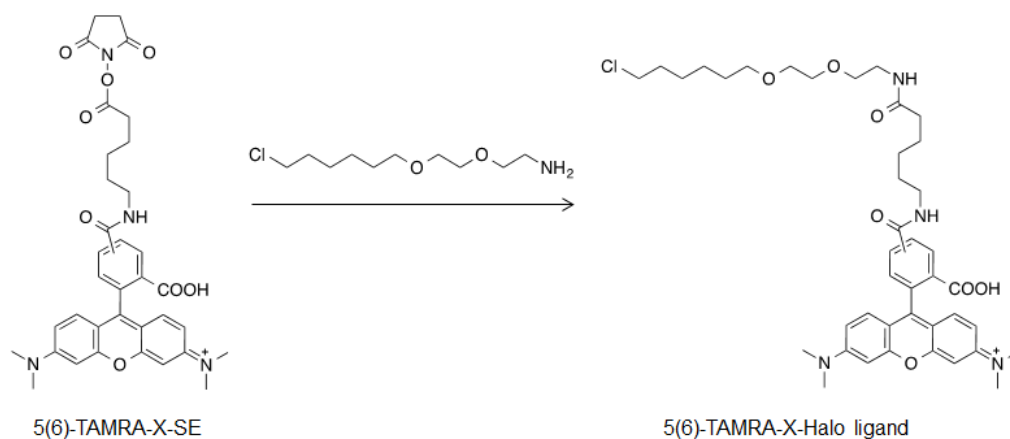
To a mixture of above DMSO solution of amino-X-HaloTag ligand (2 μL) and 50 mM DMSO solution of 5(6)-RhodamineGreen-X succinimide ester (8 μL), 100 mM NaHCO_3aq (4 μL) was added. The mixture was kept on ice for 1 hour. 0.38% formic acid (80 μL) and acetonitrile (40 μL) were added to the solution, and the crude product was purified with an analytical scale reversed-phase HPLC (XBridge, 2.5 μm , 4.6x20 mm, flow rate 1.5 ml/min, with a linear gradient of 0-100% methanol in 0.38% formic acid, over 10 min) to afford RhodamineGreen-X-X-HaloTag ligand (99.6 nmol; 50% yield (2-steps)). The product was identified by MALDI-TOF MS (calculated, 806.39 for MH^+ ; observed, 806.37).



Scheme 3-2. Synthetic scheme of RhG-X-X-Halo ligand

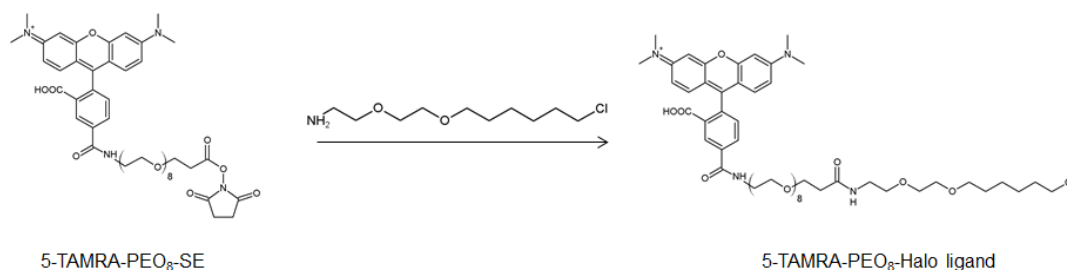
TAMRA-X-HaloTag ligand: To a mixture of 50 mM DMSO solution of 5(6)-TAMRA-X-succinimide ester (4 μL , 200 nmol) and 100 mM DMSO solution of HaloTag Amine (O_2) (1 μL , 100 nmol), 100 mM NaHCO_3aq (2 μL) was added. The mixture was kept on ice for 30 min. 0.38% formic acid (40 μL) was added to the solution, and the crude product was purified with

an analytical scale reversed-phase HPLC (XBridge, 2.5 μm , 4.6x20 mm, flow rate 1.5 ml/min, with a linear gradient of 0-100% methanol in 0.38% formic acid, over 10 min) to afford TAMRA-X-HaloTag ligand (18.5 nmol; 19% yield). The product was identified by MALDI-TOF MS (calculated, 749.37 for MH^+ ; observed, 749.32).



Scheme 3-3. Synthetic scheme of TAMRA-X-Halo ligand

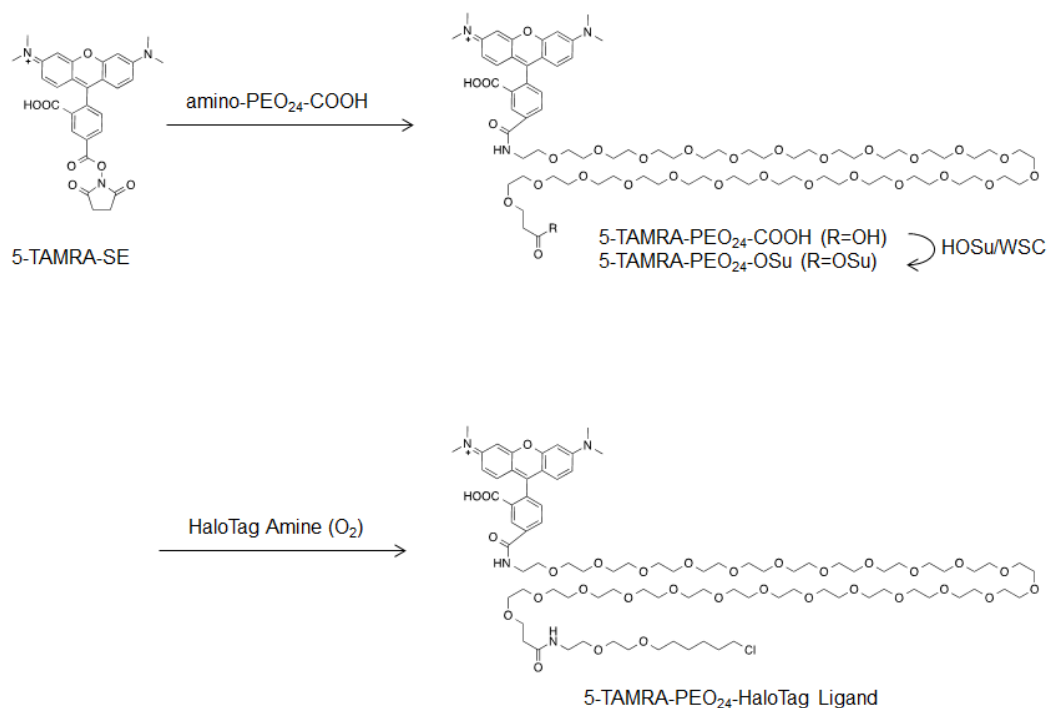
TAMRA-PEO₈-HaloTag ligand: To a mixture of 100 mM DMSO solution of HaloTag Amine (O₂) (1 μL , 100 nmol) and 50 mM DMSO solution of 5-TAMRA-PEO₈ succinimide ester (2.5 μL , 125 nmol), 100 mM NaHCO_3aq (1.25 μL) was added. The mixture was kept on ice for 1 hour. 0.38% formic acid (40 μL) and acetonitrile (5 μL) were added to the solution, and the crude product was purified with an analytical scale reversed-phase HPLC (XBridge, 2.5 μm , 4.6x20 mm, flow rate 1.5 ml/min, with a linear gradient of 0-100% methanol in 0.38% formic acid, over 10 min) to afford TAMRA-PEO₈-HaloTag ligand (25 nmol; 25% yield). The product was identified by MALDI-TOF MS (calculated, 1059.5 for MH^+ ; observed, 1059.6).



Scheme 3-4. Synthetic scheme of TAMRA-PEO₈-Halo ligand

phase HPLC (XBridge, 10 μ m, 10x50 mm, flow rate 3.0 ml/min, with a linear gradient of 0-100% methanol in 0.38% formic acid, over 15 min) to afford 5-TAMRA-PEO₂₄-OSu (274 nmol; 91% yield). The product was identified by MALDI-TOF MS (calculated, 1655.8 for MH⁺; observed, 1655.6).

To a mixture of 100 mM DMSO solution of HaloTag Amine (O₂) (4.6 μ L, 460 nmol) and 10 mM DMSO solution of 5-TAMRA-PEO₂₄-OSu (23 μ L, 230 nmol), 100 mM NaHCO₃aq (2.85 μ L) was added. The mixture was kept on ice for 1 hour. Adequate volume of 0.38% formic acid and acetonitrile was added to the solution, and the crude product was purified with a preparative scale reverse-phase HPLC (XBridge, 10 μ m, 10x50 mm, flow rate 3.0 ml/min, with a linear gradient of 0-100% methanol in 0.38% formic acid, over 15 min) to afford TAMRA-PEO₂₄-HaloTag ligand (26.6 nmol; 11.6% yield). The product was identified by MALDI-TOF MS (calculated, 1764.0 for MH⁺; observed, 1764.2).

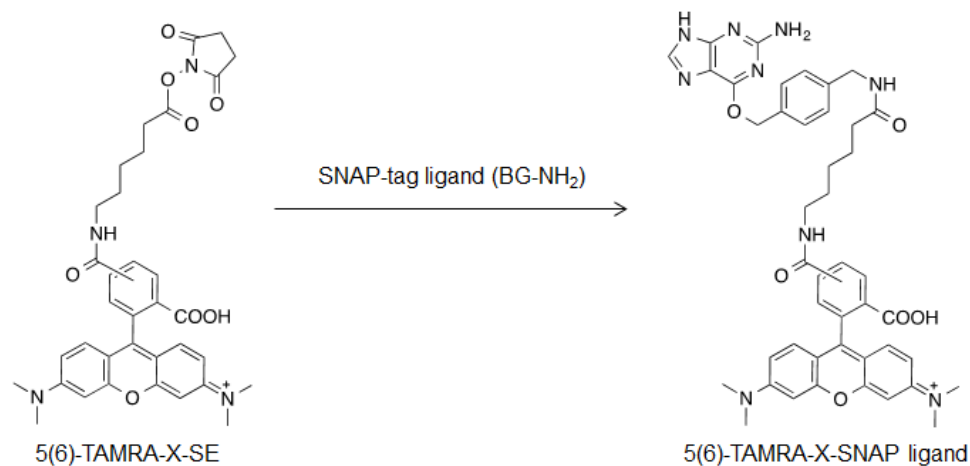


Scheme 3-6. Synthetic scheme of TAMRA-PEO₂₄-Halo ligand

3-2-5. Synthesis of fluorophore linked SNAP-tag ligand compounds

TAMRA-X-SNAP ligand: To a mixture of 50 mM DMF solution of SNAP-tag ligand (BG-NH₂) (1.2 μ L, 60 nmol) and 100 mM DMSO solution of 5(6)-TAMRA-X succinimide ester (3 μ L, 300 nmol) in DMF (130.8 μ L), 100 mM triethylamine (15 μ L, 1.5 μ mol) was added.

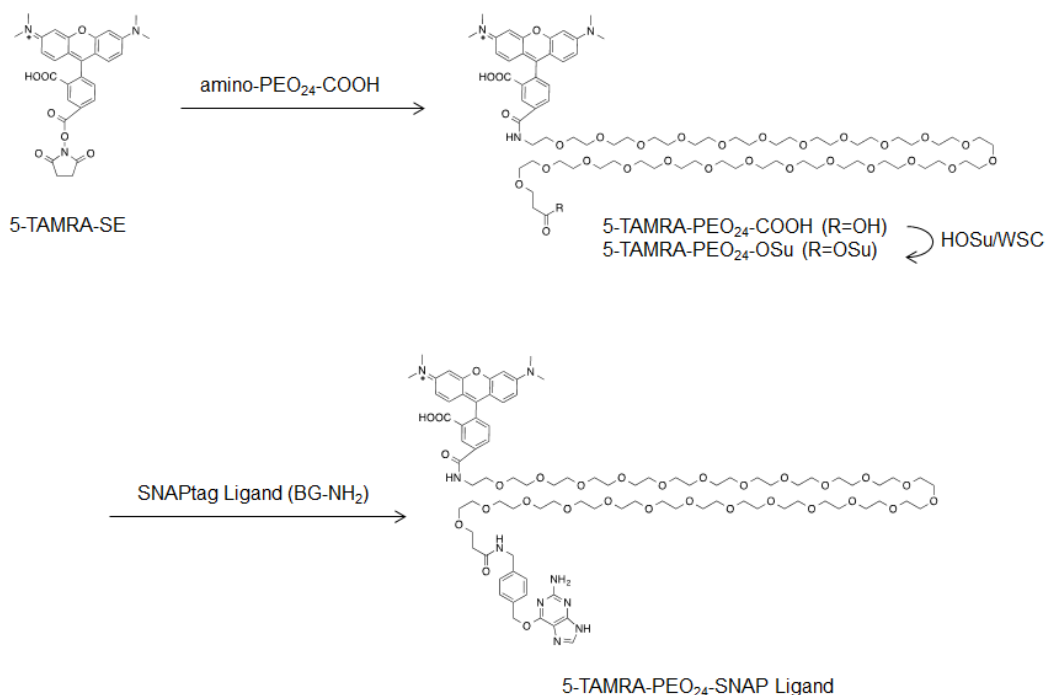
After shaking at 30 °C for 2.5 hours, additional 50 mM DMSO solution of BG-NH₂ (1.2 μL, 60 nmol) was added to the mixture. The mixture was shaken at 30 °C for 30 min. Adequate volume of 0.38% formic acid and acetonitrile were added to the solution, and the crude product was purified with a preparative scale reverse-phase HPLC (XBridge, 10 μm, 10x50 mm, flow rate 3.0 ml/min, with a linear gradient of 0-100% methanol in 0.38% formic acid, over 15 min) to afford TAMRA-X-SNAP ligand (226.6 nmol; 76% yield). The product was identified by MALDI-TOF MS (calculated, 796.4 for MH⁺; observed, 796.2).



Scheme 3-7. Synthetic scheme of TAMRA-X-SNAP ligand

TAMRA-PEO₈-SNAP ligand: To a mixture of 50 mM DMF solution of SNAP-tag ligand (BG-NH₂) (2 μL, 100 nmol) and 50 mM DMSO solution of 5-TAMRA-PEO₈ succinimide ester (2 μL, 100 nmol) in DMF (43.6 μL), 100 mM triethylamine (5 μL, 500 nmol) was added. The mixture was shaken at 30 °C for 4.5 hours. Adequate volume of 0.1% trifluoroacetic acid and acetonitrile were added to the solution, and the crude product was purified with a preparative scale reverse-phase HPLC (XBridge, 10 μm, 10x50 mm, flow rate 3.0 ml/min, with a linear gradient of 0-100% acetonitrile in 0.1% TFA, over 15 min) to afford TAMRA-PEO₈-SNAP ligand (14.1 nmol; 14% yield). The product was identified by MALDI-TOF MS (calculated, 1106.5 for MH⁺; observed, 1106.6).

(43 μL), 100 mM triethylamine (5 μL , 500 nmol) was added. The mixture was shaken at 30 $^{\circ}\text{C}$ for 45 minutes. 0.1% trifluoroacetic acid (80 μL) and acetonitrile (10 μL) were added to the solution, and the crude product was purified with a preparative scale reverse-phase HPLC (XBridge, 10 μm , 10x50 mm, flow rate 3.0 ml/min, with a linear gradient of 0-100% acetonitrile in 0.1% TFA, over 15 min) to afford TAMRA-PEO₂₄-SNAP ligand (28.6 nmol; 29% yield).



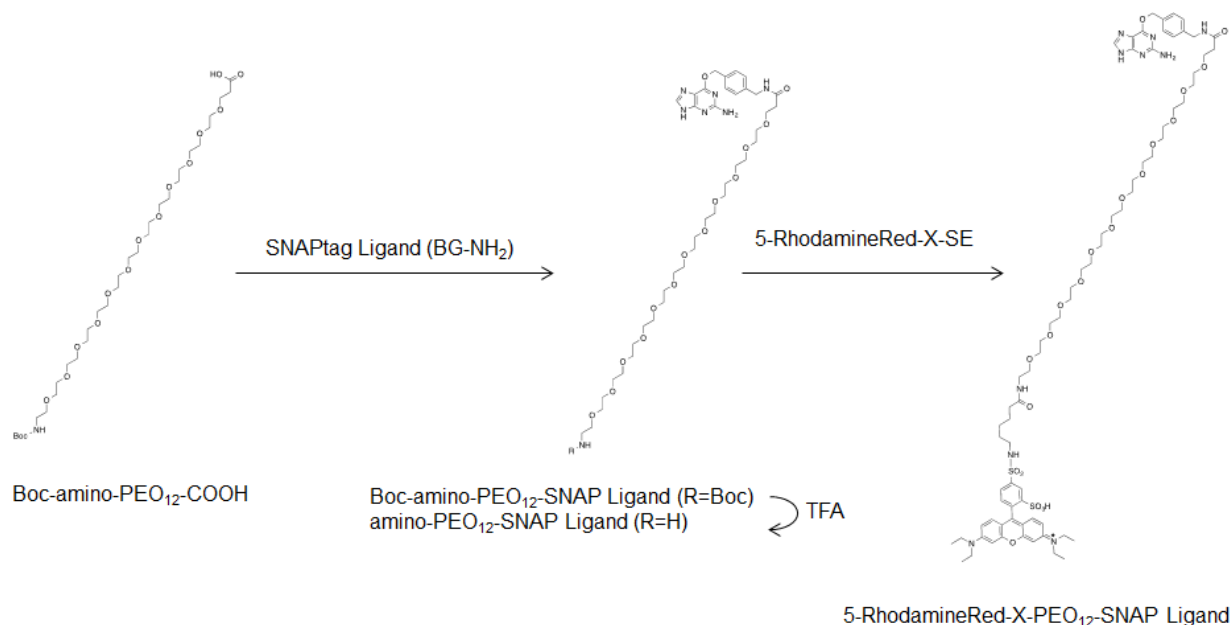
Scheme 3-10. Synthetic scheme of TAMRA-PEO₂₄-SNAP ligand

RhodamineRed-X-PEO₁₂-SNAP ligand: To a solution of 100 mM DMF solution of Boc-amino-PEO₁₂-COOH (60 μL ; 6 μmol), 125 mM DMF solution of water soluble carbodiimide (WSC) (480 μL ; 60 μmol) was added. After shaking at room temperature for 5 min, 50 mM DMF solution of SNAP-tag ligand (BG-NH₂) (15 μL ; 750 nmol) was added to the mixture, and the mixture was shaken at room temperature for 4 hours. 0.1% trifluoroacetic acid (400 μL) was added the solution, and the crude product was purified with a preparative scale reverse-phase HPLC (XBridge, 10 μm , 10x50 mm, flow rate 3.0 ml/min, with a linear gradient of 0-100% methanol in 0.38% formic acid, over 15 min) to afford Boc-amino-PEO₁₂-SNAP ligand.

The dried Boc-amino-PEO₁₂-SNAP-tag ligand was dissolved in trifluoroacetic acid (TFA) (100 μL) and placed on ice for 10 min to remove Boc group. After evaporation of TFA

by vacuum centrifuge, the pellet was washed with diethyl ether (500 μ L), and dried under vacuum to afford Amino-PEO₁₂-SNAP ligand (166 nmol; 22% yield, 2 steps).

To a mixture of 25 mM DMSO solution of 5-RhodamineRed-X succinimide ester (2.5 μ L; 62.5 nmol) and 10 mM DMSO solution of Amino-PEO₁₂-SNAP ligand (5 μ L; 50 nmol), 100 mM NaHCO₃aq (2.5 μ L; 250 nmol) was added. After keeping on ice for 1 hour, 100 mM NaHCO₃aq (2.5 μ L; 250 nmol) was added to the mixture. The mixture was shaken at room temperature for more 2 hours. 0.38% formic acid (90 μ L) and MeCN (10 μ L) were added to the solution, and the crude product was purified with a preparative scale reverse-phase HPLC (XBridge, 10 μ m, 10x50 mm, flow rate 3.0 ml/min, with a linear gradient of 0-100% acetonitrile in 0.1% TFA, over 15 min) to afford RhodamineRed-X-PEO₁₂-SNAP ligand (34 nmol; 68% yield). The product was identified by MALDI-TOF MS (calculated, 1523.7 for MH⁺; observed, 1523.8).

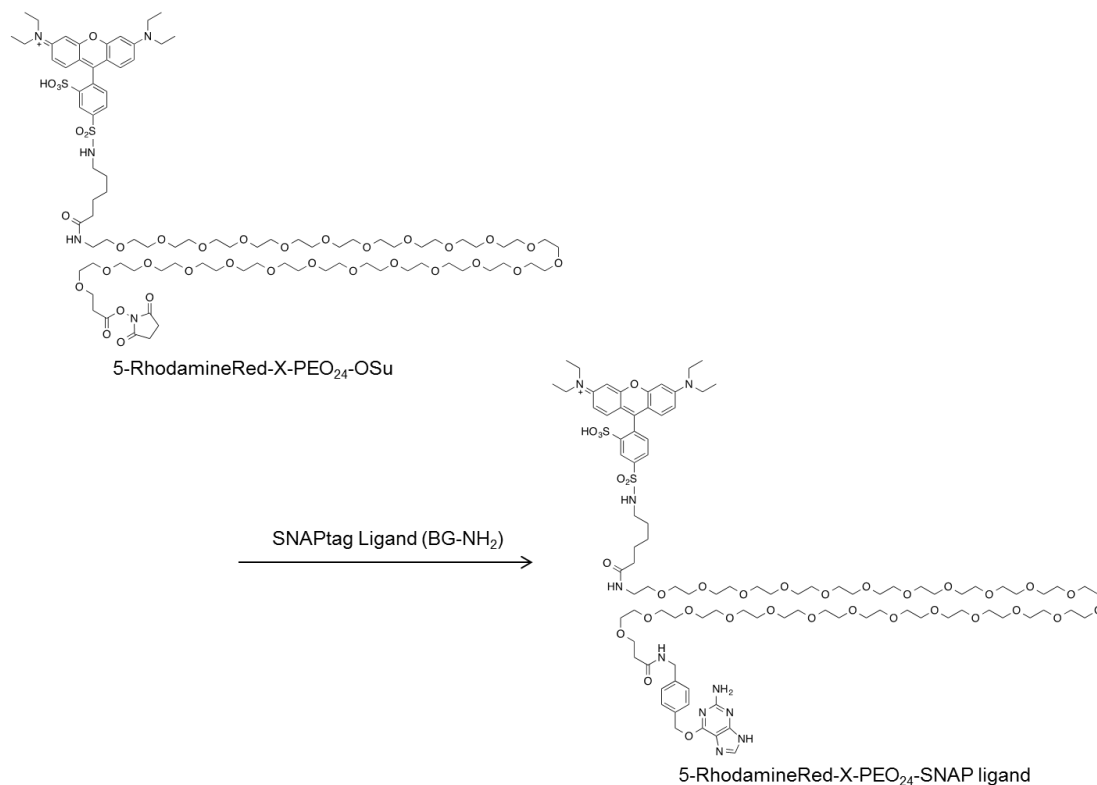


Scheme 3-11. Synthetic scheme of RhR-X-PEO₁₂-SNAP ligand

RhodamineRed-X-PEO₂₄-SNAP ligand: The synthetic scheme to RhodamineRed-X-PEO₂₄-OSu was the same as that of RhodamineRed-X-PEO₂₄-HaloTag Ligand.

To a mixture of 50 mM DMF solution of SNAP-ligand (BG-NH₂) (2.5 μ L, 125 nmol) and 10 mM DMSO solution of 5-RhodamineRed-X-PEO₂₄ succinimide ester (12.5 μ L, 125 nmol) in DMF (54.5 μ L), 100 mM triethylamine (6.25 μ L, 625 nmol) was added. The mixture was shaken at 30 °C for 1 hour. 0.1% trifluoroacetic acid (80 μ L) was added to the solution,

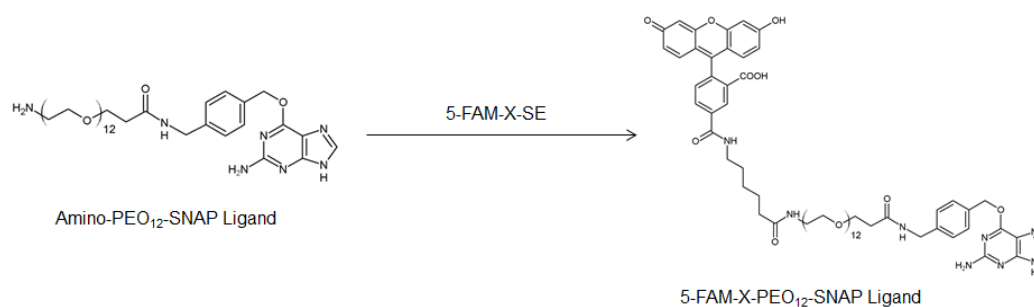
and the crude product was purified with a preparative scale reverse-phase HPLC (XBridge, 10 μ m, 10x50 mm, flow rate 3.0 ml/min, with a linear gradient of 0-100% acetonitrile in 0.1% TFA, over 15 min) to afford RhodamineRed-X-PEO₂₄-SNAP ligand (98.8 nmol; 79% yield). The product was identified by MALDI-TOF MS (calculated 2052.0 for MH⁺; observed 2052.3).



Scheme 3-12. Synthetic scheme of RhR-X-PEO₂₄-SNAP ligand

FAM-X-PEO₁₂-SNAP ligand: The synthetic scheme to amino-PEO₁₂-SNAP ligand was the same as that of RhodamineRed-X-PEO₁₂-SNAP ligand.

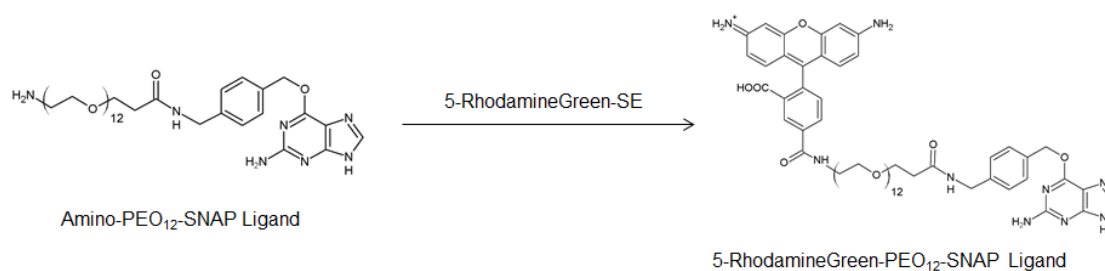
To a mixture of 100 mM DMSO solution of 5-FAM-X succinimide ester (1.75 μ L, 175 nmol) and 10 mM DMSO solution of amino-PEO₁₂-SNAP ligand (3.5 μ L, 35 nmol) in DMSO (1.75 μ L), 100 mM NaHCO₃aq (1.75 μ L, 175 nmol) was added. The mixture was kept on ice for 4 hours. Adequate volume of 0.38% formic acid and acetonitrile was added to the solution, and the crude product was purified with a preparative scale reverse-phase HPLC (XBridge, 10 μ m, 10x50 mm, flow rate 3.0 ml/min, with a linear gradient of 0-100% acetonitrile in 0.1% TFA, over 15 min) to afford FAM-X-PEO₁₂-SNAP ligand (10.6 nmol; 30% yield). The product was identified by MALDI-TOF MS (calculated, 1363.6 for (M+Na)⁺; observed, 1363.7)



Scheme 3-13. Synthetic scheme of FAM-X-PEO₁₂-SNAP ligand

RhodamineGreen-PEO₁₂-SNAP ligand: The synthetic scheme to amino-PEO₁₂-SNAP ligand was the same as that of RhodamineRed-X-PEO₁₂-SNAP ligand.

To a mixture of 50 mM DMSO solution of 5-RhodamineGreen succinimide ester (2 μ L, 100 nmol) and 10 mM DMSO solution of amino-PEO₁₂-SNAP Ligand (5 μ L, 50 nmol) in DMSO (3 μ L), 100 mM NaHCO₃aq (2.5 μ L, 250 nmol) was added. The mixture was kept on ice for 1 hour. Adequate volume of 0.38% formic acid and acetonitrile was added to the solution, and the crude product was purified with a preparative scale reverse-phase HPLC (XBridge, 10 μ m, 10x50 mm, flow rate 3.0 ml/min, with a linear gradient of 0-100% acetonitrile in 0.1% TFA, over 15 min) to afford RhodamineGreen-PEO₁₂-SNAP ligand (22 nmol; 44% yield). The product was identified by MALDI-TOF MS (calculated, 1226.6 for (M+Na)⁺; observed, 1226.6).



Scheme 3-14. Synthetic scheme of RhG-PEO₁₂-SNAP ligand

3-2-6. Cell-free translation and protein purification

Coding regions of scFv fusions were amplified by PCR and the PCR products were purified by QIAquick PCR purification kit. The transcription to mRNA was performed as described before¹⁰.

Cell-free translation was performed at final volume 120 μ L with 0.8 μ g/ μ L mRNA, 55 mM HEPES-KOH (pH 7.5), 210 mM GluK, 6.9 mM $\text{CH}_3\text{COONH}_4$, 12 mM $(\text{CH}_3\text{COO})_2\text{Mg}$, 1.2 mM ATP, 0.28 mM GTP, 26 mM phosphoenolpyruvate, 1 mM spermidine, 1.9% PEG-8000, 35 μ g/ml folinic acid, 0.1 mM of each of the 20 natural amino acid, 2 mM glutathione oxidized and 24 μ L *E.coli* S30 extract. The mixture was incubated at 37°C for 1 hour. After incubation, DMSO solution of fluorophore-linked HaloTag or SNAP-tag ligand was added to the cell-free translation mixture to final concentration 50 μ M and incubated at 25°C for 30 min to achieve labeled protein-tags. For expression of scFv(BGP)-EGFP and scFv(BGP)-Halo labeled with TAMRA-linked nonnatural amino acid, TAMRA-X-AF-tRNA_{CCCG} was added to the cell-free translation system as described in chapter 2.

The translation and labeling mixture was diluted with buffer A (20 mM sodium phosphate, 0.5M NaCl, 5 mM *imidazole*, pH 7.5) containing 10 M urea to final volume 480 μ L and mixed with 48 μ L MagneHis Ni-particles. After shaking for 30 min at room temperature, the supernatant was removed and the beads were washed once with buffer A, once with buffer A containing 8 M urea and followed by washing three times with buffer A. The His-tagged protein was eluted by buffer B (20 mM sodium phosphate, 0.5M NaCl, 500 mM *imidazole*, pH 7.5) and was gel-filtrated by Zeba Spin Desalting column (7K MWCO) equilibrated with phosphate buffer saline containing 0.05% Tween 20 (PBS-T). For EGFP and YFP fusions, buffer A containing 4 M urea was used for dilution of the translation mixture and for second wash step.

Samples for SDS-PAGE were taken at each purification step and mixed with SDS-PAGE sample buffer to final volume 20 μ L. All samples were heated at 95°C for 5 minutes before SDS-PAGE. Each sample (5 μ l) and Prestained protein marker were applied to 12% SDS-PAGE gel. SDS-PAGE gel was visualized by a fluorescence scanner (FMBIO-III; Hitachi Software Engineering, Japan). RhG and FAM were excited at 488 nm and visualized at 520 nm; TAMRA and RhRed were excited at 532 nm and visualized at 580 nm. Prestained protein marker was visualized with excitation at 635 nm and detection at 670 nm.

3-2-8. Examination of labeling efficiency of HaloTag- and SNAP tag-scFv fusions with different concentrations of fluorophore-ligands

Cell-free translation mixture (60 μ L) of Halo-(GGGS)₅-scFv(BPA) was divided into five and RhG-XX-Halo ligand was added at concentrations of 10, 50, 100, 150, and 200 μ M. The resulting mixtures were incubated at 25°C for 30 or 60 min, and 2 μ L sample from each

mixture was taken. The 2 μL sample was mixed with SDS-PAGE sample buffer to final volume 20 μL , and 5 μL sample was applied to 12% SDS-PAGE after heating at 95°C for 5 min. The SDS-PAGE gel was visualized by a fluorescence scanner (FMBIO-III; Hitachi Software Engineering, Japan), and the intensity of each protein band was measured.

In case of SNAP-tag, the experiment procedure was carried out the same as described above for HaloTag using SNAP-(GGGS)₅-scFv(BGP) and TAMRA-X-SNAP ligand.

3-2-9. Fluorescence measurement

Purified protein was diluted in PBS-T buffer to final 80 μL with various concentrations of antigens (10^{-10} - 10^{-6} M of BGP peptide and BPA, and 10^{-8} - 10^{-4} M of pTyr-containing EGF receptor substrate 2 peptide). After incubation at 25°C for 12 hours, emission spectra were measured by a Fluorolog-3 instrument (Horiba, Japan) at 25°C. Excitation and scanning for emission of each fluorophore was listed in Table 3-1. Fluorescence intensity of each fluorophore at peak emission was utilized for analysis. In case of FRET-based biosensors, fluorescence intensities at peak emission of donor and acceptor were used for calculation of fluorescence ratio (acceptor/donor). The apparent dissociation constant (K_d) was calculated by fitting the fluorescence intensity or fluorescence ratio values to a sigmoidal dose-response (variable slope) model using Graphpad Prism (GraphPad, CA, USA). All data were normalized by the value in the absence of antigen.

Table 3-1. Excitation wavelength and scanning region for each fluorophore			
<i>Fluorophore name</i>	<i>Excitation (nm)</i>	<i>Peak emission (nm)</i>	<i>Scanning region (nm)</i>
RhodamineGreen (RhG)	495	529	510 - 700
FAM	495	530	510 - 700
TAMRA	550	580	565 - 700
RhodamineRed (RhR)	570	590	580 - 700
EGFP	470	509	490 - 700
YFP	508	527	520 - 700

3-3. Results and discussion

3-3-1. Synthesis of HaloTag-scFv fusions

First of all, I utilized HaloTag for N-terminus specific fluorescence labeling of scFv instead of the incorporation of fluorophore-labeled nonnatural amino acid. HaloTag was fused to N-terminus of scFv through a flexible linker (Gly₃Ser)₅ ((GGGS)₅). The HaloTag-scFv fusion was expressed in *E. coli* cell-free translation and labeled with fluorophore-linked HaloTag ligand.

The labeling condition was determined using HaloTag-scFv against BPA (Halo-(GGGS)₅-scFv(BPA)) and RhG-X-X-Halo ligand. Halo-(GGGS)₅-scFv(BPA) was synthesized by cell-free translation at 37°C for 60 min. After translation, RhG-X-X-Halo ligand was added to the translation mixture to final concentration of 10, 50, 100, 150, and 200 μM, then, incubated at 25°C. Sample for SDS-PAGE was taken after 30 min and 60 min incubation. Fluorescence imaging of SDS-PAGE gel indicated that Halo-(GGGS)₅-scFv(BPA) was labeled at all concentrations of RhG-X-X-Halo ligand (Figure 3-2A). Analyzing of fluorescent intensity of full-length Halo-(GGGS)₅-scFv(BPA) bands revealed that the labeling efficiency was saturated from 50 μM of Halo ligand. In addition, 60 min incubation slightly improved labeling efficiency compared with 30 min incubation but this improvement was not significant (Figure 3-2B). Therefore, the concentration of fluorophore-Halo ligand at 50 μM and 30 min incubation were decided for labeling of HaloTag-scFv fusions. Since the labeling efficiency was solely dependent on the properties of protein-tag and ligand, result of this experiment can be applied for any other HaloTag-scFvs and fluorophore-ligand compounds.

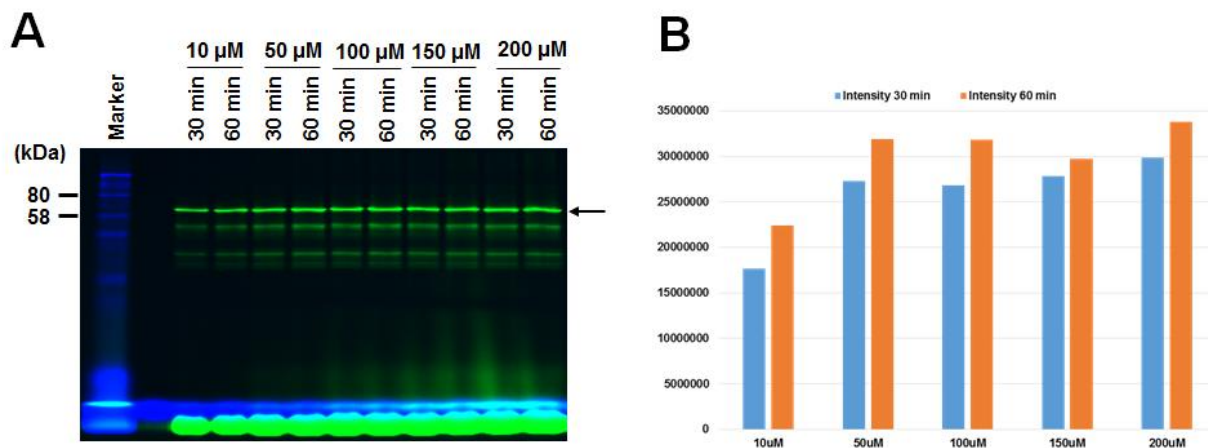


Figure 3-2. Labeling of HaloTag-scFv against BPA (Halo-(GGGS)₅-scFv(BPA)) with different concentrations of RhG-X-X-Halo ligand for 30 and 60 min. (A) Fluorescence image of SDS-PAGE gel for each labeling reaction mixture. Arrow indicated the full-length Halo-(GGGS)₅-scFv(BPA) (MW ≈ 62.5 kDa). (B) Fluorescence intensity of each band on the SDS-PAGE gel.

To examine fluorescence response of HaloTag-scFv upon antigen-binding, at first, Halo-(GGGS)₅-scFv(BPA) was synthesized and labeled with TAMRA-Halo ligand compounds containing various linker length between TAMRA and HaloTag ligand. Figure 3-3A represented a fluorescence image of SDS-PAGE gel of Halo-(GGGS)₅-scFv(BPA) labeled by TAMRA-PEO₁₂-Halo ligand indicated the desired product was successfully expressed in the cell-free translation system and labeled. Although shorter translation products were observed on the SDS-PAGE, full-length protein was purified by Ni-NTA beads against the C-terminal His₆-tag.

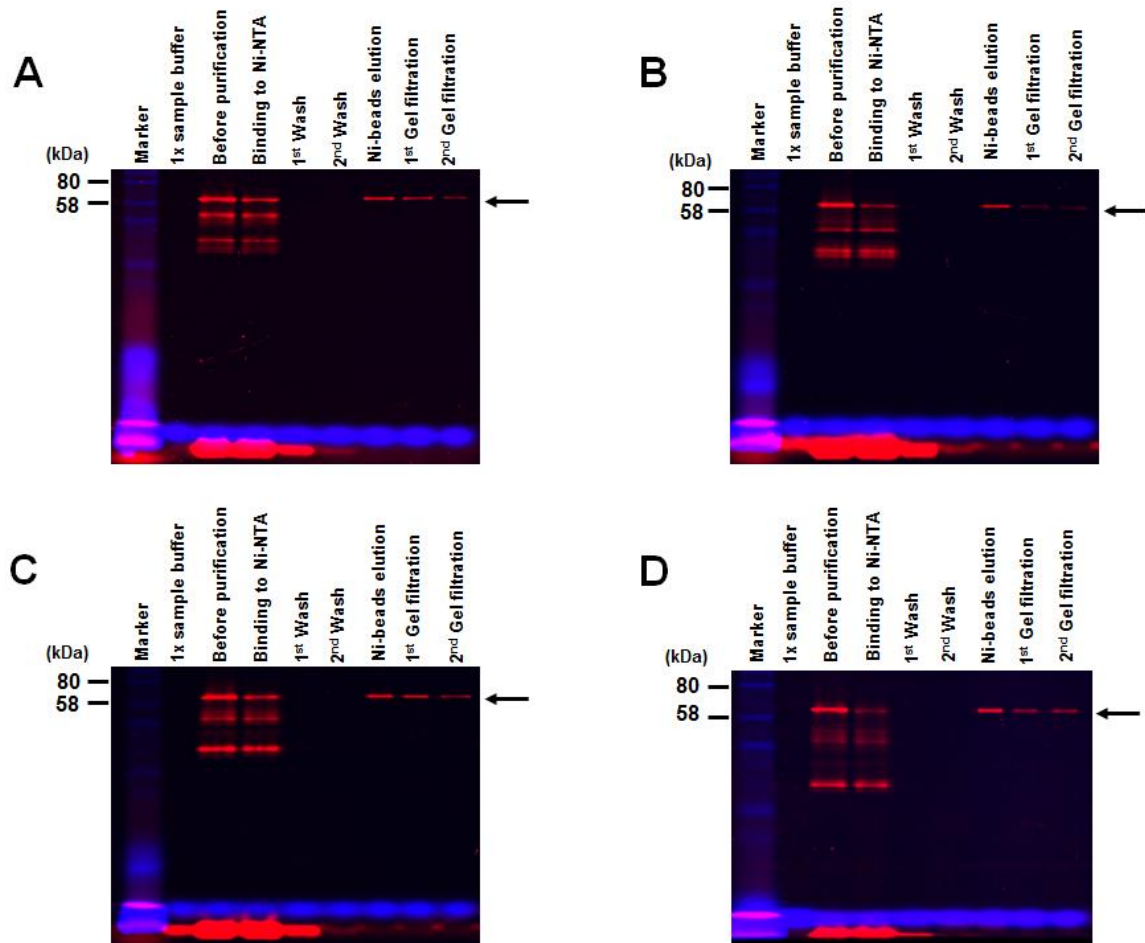


Figure 3-3. Fluorescence images of SDS-PAGE for expression and purification of HaloTag-scFvs labeled by TAMRA-PEO₁₂-Halo ligand. *Arrows* indicated full-length HaloTag-scFv. **(A)** Halo-(GGGS)₅-scFv(BPA) (MW ≈ 62.5 kDa), **(B)** Halo-(GGGS)₅-scFv(pTyr) (MW ≈ 61.5 kDa), **(C)** Halo-(GGGS)₅-scFv(BGP) (MW ≈ 61.8 kDa), **(D)** Halo-GGGS-scFv(BGP) (MW ≈ 60.6 kDa).

Next, fluorescence spectra were measured in the absence and presence of antigen to examine the quenching effect of Halo-(GGGS)₅-scFv(BPA) to TAMRA fluorophore (Figure 3-4). Fluorescence spectra of Halo-(GGGS)₅-scFv(BPA) labeled by TAMRA-PEO₁₂-Halo ligand measured by excitation TAMRA at 550nm showed fluorescence enhancement upon the addition of antigen (Figure 3-4A). This result suggested that TAMRA was quenched in the absence of antigen but the quenching effect was eliminated upon the antigen-binding as in the case of TAMRA-labeled scFv synthesized by nonnatural amino acid incorporation.

Fluorescent measurement of Halo-(GGGS)₅-scFv(BPA) labeled by TAMRA-Halo ligand with various linker length between TAMRA and HaloTag ligand revealed that no fluorescence enhancement was observed upon addition of BPA for the shortest linker (TAMRA-X-Halo ligand in which X indicates aminohexanoyl group) (Figure 3-4B). Probably, TAMRA did not interact with Trp residues in scFv due to the short linker. For 5-TAMRA-PEO₈-Halo ligand, antigen-dependent fluorescence increase was observed although the increase was smaller than that of PEO₁₂ linker. The longer linker PEO₂₄ also did not improve the fluorescence enhancement (Figure 3-4B). These results suggested that length of linker between fluorophore and HaloTag ligand was important for the interaction of fluorophore and Trp in scFv.

The apparent dissociation constants (K_d) obtained from Halo-(GGGS)₅-scFv(BPA) labeled with different linker TAMRA-Halo ligand compounds were almost identical. The K_d upon labeling with 5-TAMRA-PEO₈-Halo ligand, 5-TAMRA-PEO₁₂-Halo ligand and 5-TAMRA-PEO₂₄-Halo ligand were 1.2×10^{-8} M, 1.3×10^{-8} M and 5.3×10^{-9} M, respectively. These values were approaching the K_d value determined for TAMRA-labeled scFv(BPA) synthesized by nonnatural amino acid mutagenesis (2×10^{-8} M)¹¹. This indicated that fusion of HaloTag and labeling with TAMRA-ligands did not affect affinity of scFv(BPA) to antigen.

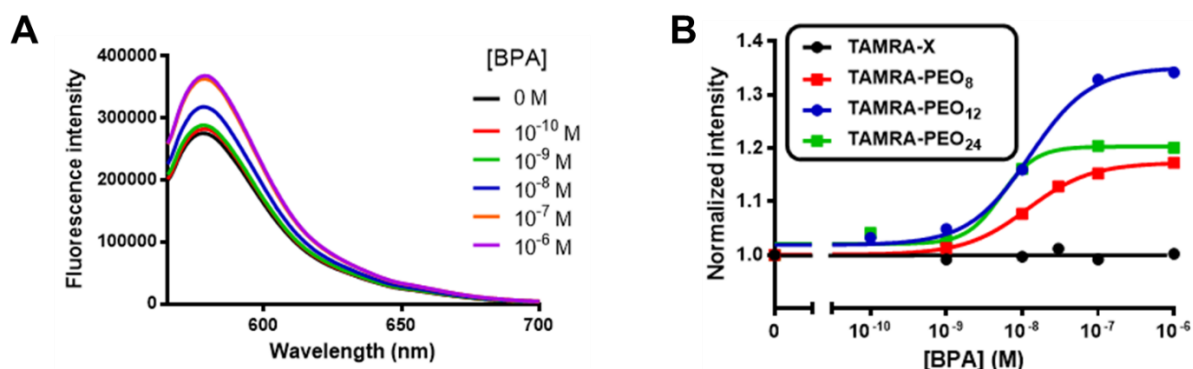


Figure 3-4. Fluorescence change of Halo-(GGGS)₅-scFv(BPA) upon antigen binding. (A) Fluorescence spectral change of Halo-(GGGS)₅-scFv(BPA) labeled by TAMRA-PEO₁₂-Halo ligand upon addition of antigen. (B) The titration curves of fluorescence intensity of Halo-(GGGS)₅-scFv(BPA) labeled by TAMRA-Halo ligands having different linkers.

Since TAMRA-PEO₁₂-Halo ligand showed the best result among tested TAMRA-Halo ligand compounds, I used it for the synthesis of HaloTag-scFv fusions against BGP and pTyr (Figure 3-3B and C). Both Halo-(GGGS)₅-scFv(BGP) and Halo-(GGGS)₅-scFv(pTyr) showed very low fluorescence enhancement (1.04- and 1.06-fold, respectively) in the presence of antigens (Figure 3-5). In case of anti-BGP scFv, Halo-GGGS-scFv(BGP) having a shorter linker peptide was also synthesized (Figure 3-3D) but showed no response to antigen addition (Figure 3-5).

The calculated K_d of Halo-(GGGS)₅-scFv(BGP) (3.4×10^{-9} M) indicated that affinity to antigen of anti-BGP scFv was comparable with the K_d of TAMRA-scFv synthesized using nonnatural amino acid mutagenesis (6.2×10^{-9} M). The K_d of Halo-(GGGS)₅-scFv(pTyr) was calculated as 6.4×10^{-7} M which also compared well to the K_d estimated for TAMRA-scFv synthesized using nonnatural amino acid mutagenesis (2.6×10^{-6} M).

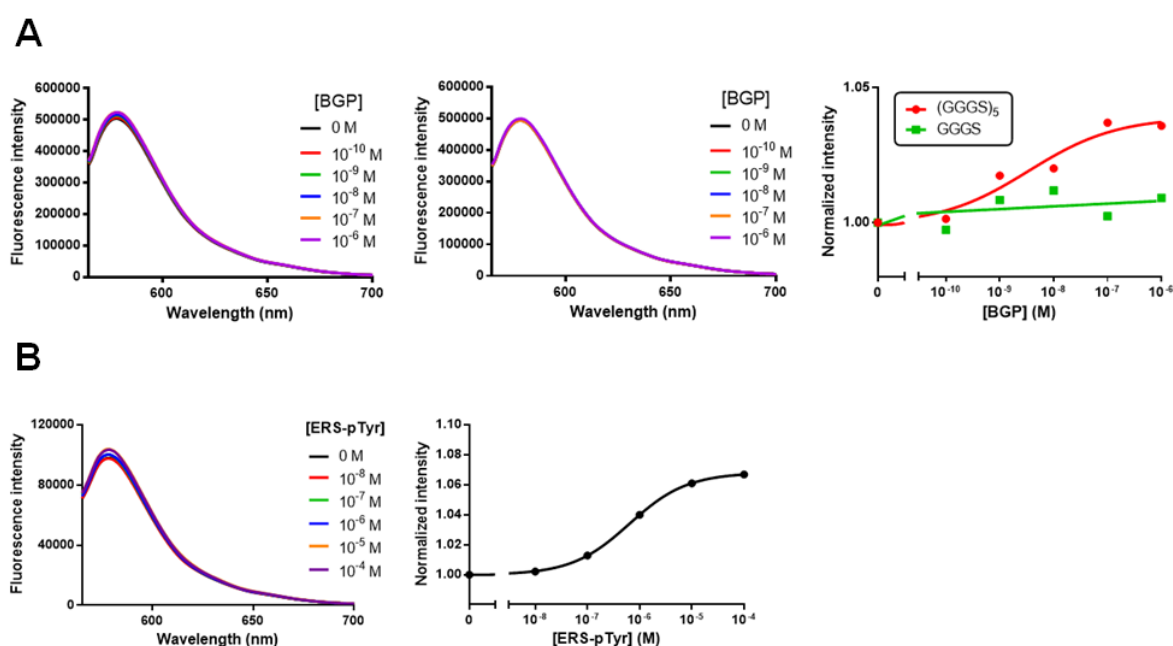


Figure 3-5. Fluorescence changes of Halo-(GGGS)_n-scFv(BGP) ($n = 1, 5$) and Halo-(GGGS)₅-scFv(pTyr) labeled by 5-TAMRA-PEO₁₂-Halo ligand upon antigen-binding. (A) *left*: Fluorescence spectra of Halo-(GGGS)₅-scFv(BGP), *middle*: Fluorescence spectra of Halo-GGGS-scFv(BGP), *right*: Titration curves. (B) *left*: Fluorescence spectra and *middle*: Titration curve of Halo-(GGGS)₅-scFv(pTyr).

3-3-3. Synthesis and fluorescence measurement of SNAP-scFvs

Although substitution of fluorophore-labeled nonnatural amino acid by HaloTag and its fluorescent ligand generated fluorescent-labeled scFvs which exhibited antigen-dependent enhancement of fluorescence intensity, the enhancements were very low. Therefore, I tried to replace HaloTag by SNAP-tag and constructed SNAP-(GGGS)₅-scFvs against BPA, BGP and pTyr. In fact, the molecular weight of SNAP-tag is smaller than HaloTag (19 kDa and 33 kDa, respectively), therefore, SNAP-tag is expected to be more flexible due to small size, and labeled fluorophore can easily interact with scFv.

SNAP-scFv fusions were synthesized by cell-free translation and subsequently labeled by fluorophore-SNAP ligand compounds. The reaction condition of the labeling with fluorophore-SNAP ligand was determined using SNAP-(GGGS)₅-scFv(BGP) and TAMRA-X-SNAP ligand. The results of fluorescence imaging of SDS-PAGE showed that 50 μ M fluorophore-SNAP ligand and 30 min incubation were suitable for labeling of SNAP-scFv fusions. Labeled proteins containing His₆-tag were purified by Ni-NTA magnetic beads. The synthesis and purification were analyzed by fluorescence imaging of SDS-PAGE gel (Figure 3-6) which indicated that all the SNAP-(GGGS)₅-scFvs against BPA, BGP, and pTyr were successfully synthesized and purified.

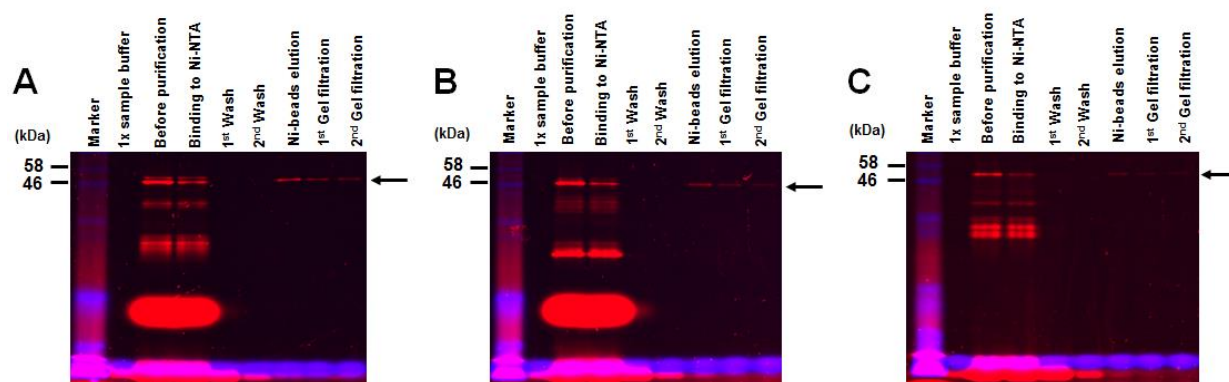


Figure 3-6. Fluorescence images of SDS-PAGE gels to analyze protein synthesis and purification of (A) SNAP-(GGGS)₅-scFv(BPA) (MW \approx 48.3 kDa), (B) SNAP-(GGGS)₅-scFv(BGP) (MW \approx 47.6 kDa and (C) SNAP-(GGGS)₅-scFv(pTyr) (MW \approx 47.3 kDa) labeled by TAMRA-PEO₁₂-SNAP ligand. Arrow indicated full-length SNAP-scFv fusion.

Fluorescence spectra of the three SNAP-(GGGS)₅-scFvs labeled by TAMRA-PEO₁₂-SNAP ligand exhibited significant fluorescence enhancement (Figure 3-7, *left*). The increases in fluorescence intensity were larger than those of HaloTag-(GGGS)₅-scFvs (Figure 3-7, *right*). The fluorescence increases of SNAP-(GGGS)₅-scFvs against BPA (1.8-fold) and pTyr (1.3-fold) were comparable to those obtained from TAMRA-scFvs synthesized by nonnatural amino acid mutagenesis (2-fold and 1.23-fold, respectively).

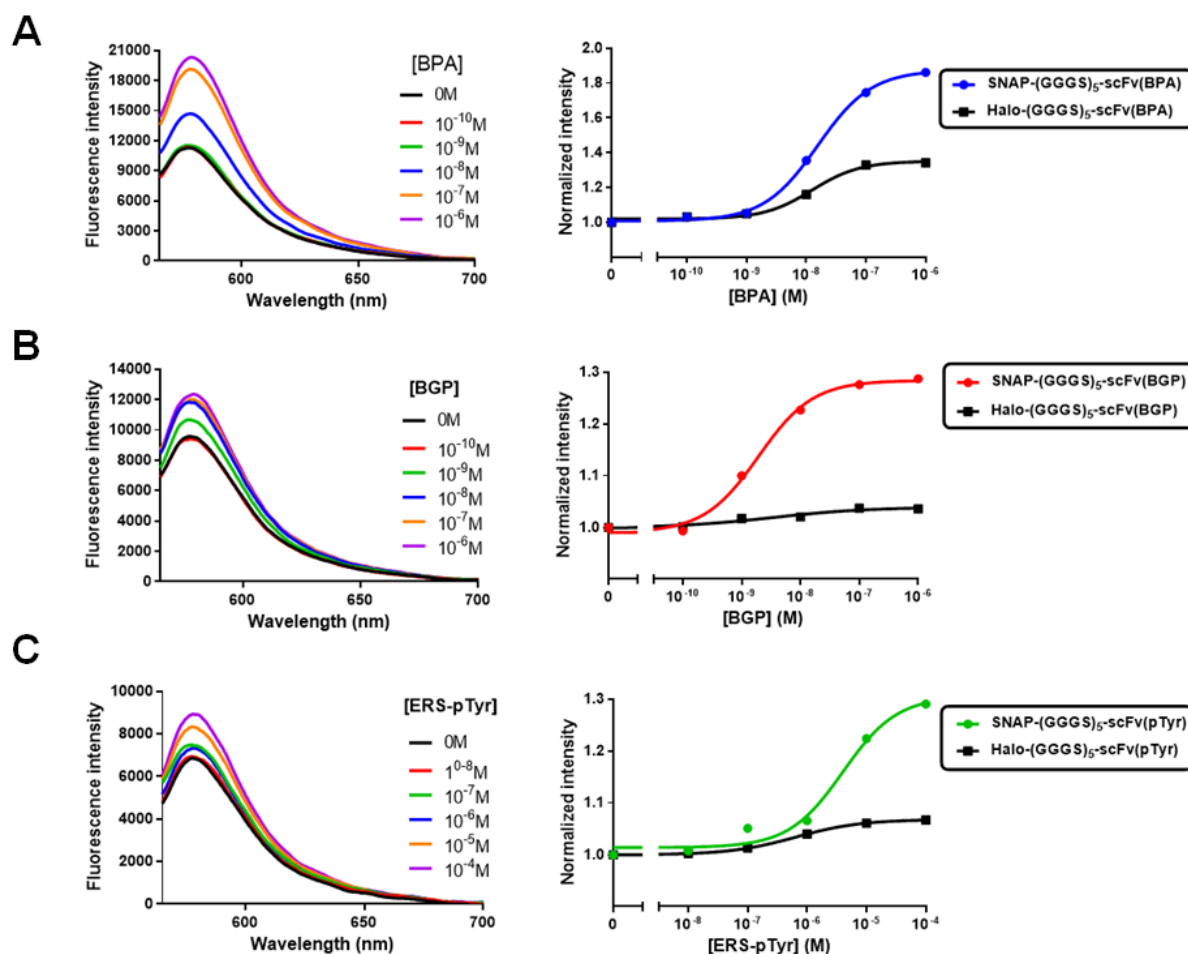


Figure 3-7. Fluorescence changes upon antigen-binding of (A) SNAP-(GGGS)₅-scFv(BPA), (B) SNAP-(GGGS)₅-scFv(BGP) and (C) SNAP-(GGGS)₅-scFv(pTyr) labeled with TAMRA-PEO₁₂-SNAP ligand. *Left*: fluorescence spectra of SNAP-scFvs. *Right*: comparison of titration curves of SNAP-(GGGS)₅-scFvs and HaloTag-(GGGS)₅-scFvs.

The apparent K_d values of the SNAP-(GGGS)₅-scFvs against BPA, BGP, and pTyr (1.6×10^{-8} M, 1.9×10^{-9} M, 4.0×10^{-6} M, respectively) were comparable to those of TAMRA-scFvs synthesized by nonnatural amino acid incorporation. Hence, fusion of SNAP-tag did not affect affinity of the scFvs to antigen as in case of HaloTag.

To explain the reason why SNAP-scFvs improved the fluorescence increase upon antigen-binding compared with HaloTag-scFvs, a hypothesis that the orientation of fluorophore-ligand to scFv was important for quenching effect was suggested. Analyzing the crystal structures of SNAP-tag and HaloTag (Figure 3-8) revealed that SNAP-tag ligand-binding site is close to C-terminus, as a result, labeled fluorophore can easily interact with scFv. But in case of HaloTag, the HaloTag ligand-binding site is close to N-terminus, thus, labeled fluorophore is brought far to scFv causing low quenching effect (Figure 3-8).

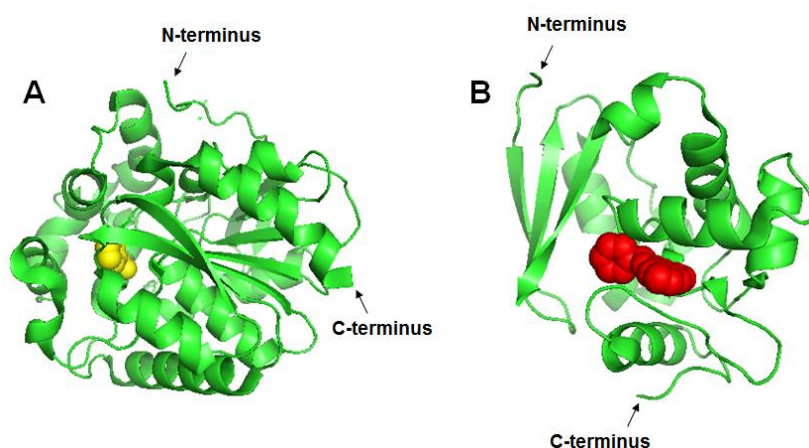


Figure 3-8. (A) Crystal structure of HaloTag¹² with ligand (benzoic acid) colored in *yellow* (Protein data bank (PDB) code: 3FBW). (B) Crystal structure of SNAP-tag¹³ with ligand (6-(benzyloxy)-9H-purin-2-amine) colored in *red* (PDB code: 3KZZ).

To check this hypothesis, I synthesized and analyzed scFv(BGP)-(GGGS)₂-Halo in which HaloTag was fused to C-terminus of scFv, consequently, HaloTag ligand binding site was expected to be in close distance to scFv. The resulting scFv(BGP)-(GGGS)₂-Halo labeled by TAMRA-PEO₁₂-Halo ligand exhibited an improvement of fluorescence enhancement (1.15-fold) compared with Halo-(GGGS)₅-scFv(BGP) (1.03-fold enhancement) (Figure 3-9). This indicated that the location of ligand-binding site of HaloTag is also an important factor, nonetheless N-terminal SNAP tag is more preferable than C-terminal HaloTag. The estimated

K_d of scFv(BGP)-(GGG)₂-Halo was 1.4×10^{-10} M, suggesting that fusion of HaloTag to C-terminus did not affect the antigen binding activity.

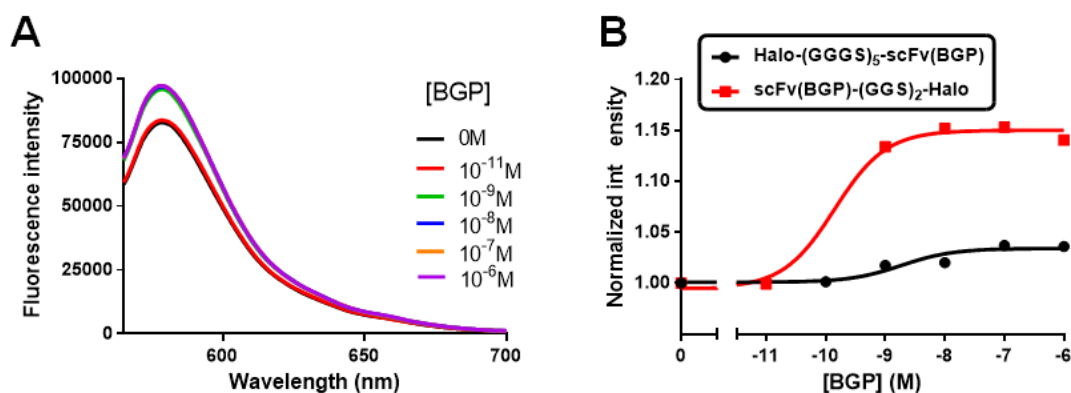


Figure 3-9. (A) Fluorescence spectral change of scFv(BGP)-(GGG)₂-Halo labeled with TAMRA-PEO₁₂-Halo ligand upon addition of BGP. (B) Comparison of titration curves of scFv(BGP)-(GGG)₂-Halo and Halo-(GGG)₅-scFv(BGP) labeled with TAMRA-PEO₁₂-Halo ligand.

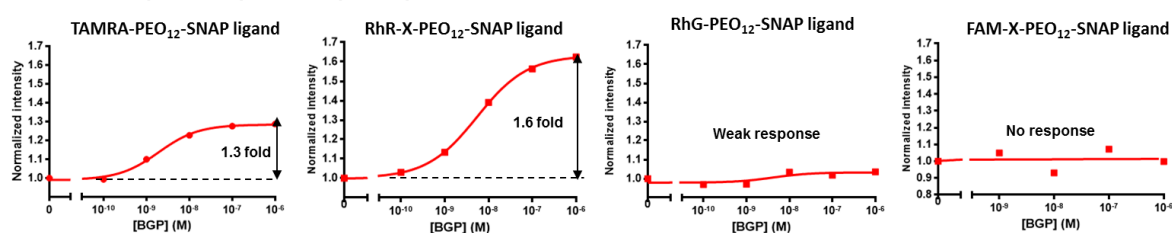
3-3-4. Quenching effect of SNAP-scFvs to different fluorophores

It has been reported that fluorescence response of fluorescent-labeled scFvs synthesized by nonnatural amino acid mutagenesis depends on the type of fluorophores¹⁴. According to this fact, I examined the use of different fluorophores to labeled SNAP-scFvs. Fluorophore-SNAP ligands such as RhR-X-PEO₁₂-, RhG-PEO₁₂- and FAM-X-PEO₁₂-SNAP ligands were chemically synthesized and conjugated to SNAP-(GGG)₅-scFvs against BGP, BPA, and pTyr. Fluorescence spectral changes upon the antigen-binding indicated that type of fluorophore affects the quenching effect of scFvs. In case of anti-BGP scFv, RhR-X-PEO₁₂-SNAP ligand produced 1.6-fold fluorescence enhancement, however, no or very little fluorescence enhancement was observed for RhG-PEO₁₂- and FAM-X-PEO₁₂-SNAP ligands (Figure 3-10A). Similarly, anti-BPA scFv labeled with RhR-X-PEO₁₂-SNAP ligand showed improved fluorescence response with 2.0-fold enhancement (Figure 3-10B) which was comparable to TAMRA-scFv(BPA) synthesized by nonnatural amino acid mutagenesis¹¹. On the other hand, SNAP-(GGG)₅-scFv(pTyr) showed similar fluorescence response when labeled with RhR-X-

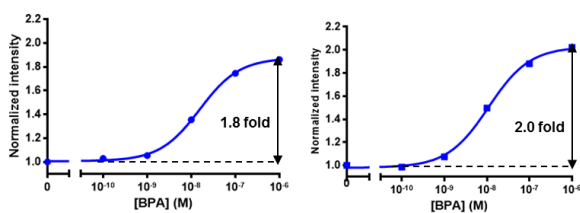
PEO₁₂-, RhG-PEO₁₂- and FAM-X-PEO₁₂-SNAP ligands, although TAMRA-PEO₁₂-SNAP ligand exhibited the highest fluorescence increase with 1.3-fold (Figure 3-10C).

These results suggested that the same fluorophore exhibited different fluorescence response for different scFvs. For example, when labeled by RhR-X-PEO₁₂-SNAP ligand, SNAP-(GGGS)₅-scFvs against BGP, BPA, and pTyr exhibited fluorescence increase 1.6-fold, 2.0-fold and 1.2-fold, respectively. FAM-X-PEO₁₂-SNAP ligand showed fluorescence response for anti-pTyr scFv but not for anti-BGP scFv.

A. SNAP-(GGGS)₅-scFv(BGP)



B. SNAP-(GGGS)₅-scFv(BPA)



C. SNAP-(GGGS)₅-scFv(pTyr)

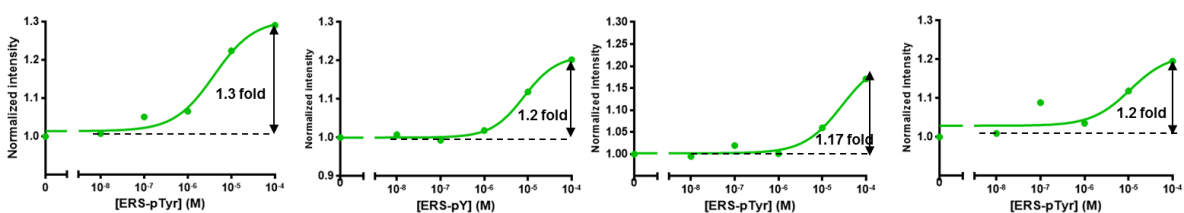


Figure 3-10. Antigen titration curves of fluorescence of SNAP-(GGGS)₅-scFvs labeled by different fluorophores. *From left to right* are data of TAMRA-PEO₁₂-, RhR-X-PEO₁₂-, RhG-PEO₁₂- and FAM-X-PEO₁₂-SNAP ligands.

3-3-5. Effect of linker length on fluorescence response

The effect of linker length of fluorophore-SNAP ligand as well as linker peptide length between SNAP-tag and scFv were examined. In case of Halo-(GGGS)₅-scFv(BPA), linker length between fluorophore and HaloTag ligand affected the quenching effect (Figure 3-4B). Therefore, TAMRA-SNAP ligands with different linkers were synthesized and conjugated to SNAP-(GGGS)₅-scFv against BPA. Fluorescence response upon antigen addition showed that the fluorescence enhancement strongly depended on the linker length, and PEO₈ and PEO₁₂ were the most suitable while longer and shorter linkers caused a decrease in fluorescence response (Figure 3-11A). On the other hand, SNAP-(GGGS)₅-scFv(BPA) labeled with RhR-SNAP ligand carrying X-PEO₁₂ or X-PEO₂₄ linker revealed that the longer linker showed slightly better fluorescence response (Figure 3-11B).

In case of SNAP-(GGGS)₅-scFv against BGP, the effect of linker length between TAMRA-SNAP ligand and RhR-SNAP ligand were also examined. Fluorescence measurement suggested that length of linker also affected fluorescence response of this biosensor to antigen (Figure 3-12), although in a less significant manner than SNAP-(GGGS)₅-scFv(BPA) labeled by TAMRA-SNAP ligands.

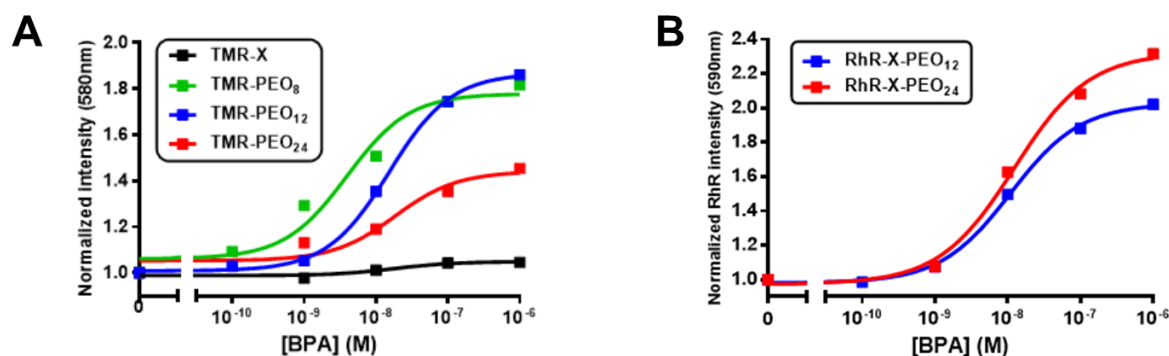


Figure 3-11. Titration curves of fluorescence of SNAP-(GGGS)₅-scFv(BPA) labeled by fluorophore-SNAP ligands with various linker length. (A) TAMRA-SNAP ligands, (B) RhR-SNAP ligands.

3-3-6. Construction of double labeled scFvs by fusing SNAP-tag and fluorescent protein

In previous chapter, double labeled anti-pTyr scFv with TAMRA-linked nonnatural amino acid and fluorescent proteins (EGFP or HaloTag labeled with RhG-Halo ligand) had been synthesized, which showed fluorescence ratio change upon the antigen-binding. Double labeled scFvs enable ratiometric detection of antigen, and therefore, are available under heterogeneous conditions such as in live cells where the labeled scFv concentration cannot be determined.

Prior to the synthesis of double labeled scFvs by fusing SNAP-tag and fluorescent proteins, double labeled anti-BGP scFvs were synthesized by introducing TAMRA-X-AF and fusing with EGFP or HaloTag in order to confirm anti-BGP scFv is available to double labeling as well as anti-pTyr scFv. TAMRA-scFv(BGP)-EGFP and TAMRA-scFv(BGP)-Halo, which was subsequently labeled by RhG-X-Halo ligand, were synthesized and purified. Fluorescence imaging of SDS-PAGE gel indicated successful synthesis and purification of TAMRA-scFv fused with EGFP or RhG-conjugated HaloTag (Figure 3-14).

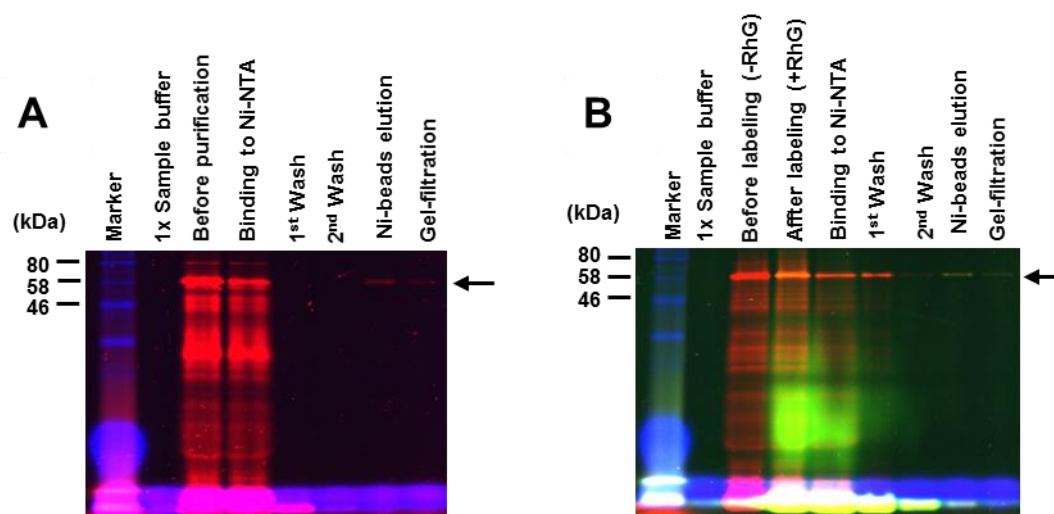


Figure 3-14. Fluorescence images of SDS-PAGE gels of (A) TAMRA-scFv(BGP)-EGFP and (B) TAMRA-scFv(BGP)-Halo labeled with RhG-Halo ligand. Arrow indicated full-length protein, molecular weight of TAMRA-scFv(BGP)-EGFP and TAMRA-scFv(BGP)-Halo were 55 kDa and 62 kDa, respectively.

To examine FRET between EGFP and TAMRA, EGFP was excited at 470 nm. Without antigen, very low TAMRA fluorescence was observed at 580 nm, but the TAMRA fluorescence increased dependently on BGP concentration without significant change in EGFP fluorescence (Figure 3-15A). Fluorescence ratio of TAMRA/EGFP exhibited 2.4-fold increase. The estimated K_d (4.8×10^{-9} M) was almost identical to that of TAMRA-scFv(BGP), suggesting that EGFP did not affect the affinity of scFv to antigen. The antigen-dependent enhancement of TAMRA intensity was also detected by directly exciting TAMRA at 550 nm. TAMRA-scFv(BGP)-Halo labeled with RhG showed similar fluorescence ratio change (2.4-fold) with estimated K_d of 3.3×10^{-9} M (Figure 3-13B). These results demonstrated that fusion of anti-BGP scFv with fluorescent proteins was available to generate double-labeled scFvs without affecting the antigen-binding affinity as in the case of anti-pTyr scFv.

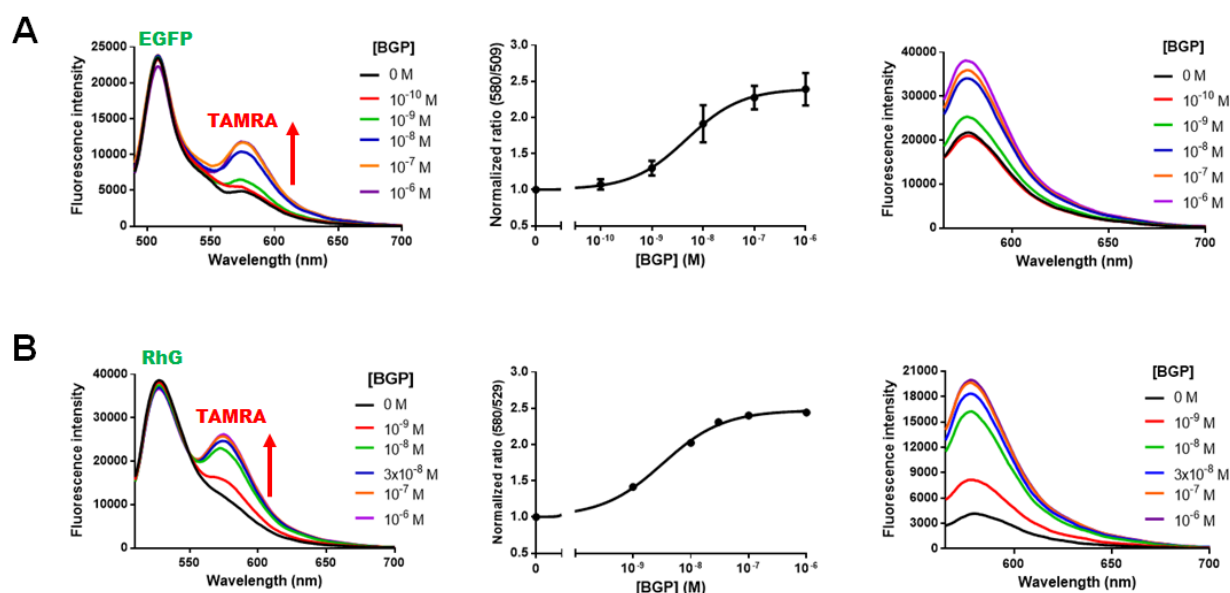


Figure 3-15. Fluorescence analysis of (A) TAMRA-scFv(BGP)-EGFP and (B) TAMRA-scFv(BGP)-Halo labeled with RhG-X-Halo ligand. *Left:* Fluorescence spectral change upon antigen addition with excitation of EGFP at 470 nm or RhG at 495 nm, *Middle:* Titration curve of the fluorescence intensity ratio (data of TAMRA-scFv(BGP)-EGFP are mean \pm SD of three analyses), *Right:* Fluorescence spectral change upon antigen addition with excitation of TAMRA at 550 nm.

Next, SNAP-scFv against BGP was fused with EGFP at the N-terminus to form double labeled scFvs which allowed FRET between EGFP and fluorophore linked to SNAP ligand. In addition, yellow fluorescent protein (YFP) was also employed as a FRET donor. The double labeled scFvs were synthesized by cell-free translation and subsequently labeled by RhR-X-PEO₁₂-SNAP ligand. Then, the His₆-tag-containing full-length products were purified by Ni-NTA magnetic beads. Protein synthesis and purification were analyzed by SDS-PAGE. Fluorescence imaging of SDS-PAGE gel confirmed that double labeled scFvs were synthesized and purified (Figure 3-16).

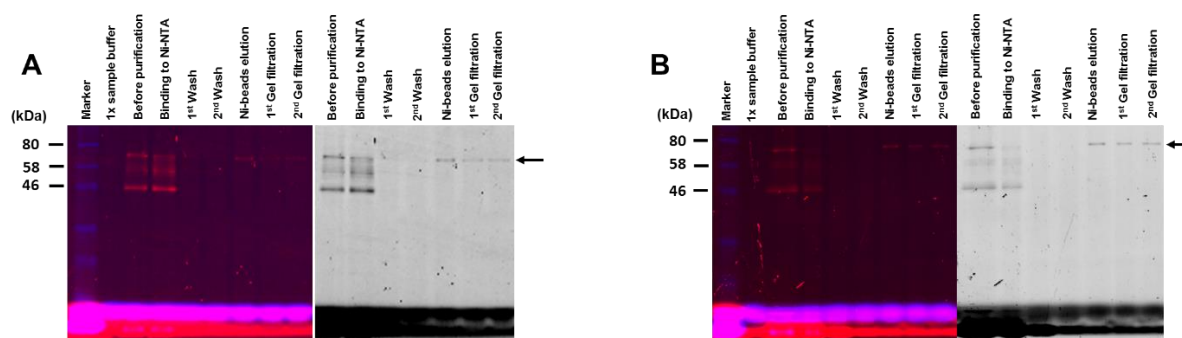


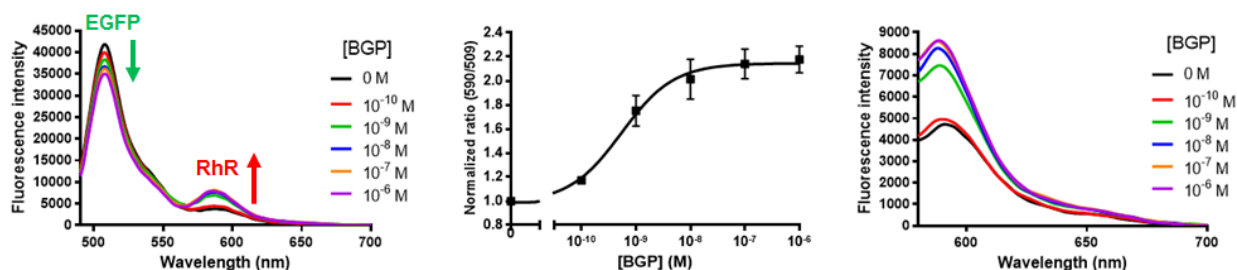
Figure 3-16. Fluorescence image of SDS-PAGE gels of (A) EGFP-SNAP-scFv(BGP) and (B) YFP-SNAP-scFv(BGP) labeled by RhR-X-PEO₁₂-SNAP ligand (estimated molecular weight of both proteins were 73 kDa). Arrow indicated full-length product.

Fluorescence measurement of EGFP-SNAP-scFv(BGP) labeled by RhR-X-PEO₁₂-SNAP ligand was performed by exciting EGFP at 470 nm (Figure 3-17A). In the absence of antigen, the peak of EGFP at 509 nm is dominant and small peak of RhR at 590 nm was observed. In the presence of antigen, RhR intensity exhibited antigen-dependent enhancement. EGFP fluorescence slightly decreased, suggesting that FRET between EGFP and RhR occurred and was slightly enhanced in the presence of antigen. As a result of these fluorescence intensity changes, the fluorescence intensity ratio (RhR/EGFP) increased 2-fold. Excitation of RhR at 570 nm also showed enhancement of RhR intensity upon antigen addition, confirming the enhancement of RhR fluorescence under excitation of EGFP was due to quenching of RhR by scFv and antigen-dependent removal of quenching effect.

In addition, YFP-SNAP-scFv(BGP) labeled by RhR-X-PEO₁₂-SNAP ligand was analyzed by exciting YFP at 508 nm (Figure 3-17B). Upon addition of antigen, similar fluorescence spectral change was observed. Fluorescence ratio of RhR/YFP increased 1.8-fold.

The antigen-dependent enhancement of RhR intensity was confirmed by measuring fluorescence of RhR with excitation wavelength at 570 nm.

A



B

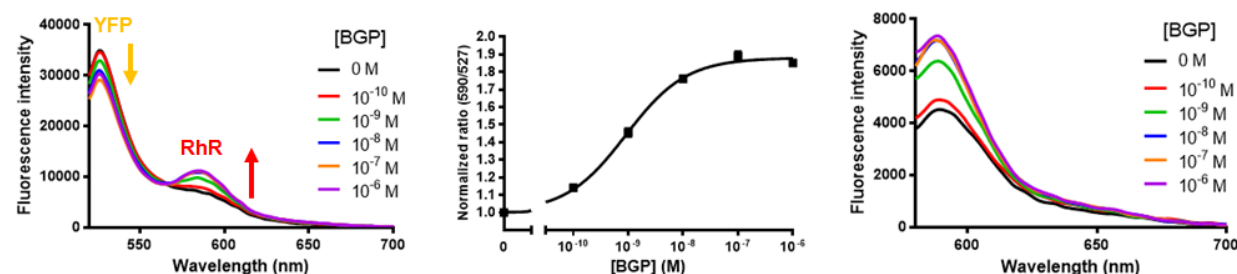


Figure 3-17. Fluorescence analysis of (A) EGFP-SNAP-scFv(BGP) and (B) YFP-SNAP-scFv(BGP) labeled by RhR-X-PEO₁₂-SNAP ligand. *Left:* Fluorescence spectral change upon antigen addition. Excitation wavelength was 470 nm for EGFP and 508 nm for YFP. *Middle:* Titration curve of fluorescence intensity ratio (fluorescence ratio values were mean \pm SD of three (EGFP fusion) or two (YFP fusion) analyses). *Right:* Fluorescence spectral change under excitation of RhR at 570 nm.

The apparent K_d values were estimated as 5.5×10^{-10} M and 9.1×10^{-10} M for EGFP- and YFP-fused SNAP-scFvs, respectively. These values were comparable to that of SNAP-scFv without fluorescent protein, suggesting that the fluorescent proteins did not affect the antigen-binding affinity of scFv.

Taken together, these results demonstrated that fluorescent protein-SNAP-scFv fusion labeled with fluorophore-SNAP ligand is a useful tool for ratiometric detection of antigen. Compared with conventional FRET probes that exhibit FRET change upon ligand-induced conformational change, the double labeled scFv does not require conformational change and can be generated against a wide variety of target molecules. This antibody-based fluorescent ratio biosensor is genetically-encoded, and therefore, it will be available to live cell imaging.

3-4. Conclusion

In this chapter, antibody-based genetically-encoded fluorescent biosensors which can be expressed without introducing fluorophore-linked nonnatural amino acid were developed by using protein-tag (HaloTag or SNAP-tag) and their fluorescent ligands. The Halo-scFvs and SNAP-scFvs exhibited fluorescence enhancement in the presence of antigen. Orientation of protein-tag to scFv, type of fluorophore, type of scFv and linker length between fluorophore–ligand was found to significantly affect fluorescence response of the biosensors. In addition, the affinity of scFv was not changed by fusion of HaloTag and SNAP-tag.

Double labeled scFvs were developed as antibody-based genetically-encoded fluorescent ratio biosensors by linking the SNAP-scFv with fluorescent proteins (FP). EGFP-SNAP-scFv and YFP-SNAP-scFv allowed FRET between FP and labeled fluorophore and antigen-dependent fluorescence enhancement of fluorophore, as consequence, antigen-dependent fluorescence ratio enhancement of fluorophore/FP ratio.

3-2. References

- (1) Imamura H., Huynh Nhat K.P., Togawa H., Saito K., Iino R., Kato-Yamada Y., Nagai T., Noji H. Visualization of ATP levels inside single living cells with fluorescent resonance energy transfer-based genetically encoded indicators. *Proc. Natl. Acad. Sci. USA* **106**(37): 15651-15656 (2009).
- (2) Sato M., Ozawa T., Inukai K., Asano T., Umezawa Y. Fluorescent indicators for imaging protein phosphorylation in single living cells. *Nat. Biotechnol.* **20**: 287-294 (2002)
- (3) Los G. V., Encell L. P., McDougall M. G., Hartzell D. D., Karassina N., Zimprich C., Wood M. G., Learish R., Ohana R. F., Urh M., Simpson D., Mendez J., Zimmerman K., Otto P., Vidugiris G., Zhu J., Darzins A., Klaubert D. H., Bulleit R. F., Wood K. V. HaloTag: a novel protein labeling technology for cell imaging and protein analysis. *ACS Chem. Biol.* **3**(6): 373-382 (2008)
- (4) Keppler A., Gendreizig S., Gronemeyer T., Pick H., Vogel H., Johnsson K. A general method for the covalent labeling of fusion proteins with small molecules in vivo. *Nat. Biotechnol.* **21**: 86-89 (2003)
- (5) Juillerat A., Gronemeyer T., Keppler A., Gendreizig S., Pick H., Vogel H., Johnsson K. Directed evolution of O⁶-alkylguanine-DNA alkyltransferase for efficient labeling of fusion proteins with small molecules in vivo. *Chem. Biol.* **10**: 313-317 (2003)
- (6) Gautier A., Juillerat A., Heinis C., Corrêa, Jr. I. R., Kindermann M., Beaufils F., Johnsson K. An engineered protein tag for multiprotein labeling in living cells. *Chem. Biol.* **15**: 128-136 (2008)
- (7) Rezq R., El-Fazaa S., Gharbi N., Mornaqui B. Bisphenol A and human chronic diseases: current evident, possible mechanisms, and future perspectives. *Environ. Int.* **64**: 83-90 (2014)
- (8) Robinson L., Miller R. The impact of bisphenol A and phthalates on allergy, asthma, and immune function: a review of latest findings. *Curr. Environ. Health. Rep.* **2**(4): 379-387 (2015)
- (9) Tsutsui H., Jinno Y., Tomita A., Niino Y., Yamada Y., Mikoshiba K., Miyawaki A., Okamura Y. Improved detection of electrical activity with a voltage probe based on a voltage-sensing phosphatase. *J. Physiol.* **591**(18): 4427-4437 (2013)

- (10) Hohsaka T., Kajihara D., Ashizuka Y., Murakami H., Sisido M. Efficient incorporation of non-natural amino acids with large aromatic groups into streptavidin in vitro protein synthesizing systems. *J. Am. Chem. Soc.* **121**: 34-40 (1999)
- (11) Abe R., Ohashi H., Iijima I., Ihara M., Takagi H., Hohsaka T., Ueda H. “Quenchbodies”: Quench-based antibody probes that show antigen-dependent fluorescence. *J. Am. Chem. Soc.* **133**: 17386-17394 (2011)
- (12) Stsiapanava A., Dohnalek J., Gavira J. A., Kutý M., Koudelakova T., Damborsky J., Kuta Samatanova I. Atomic resolution studies of haloalkane dehalogenases DhaA04, DhaA14 and DhaA15 with engineered access tunnels. *Acta, Crystallogr., Sect. D*, **66**: 962-969 (2010)
- (13) Mollwitz B., Brunk E., Schmitt S., Pojer F., Bannwarth M., Schiltz M., Rothlisberger U., Johnsson K. Directed evolution of the suicide protein O6-Alkylguanine-DNA Alkyltransferase for increased reactivity results in an alkylated protein with exceptional stability. *Biochemistry* **51**(5): 986-994 (2012)
- (14) Ueda H., Dong, J. From fluorescence polarization to Quenchbody: Recent progress in fluorescent reagentless biosensors based on antibody and other binding proteins. *Biochim. Biophys. Acta.* **1844**(11): 1951-1959 (2014)

Chapter 4

Application of genetically-encoded antibody-based biosensor to live-cell imaging

4-1 Introduction

In chapter 3, antibody-based fluorescent ratio biosensors have been developed by fusion of fluorescent protein (EGFP or YFP) and SNAP-tag to scFvs. The biosensors are single chain, genetically-encoded, therefore, can be expressed in live cells. In this chapter, I investigated the availability of the genetically-encoded fluorescent ratio biosensor to live cell imaging. To this purpose, EGFP-SNAP-scFv against BGP ((bone gla protein, or osteocalcin) was expressed on the surface of mammalian cells to detect extracellular BGP. It has been reported that functional scFv can be expressed on mammalian cells surface¹.

BGP is a non-collagenous protein which is produced by osteoblasts during bone formation. Initially, this 5.6 kDa protein is used as a biomarker of osteoblastic bone formation, however, recent studies reveal that BGP also acts as a hormone which regulates metabolism, reproduction and cognition²⁻³. Conventional method for BGP detection is enzyme-linked immunosorbent assay (ELISA). Recently, fluorescent biosensors named Ultra Q-body have been reported and demonstrated detection of BGP secreted by differentiated osteosarcoma cells U2OS⁴. However, Ultra Q-body requires chemical modification that limits its expression in live cells.

Figure 4-1 illustrates the detection of BGP on cell surface using EGFP-SNAP-scFv labeled with fluorophore-SNAP ligand. The biosensor is expressed on osteosarcoma U2OS cells to detect secreted BGP during differentiation of U2OS cells to osteoblasts. The expected mechanism is as follows: without BGP secretion, FRET from EGFP to fluorophore occurs, while the fluorophore is quenched by scFv. When U2OS cells are induced to differentiate to osteoblast, they secrete BGP to extracellular environment. Binding of BGP to EGFP-SNAP-scFv(BGP) eliminates the fluorescence quenching and enhances the fluorophore fluorescent intensity. As consequence, fluorescence ratio of fluorophore and EGFP is expected to increase as observed *in vitro*. Fluorescence of cells expressing the biosensor is visualized under confocal fluorescence microscope. In addition to U2OS cells, Hela S3 cells expressing EGFP-SNAP-scFv on cell surface were also used to detect exogenously added BGP peptide at defined concentration.

The successful development of the present methodology will enable us to detect a variety of target molecules in live cells and become a novel and powerful technique for bio-imaging.

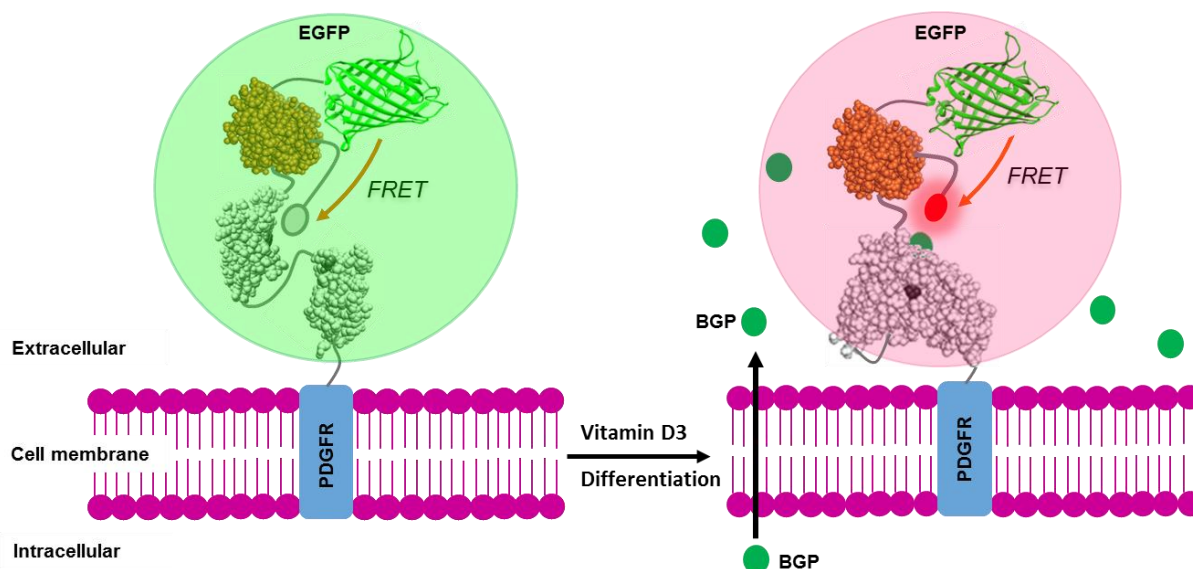


Figure 4-1. Detection of BGP secreted by osteosarcoma U2OS cells during differentiation to osteoblasts. EGFP-SNAP-scFv(BGP) is expressed and incorporated on the membrane of U2OS cells by fusion with the platelet derived growth factor receptor (PDGFR) transmembrane domain. Expressed EGFP-SNAP-scFv(BGP) is labeled by RhR-X-PEO₁₂-SNAP ligand. Without BGP, fluorescence ratio RhR/EGFP is low because of quenching of RhR. When U2OS cells are induced to differentiate to osteoblasts, they secrete BGP to extracellular environment. Binding of BGP to EGFP-SNAP-scFv(BGP) results in enhancement of RhR fluorescence, and as consequence, fluorescence ratio RhR/EGFP.

4-2. Materials and Method

4-2-1. Materials

KOD-Plus DNA polymerase was purchased from TOYOBO (Osaka, Japan). Primers for PCR were custom synthesized by Eurofins Genomics (Italy). In-Fusion HD Cloning kit was from Clontech (USA). pDisplay vector was from Invitrogen (USA), Genopure Plasmid Midi Kit was purchased from Roche (Germany), *E. coli* DH5 α was from TaKaRa (USA), FuGENE HD transfection reagent was obtained from Promega (USA). PlusgrowII, DMEM (high glucose), D-PBS(-), 0.25% Trypsin/1mM EDTA were purchased from Nacalai tesque (Japan). DMEM (high glucose, without L-Glutamine and phenol red), Penicillin/Streptomycin/Amphotericin B suspension (100X), L-Glutamine solution (100X) were from Wako (Japan). Fetal Bovine Serum was from Biowest (France). Opti-MEM (1X) was obtained from Gibco (USA). Cholecalciferol (vitamin D3) was from Tokyo Chemical Industry (Japan). The human cervical cancer cell HeLa S3 was obtained from RIKEN (Japan). The human osteosarcoma cell U2OS (ATCC[®] HTB-96[™]) was purchased from American Type Culture Collection (USA). 35 mm polystyrene cell culture dishes were purchased from Trueline (USA), 35 mm collagen-coated glass bottom dishes were from Matsunami (Japan).

4-2-2. Vector for mammalian cell expression

The cDNA of EGFP-SNAP-scFv(BGP) was amplified by PCR with forward primer (5'-GGG GCC CAG CCG GCC ATG AGT AAA GGA GAA GAA CTT TTC ACT GGA G-3') and reverse primer (5'-GTT CGT CGA CCT GCA GAG AGC CAC CGC CCC GTT TTA TTT CCA GCT TGG-3'). The vector for mammalian cell surface expression pDisplay was linearized by PCR with forward primer (5'-CTG CAG GTC GAC GAA CAA AAA CTC ATC TCA G-3') and reverse primer (5'-GGC CGG CTG GGC CCC AGC ATA ATC TGG AAC-3'). PCR products were analyzed by agarose gel electrophoresis and purified. DNA fragment of EGFP-SNAP-scFv(BGP) was cloned between Ig κ -chain leader sequence and the *myc* epitope/PDGFR-transmembrane domain (PDGFR-TM) using In-Fusion cloning kit.

E. coli DH5 α carrying pDisplay-EGFP-SNAP-scFv(BGP) was cultured in 50 ml PlusgrowII containing 100 μ g/ml Ampicillin to amplify the number of plasmid. After overnight culture at 37°C, *E. coli* cells were lysed and the plasmid was purified by Genopure plasmid midi kit.

4-2-3. Expression of EGFP-SNAP-scFv(BGP) in HeLa and U2OS cells

HeLa S3 cells and U2OS cells were maintained in DMEM (10% FBS, 1X antibiotics) at 37°C, 5% CO₂. To check the expression of EGFP-SNAP-scFv(BGP), HeLa S3 cells and U2OS cells were seeded on 35 mm polystyrene dish and cultured until about 50-60% confluency in DMEM (10% FBS, 1X antibiotics) at 37°C, 5% CO₂. The cells were transiently transfected with 1 µg plasmid by FuGENE HD transfection reagent. After 36 hour incubation at 37°C, 5% CO₂, the expressed EGFP-SNAP-scFv(BGP) on cell surface was labeled with RhR-X-PEO₁₂-SNAP ligand. The cells were incubated in DMEM (-Phenol red/10%FBS) containing 5 µM RhR-X-PEO₁₂-SNAP ligand at 37°C, 5% CO₂ for 30 min. Then, the cells were washed once with DMEM (-Phenol red/10%FBS), three times with D-PBS(-) to remove unbound RhR-SNAP ligand, and DMEM (-Phenol red/-FBS) was added to check the labeling result under inverted fluorescence microscope Olympus FSX100 (Olympus, Japan). EGFP was excited at 460 – 495 nm and emission was recorded at 505 nm. RhR was excited at 530-550 nm and emission was recorded at 570 nm.

Cell lysis was performed by detaching the cells with 0.25% Trypsin in 1 mM EDTA, then, DMEM (10% FBS) was added to inhibit Trypsin and suspended the cells. Cell pellet was collected by centrifugation and lysed by addition of lysis buffer containing 20 mM Tris-HCl (pH 7.5), 150 mM NaCl, 0.5% (w/v) sodium deoxycholate, 0.1% (w/v) SDS, 1% (w/v) Triton-X100, 1X protease inhibitor cocktail and 1mM EDTA. The lysis mixture was shake for 5 min at room temperature. Crude fraction was taken after cell lysis, and soluble fraction was taken after the lysis mixture was centrifuged to separate soluble phase and insoluble phase. The samples were mixed with SDS-PAGE sample buffer and heated at 95°C for 5 min (excepted samples from U2OS cells) before applying to 12% polyacrylamide SDS-PAGE gels. The SDS-PAGE gels were visualized by a fluorescence scanner (FMBIO-III; Hitachi Software Engineering, Japan) to check expression of EGFP-SNAP-scFv(BGP) in HeLa S3 cells and U2OS cells. EGFP was excited at 488 nm and visualized at 520 nm, RhR was excited at 532 nm and visualized at 580 nm. Prestained marker was visualized with excitation at 635 nm and detection at 670 nm.

4-2-4. Fluorescence imaging of cells expressing pDisplay-EGFP-SNAP-scFv(BGP)

HeLa S3 cells were cultured in 35 mm collagen-coated glass bottom dish until about 50-60% confluency in DMEM (10% FBS, 1X antibiotics) at 37°C, 5% CO₂. The cells were transiently transfected with 1 µg plasmid by FuGENE HD transfection reagent. After 36 hour

incubation at 37°C, 5% CO₂, the expressed EGFP-SNAP-scFv(BGP) was labeled by 5 μM RhR-X-PEO₁₂-SNAP ligand in DMEM (- Phenol red/10% FBS) and incubate at 37°C, 5% CO₂ for 30 min. After labeling, the cells were washed once with DMEM (-Phenol red/10%FBS), three times with D-PBS(-) to remove unbound RhR-X-PEO₁₂-SNAP ligand.

Cells were incubated in 2 mL DMEM (- Phenol red/-FBS) at 37°C, 5% CO₂ for 12 hours, and subjected to fluorescence imaging. To examine the response upon addition of BGP peptide, 2 mL DMEM (- Phenol red/-FBS) containing 10⁻⁴ M BGP-C7 peptide was added and cells were incubated at 37°C, 5% CO₂ for 12 hours before imaging.

Fluorescence imaging was performed by laser scanning confocal microscope Olympus Fluoview FV1000 (Olympus, Japan) with 60X oil immerse objective lens. At the time of imaging, cells were about 80-90% confluency. Live-cell imaging was performed at room temperature. To observe FRET between EGFP and RhR, EGFP was excited at 473 nm. EGFP emission was recorded from 490 nm to 540 nm and RhR emission was recorded from 595 nm to 675 nm.

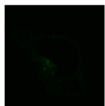
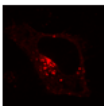
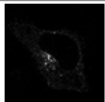
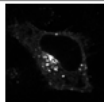
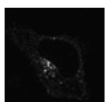
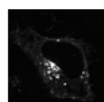
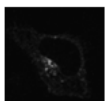
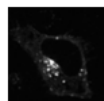
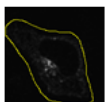
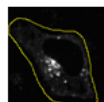
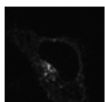

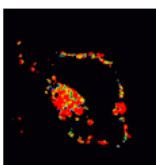
In case of U2OS cells, cell culture, transient transfection of pDisplay-EGFP-SNAP-scFv(BGP) and labeling by RhR-X-PEO₁₂-SNAP ligand were performed same as HeLa S3 cells. For osteoblast induction, after labeling, the cells were incubated in DMEM (-Phenol red/-FBS) for 24 hours at 37°C, 5% CO₂. Then, the cells were incubated at 37°C, 5% CO₂ for 36 hours in DMEM (-Phenol red) supplemented with 0.1% FBS and 10⁻⁷ M vitamin D3 (Cholecalciferol). After the treatment, the cells were used for fluorescence imaging. As a control, non-induced cells were used for fluorescence imaging without incubation with vitamin D3. The fluorescence imaging was carried out same as HeLa S3 cells.

4-2-5. Image analysis

Fluorescence images obtained from confocal microscope were analyzed by ImageJ software (<http://imagej.nih.gov/ij/>). The analysis method was similar to that described by Kardash E. and coworkers⁵. Table 4-1 represented data processing steps and output images.

The fluorescence intensity obtained from EGFP and RhR images were used for calculation of fluorescence ratio (RhR/EGFP) of each cell. The histograms represent the distribution of fluorescence ratio of cells in tested sample and control sample were made with bin width 0.25 for HeLa S3 cells and bin with 0.025 for U2OS cells. The histograms were fitted with Lorentzian distribution for HeLa S3 cells and Sum of two Lorentzian distribution for U2OS cells by GraphPad Prism (GraphPad, CA, USA).

Table 4-1. Fluorescence image analysis by ImageJ software

Processing step	ImageJ command	Output
Select region of interest and crop image	Select ROI → Image → Crop	<div>EGFP</div>  <div>RhR</div> 
Image type conversion (RGB to 32bit)	Image → Type → 32 bit	 
Background correction	Process → Subtract background (rolling ball radius 50)	 
Align RhR image to EGFP image	Plugins → MultistackReg	 
Smooth filter	Process → Smooth	
Measure fluorescent intensity	Select ROI → Analyze → Measure	 
Threshold (RhR image only)	Image → Adjust → Threshold	 
Ratio calculation (RhR/GFP)	Plugins → Ratio Plus	 <div>Ratio RhR/EGFP</div> <div>8.0</div> <div>4.0</div>
Look up table assignment	Plugins → Lookup Tables → Blue Green Red	
Range adjustment	Image → Adjust → Brightness/Contrast	
Export image	Image → Type → RGB color → Save as	

4-3. Results and discussion

4-3-1. Expression of EGFP-SNAP-scFv(BGP) in HeLa S3 cells and U2OS cells

In order to express EGFP-SNAP-scFv(BGP) on cell surface, EGFP-SNAP-scFv(BGP) gene was cloned into pDisplay expression vector, upstream to the platelet-derived growth factor receptor transmembrane domain (PDGFR-TM). The resulting pDisplay-EGFP-SNAP-scFv(BGP) was transfected into cells, followed by labeling with RhR-X-PEO₁₂-SNAP ligand. The expression as well as fluorescence labeling in cells was confirmed by fluorescence microscope. The protein expression was also examined by fluorescence imaging of SDS-PAGE gel for crude and soluble fractions of cell extract.

When pDisplay-EGFP-SNAP-scFv(BGP) was transfected into HeLa S3 cells, both EGFP and RhR fluorescence were observed by fluorescence microscope imaging of the cells (Figure 4-2A). Fluorescence imaging of SDS-PAGE gel for the cell extract with excitation of RhR at 532 nm showed that full-length Igκ-EGFP-SNAP-scFv(BGP)-PDGFR-TM (MW \approx 83 kDa) was successfully expressed in HeLa S3 cells in soluble form (Figure 4-2B). These results supported the expression and fluorescence labeling of EGFP-SNAP-scFv(BGP) in HeLa S3 cells.

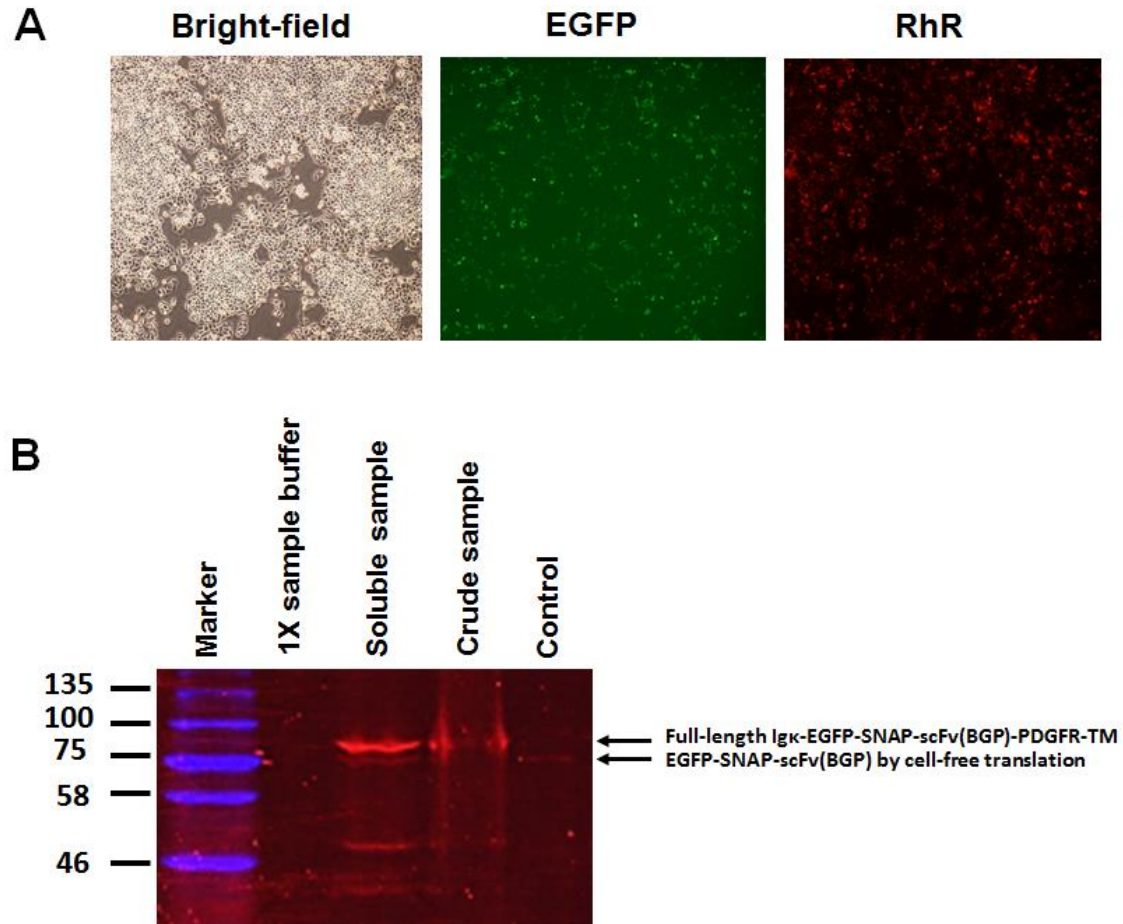


Figure 4-2. Expression of EGFP-SNAP-scFv(BGP) labeled with RhR-X-PEO₁₂-SNAP ligand in HeLa S3 cells. **(A)** Fluorescent microscope images of HeLa S3 cells observed in bright-field, EGFP fluorescence channel, and RhR fluorescence channel. **(B)** Fluorescence image of SDS-PAGE gel for crude and soluble fractions of the cell extract with excitation of RhR at 532 nm and emission at 580 nm. EGFP-SNAP-scFv(BGP) obtained from cell-free translation was applied as a control. Molecular weights of Igκ-EGFP-SNAP-scFv(BGP)-PDGFR-TM and EGFP-SNAP-scFv(BGP) are 83 kDa and 73 kDa, respectively.

Next, the expression of EGFP-SNAP-scFv(BGP) was investigated in U2OS cells. The experiment was performed same as HeLa S3 cells. In fluorescence microscope images, both EGFP and RhR fluorescence were observed although the number of fluorescent cells was lower than HeLa S3 cells (Figure 4-3A). Due to the low expression level of the protein in U2OS cells, RhR-labeled EGFP-SNAP-scFv(BGP) was not detected in SDS-PAGE gel with denatured samples. Therefore, non-denatured samples were used for SDS-PAGE to visualize EGFP fluorescence. Upon excitation of EGFP at 488 nm, a protein band exhibiting EGFP fluorescence

with equal molecular weight as the protein expressed in HeLa S3 cells was observed in both crude and soluble fractions of U2OS cell extract (Figure 4-3B). This result suggested that full-length Ig κ -EGFP-SNAP-scFv(BGP)-PDGFR-TM was also expressed in U2OS cells although the labeling with RhR-SNAP ligand was not efficient. Full-length Ig κ -EGFP-SNAP-scFv(BGP)-PDGFR-TM may remain inside the cells and be not labeled with RhR-SNAP ligand on the cell surface.

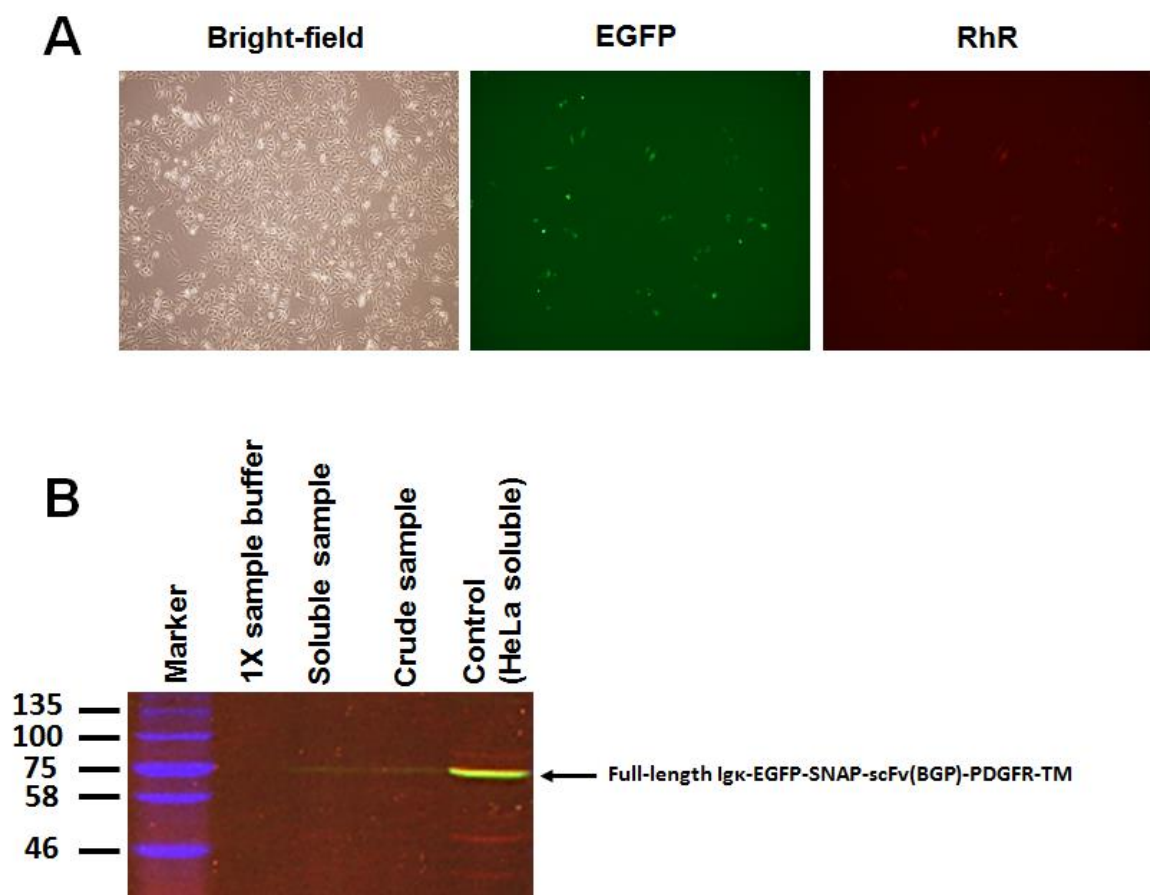


Figure 4-3. Expression of EGFP-SNAP-scFv(BGP) labeled with RhR-X-PEO₁₂-SNAP ligand in U2OS cells. **(A)** Fluorescence microscope images of U2OS cells observed in bright-field, EGFP fluorescence channel, and RhR fluorescence channel. **(B)** Fluorescence image of non-denaturing SDS-PAGE gel for crude and soluble fractions of the cell extract with excitation of EGFP at 488 nm and emissions at 520 nm and with excitation of RhR at 532 nm and emissions at 580 nm. Soluble fraction of the HeLa S3 cell extract was applied as a control.

4-3-2. Fluorescence imaging of HeLa S3 cells expressing EGFP-SNAP-scFv(BGP)

HeLa S3 cells expressing EGFP-SNAP-scFv(BGP) and labeled by RhR-X-PEO₁₂-SNAP ligand were incubated with 10⁻⁴ M BGP peptide for 12 hours before imaging. Control cells which were incubated without BGP peptide was used for comparison. Fluorescence of HeLa S3 cells was visualized under a laser scanning confocal microscope. Fluorescence images of EGFP and RhR channels with excitation of EGFP at 473 nm were recorded and fluorescence ratio images were obtained using ImageJ software.

Fluorescence ratio images of HeLa S3 cells incubated with BGP peptide showed higher fluorescence ratio (RhR/EGFP) compared with those incubated in the absence of BGP (Figure 4-4A). The histograms of fluorescence ratio of individual cells also confirmed that the distribution of fluorescence ratio of BGP addition cells was shifted to higher ratio range compared with control cells (Figure 4-4B). This result suggested that the fluorescence ratio of RhR/EGFP was enhanced due to the binding of EGFP-SNAP-scFv(BGP) expressed on HeLa cell surface with BGP and the removal of the quenching effect on RhR.

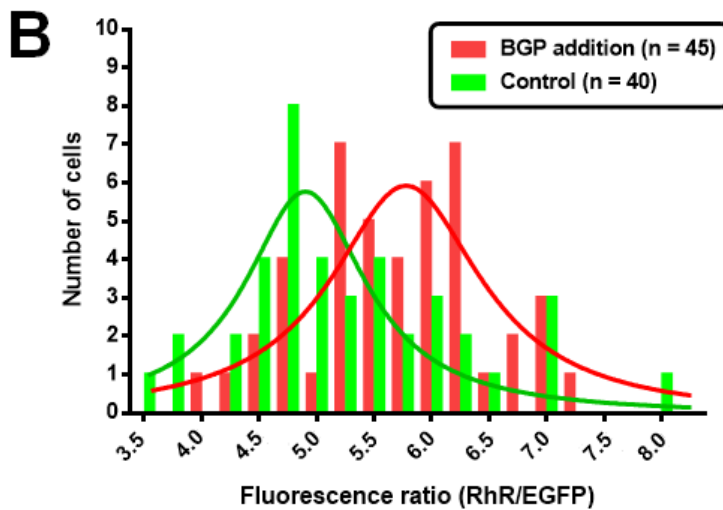
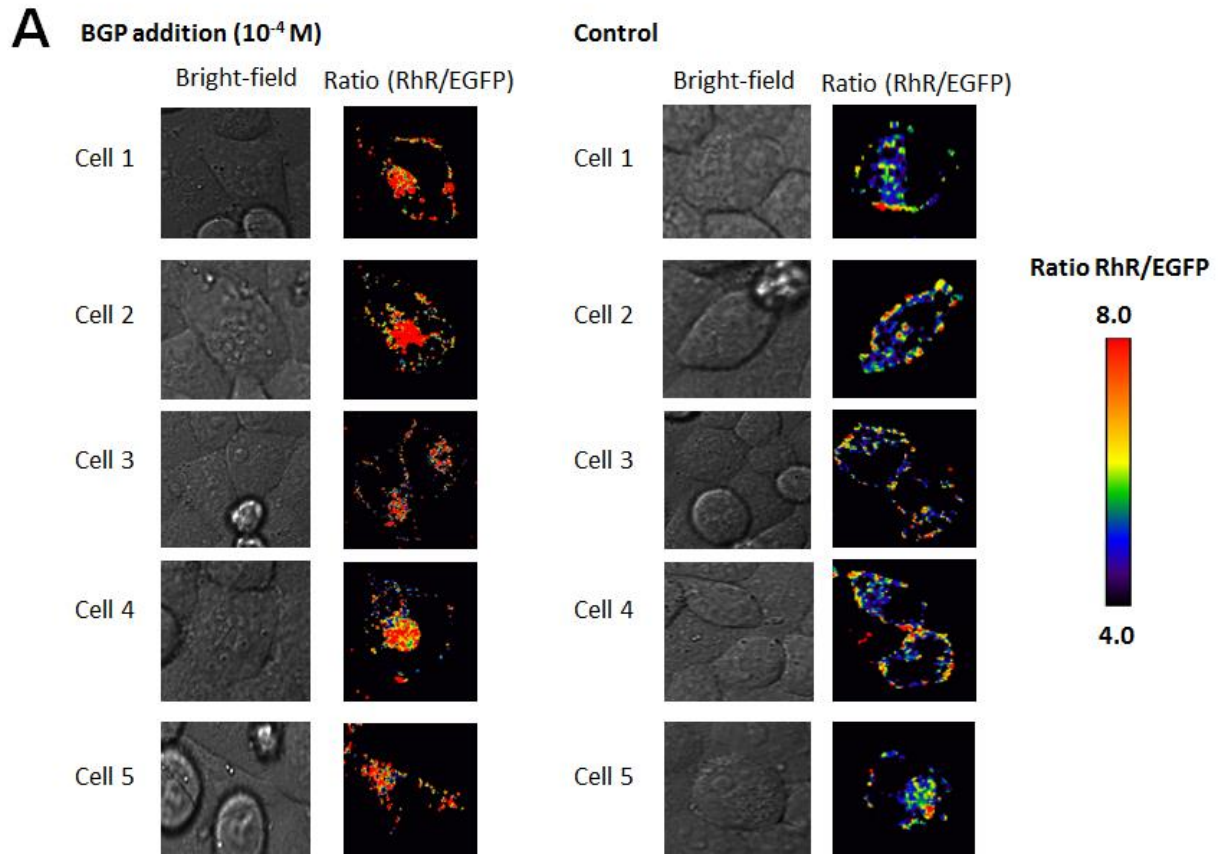


Figure 4-4. (A) Fluorescence ratio images of HeLa S3 cells expressing EGFP-SNAP-scFv(BGP) labeled by RhR-X-PEO₁₂-SNAP ligand in the presence (BGP addition) and in the absence of antigen (control). (B) Histograms representing the distribution of fluorescence ratio (RhR/EGFP) values of individual cells in BGP addition sample and control sample (n: number of cells analyzed).

4-3-3. Fluorescence imaging of U2OS cells expressing EGFP-SNAP-scFv(BGP)

U2OS cells expressing EGFP-SNAP-scFv(BGP) and labeled by RhR-X-PEO₁₂-SNAP ligand were induced to differentiate to osteoblasts by incubating in medium containing 0.1% FBS and 10⁻⁷ M vitamin D3. It has been reported that U2OS cells produce about 0.4 ng/ml (0.07 nM) BGP upon differentiation⁶. After 36 hours incubation, the cells were observed by laser scanning confocal microscope. Control cells without induction for differentiation were also subjected to fluorescence imaging.

Fluorescence ratio images of cells exhibiting fluorescence ratio (RhR/EGFP) values above 0.4 indicated that differentiated U2OS cells with osteoblast induction showed higher fluorescence ratio compared with control cells (Figure 4-5A). The histograms of fluorescence ratio values of individual cells also confirmed that the distribution of fluorescence ratio was shifted to higher values in osteoblast induction cells compared with control cells at a range above 0.4 (Figure 4-5B). This result was consistent with the result obtained from HeLa S3 cells, suggesting that EGFP-SNAP-scFv(BGP) on the surface of U2OS cells could bind to the secreted BGP and the quenching effect on RhR was eliminated upon BGP binding.

On the other hand, no shift in fluorescence ratio values between control and osteoblast induction cells was observed at a range below 0.4 (Figure 4-5B). The osteoblast induction-independent low fluorescence ratio cells may be resulted from cells expressing only intracellular EGFP-SNAP-scFv. As suggested in Figure 4-3, considerable amount of EGFP-SNAP-scFv may remain inside the cells without labeling with RhR-SNAP ligand. In addition, the results in Figures 4-4 and 4-5 indicated that the fluorescence ratio values of U2OS cells were much lower than those of HeLa S3 cells. Probably, the non-labeled EGFP-SNAP-scFv might increase the background EGFP signal and decrease fluorescence ratio values in U2OS cells. The intracellular EGFP-SNAP-scFv may become a drawback for live-cell imaging using this biosensor since it reduces the fluorescence ratio of RhR/EGFP. To further improve this biosensor, the use of another protein-tag (such as HaloTag or CLIP-tag) and its membrane impermeable green fluorescent ligand in place of EGFP would be effective to avoid the fluorescence of EGFP-SNAP-scFv inside the cells.

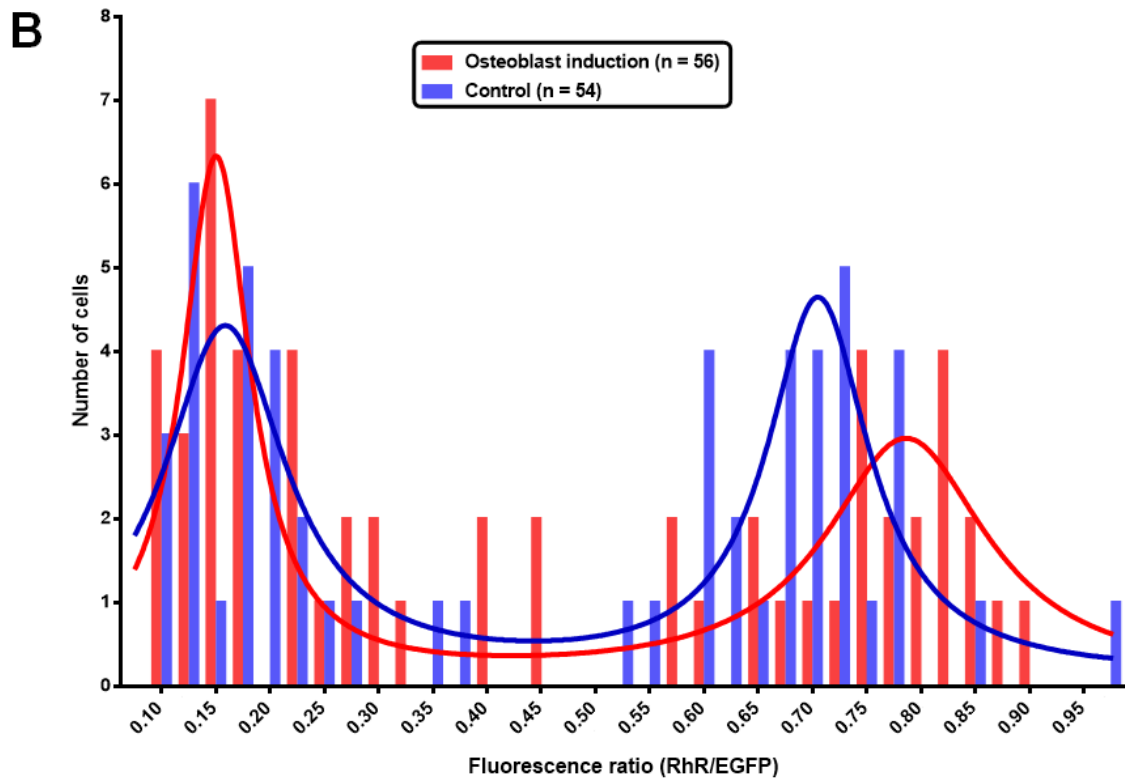
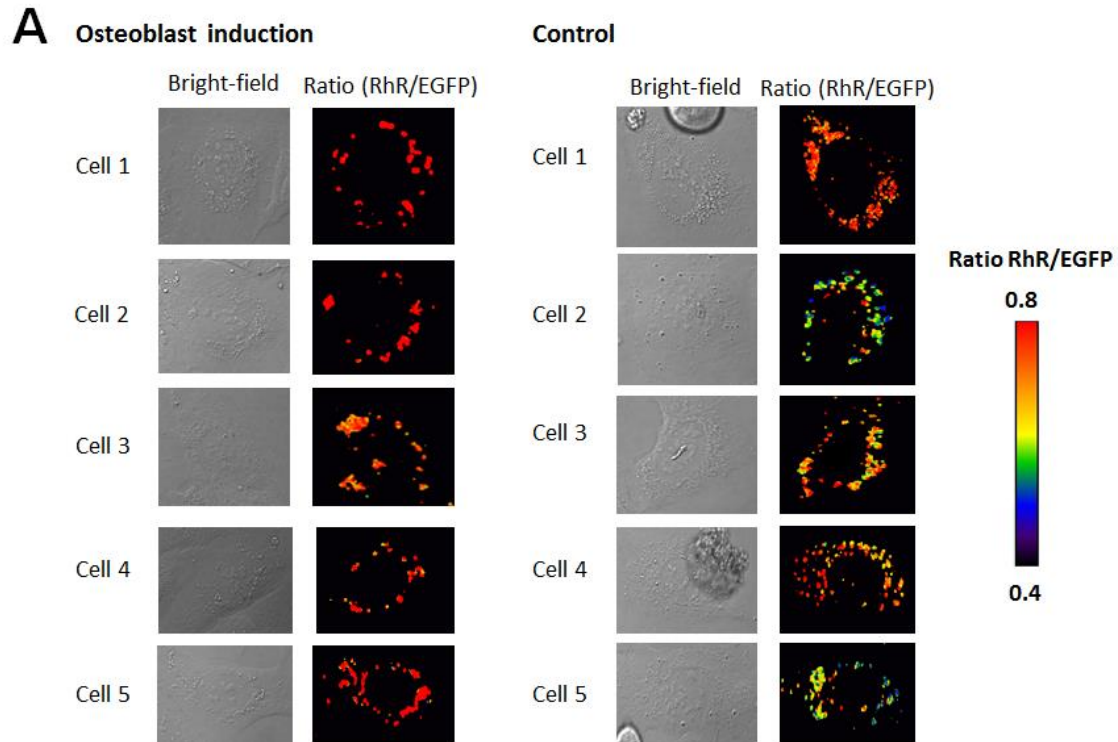


Figure 4-5. (A) Fluorescence ratio images of differentiated U2OS cells with osteoblast induction and control cells without induction. (B) Histograms representing the distribution of fluorescence ratio (RhR/EGFP) values of individual cells with osteoblast induction and without osteoblast induction (control) (n: number of cells analyzed).

4-4. Conclusion

In this chapter, I investigated an application of the fluorescent ratiometric biosensor EGFP-SNAP-scFv(BGP) to live cell imaging for detection of BGP. The EGFP-SNAP-scFv was successfully expressed and labeled with RhR-SNAP ligand on the cell surface of both HeLa S3 and U2OS cells. Fluorescence imaging using confocal microscope exhibited an increase of fluorescence ratio RhR/EGFP in response to exogenous addition of BGP peptide in HeLa S3 cells and BGP secretion with osteoblast induction in U2OS cells, suggesting that the binding of BGP to scFv eliminated the quenching of RhR fluorescence as observed *in vitro*. In addition, SNAP-tag has been reported to be labeled *in vivo* and even in animal⁷, hence, the application of this type of biosensors can be expanded to a wide variety of bio-imaging. Moreover, using of membrane-permeable fluorescent SNAP ligands and antibodies that works inside cells (intrabodies), this type of biosensors can be applied for fluorescence imaging inside cells.

4-4. References

- (1) Ho M., Nagata S., Pastan I. Isolation of anti-CD22 Fv with high affinity by Fv display on human cells. *Proc. Natl. Acad. Sci. USA* **103**(25): 9637-9642 (2006)
- (2) Wei J., Karsenty G. An overview of the metabolic functions of osteocalcin. *Curr. Osteoporos. Rep.* **13**(3): 180-185 (2015)
- (3) Zoch M. L., Clemens T. L., Riddle R. C. New insights into the biology of osteocalcin. *Bone* **82**: 42-49 (2016)
- (4) Abe R., Jeong H. J., Arakawa D., Dong J., Ohashi H., Kaigome R., Saiki F., Yamane K., Takagi H., Ueda H. Ultra Q-bodies: quench-based antibody probes that utilized dye-dye interactions with enhanced antigen-dependent fluorescence. *Sci. Rep.* **4**: 4640 (2014)
- (5) Kardash E., Bandemer J., Raz E. Imaging protein activity in live embryos using fluorescence resonance energy transfer biosensors. *Nat. Protoc.* **6**(12): 1835-1846 (2011)
- (6) Matsugaki T., Zenmyo M., Hiraoka K., Fukushima N., Shoda T., Komiya S., Ono M., Kuwano M., Nagata K. M-myc downstream-regulated gene 1/Cap43 expression promotes cell differentiation of human osteosarcoma cells. *Oncol. Rep.* **24**(3): 721-725 (2010).
- (7) Bojkowska K., Santoni de Sio F., Barde I., Offner S., Verp S., Heinis C., Johnsson K, Trono D. Measuring in vivo protein half-life. *Chem. Biol.* **18**(6): 805-815 (2011)

Chapter 5

Conclusion

In chapter 2, I developed novel fluorescent biosensor for detection of phosphotyrosine containing peptides based on antigen-dependent removal of quenching effect on a fluorophore attached to antibody single-chain variable domain. The biosensor consists of an anti-phosphotyrosine single-chain variable domain (scFv(pTyr)) fluorescently labeled at N-terminus by a fluorophore-nonnatural amino acid. The biosensor exhibited antigen-dependent enhancement of fluorescence. Fusion of fluorescent protein (FP) to this biosensor generated a double labeled biosensor which allowed FRET between FP and fluorophore and antigen-dependent fluorescent enhancement of the fluorophore. The result obtained here demonstrated that fluorescent protein-fusion and fluorescent-labeled scFv are useful to generate fluorescent ratiometric biosensors.

In chapter 3, I substituted the fluorophore-nonnatural amino acid at N-terminal domain of scFv by protein-tag and its fluorescent ligand to obtain antibody-based genetically encoded biosensor. The resulting biosensors allowed detection of antigens based on antigen-dependent removal of quenching effect on fluorophore attached to protein-tag without using nonnatural amino acid mutagenesis. In addition, orientation of protein-tag to scFv, type of fluorophore, linker length between fluorophore-ligand and peptide linker between protein-tag and scFv were found to significantly affect fluorescent enhancement of the biosensor. Double labeled biosensor was achieved by fusion of FP to SNAP-scFv. These biosensor showed fluorescence ratio change in an antigen-dependent manner based on FRET and antigen-dependent removal of fluorescence quenching effect.

In chapter 4, I demonstrated an application of newly synthesized EGFP-SNAP-scFv(BGP) labeled with RhodamineRed-SNAP ligand to detection of extracellular BGP. The biosensor was expressed on the surface of HeLa S3 cells as well as osteosarcoma U2OS cells. HeLa S3 cells showed enhanced fluorescence ratio (RhodamineRed/EGFP) in response to exogenously added BGP peptide. Similarly, upon induction of U2OS cells to differentiate to osteoblasts during which BGP was secreted, the induced U2OS cells exhibited higher fluorescent ratio (Rhodaminered/EGFP) compared with non-induced cells.

Throughout this study, I have successfully constructed antibody-based genetically encoded fluorescent biosensors which can be expressed both in cell-free translation system and in live cells. Conventional FRET-based biosensors usually require the protein backbone to undergo a large conformational change upon interaction with target molecules and careful design of fluorescent protein orientation to achieve good FRET change. These requirements limit the development of FRET-based biosensors. However, the present strategy in combination of FRET and antigen-dependent removal of quenching effect does not require conformational change of protein. In addition, antibody-based biosensors can be available for various antigens. These advantages of this strategy will allow a wide range of applications including diagnostic analysis of biomarkers and live cell imaging.

List of Publication

Kim Phuong Huynh Nhat, Takayoshi Watanabe, Kensuke Yoshikoshi, Takahiro Hohsaka. Antibody-Based Fluorescent and Fluorescent Ratiometric Indicators for Detection of Phosphotyrosine, *J. Biosci. Bioeng.*, *in press*.

Kim Phuong Huynh Nhat, Takayoshi Watanabe, Keisuke Fukunaga, Takahiro Hohsaka. Genetically-Encoded Antibody-Based Biosensors by Fusion of Protein-Tag and Fluorescent Protein to Single-Chain Antibody, *in preparation*.

Acknowledgement

This study was carried out at School of Materials Science, Japan Advanced Institute of Science and Technology (JAIST) under the supervision of Professor Takahiro Hohsaka since 2013. I would like to express my sincere thanks to his kind, long-standing guidance and encouragement throughout the study.

I specially acknowledge Professor Yuzuru Takamura, Professor Kenzo Fujimoto, Associate Professor Kazuaki Matsumura, Associate Professor Hidekazu Tsutsui (JAIST) and Professor Masaru Kawakami (Yamagata University) for kind instructions as well as materials and instrument support.

I am grateful to Assistant Professor Takayoshi Watanabe for his kind guidance and support of fluorophore-protein-tag ligands. I specially thank Dr. Keisuke Fukunaga for microscopic instructions. And I greatly appreciate all members of Hohsaka laboratory for their kindness, encouragement as well as valuable advice, discussion during the study.

I am thankful to the “Doctoral Research Fellow” (DRF) program of Japan Advanced Institute of Science and Technology (JAIST) for financial support.

Finally, I wish to express my gratefulness to my family, my friends for their kind support and encouragement during my PhD course.